2-P (MIX)

April 1971

DEVELOPMENT AND TEST OF A FLIGHT PROTOTYPE POWER CONDITIONER FOR 20 CM MERCURY BOMBARDMENT ELECTRIC THRUSTER SYSTEM

Contract No. JPL 952297

HUGHES
HUGHES AIRCRAFT COMPANY

SCG 10167R

April 1971

DEVELOPMENT AND TEST OF A FLIGHT PROTOTYPE POWER CONDITIONER FOR 20 CM MERCURY BOMBARDMENT ELECTRIC THRUSTER SYSTEM

Contract No. JPL 952297

This work was performed for the Jet Propulsion Laboratory, California Institute of Technology, sponsored by the National Aeronautics and Space Administration under Contract NAS7-100.

HUGHES
HUGHES AIRCRAFT COMPANY

SCG 10167R

CONTRIBUTORS

The work that is reported in the following sections has been the combined effort of a number of key people. Although each person was involved in all phases of the program, the greatest area participation is noted. Project engineering responsibility shifted prior to the breadboard modification or the second phase.

KEY PERSONNEL

J. H. Molitor	Project Manager
W. J. Muldoon	Project Engineer, Phase I
D. R. Garth	Project Engineer, Phase II
G. C. Benson	Systems Engineer
P. C. Chapman	Supervisor, Fabrication

ACKNOWLEDGMENTS

The author wishes to thank the Jet Propulsion Laboratory personnel listed below for their contributions, forbearance, and aid in the success of this program.

D. J. Kerrisk

T. D. Masek

T. W. Macie

E. N. Costogue

W. C. Schaefer

CONTENTS

1. INTRODUCTION AND SUMMARY

INTRODUCTION

In July, 1968, a program was initiated at Hughes Aircraft Company under contract to the Jet Propulsion Laboratory to design and fabricate one breadboard and two experimental model power conditioners to prove the feasibility and state of the art of a lightweight, high efficiency power conditioner for use in deep space on a solar electric propelled mission. The results of the breadboard and experimental phases indicate that power conditioning technology has reached a state that is compatible with mission constraints in terms of weight, reliability, and efficiency.

During the design and fabrication of the breadboard model, studies and analyses of reliability, weight, and efficiency were performed. The unit fabricated incorporated the study results and was fabricated as an engineering prototype unit. The breadboard unit therefore provided initial information as to severity of EMI problems, expected final experimental system weights, and thermal data. Design changes in the experiment units were made as the result of the breadboard unit weight, EMI levels, and system efficiency requirements.

Prior to fabrication of the experimental systems, the thruster design was changed to incorporate a hollow cathode. The detail of modifications made to the breadboard unit is described, as is the impact on weight and reliability.

Fabrication techniques to reduce weight and circuit changes from the breadboard system are described. Reliability and efficiency analyses were performed with the summary included. The acceptance test results are tabulated and integration testing is discussed.

SUMMARY

The purpose of this effort was to prove that a power conditioner fulfilling the requirements of reliability, weight, and efficiency could be fabricated for operation with a 20 cm mercury bombardment ion thruster. The program included the design, development, and testing of a breadboard and two experimental units. The breadboard was to be an electrical

evaluation unit, while the experimental systems were to prove the environmental designs. It was elected to build the breadboard as an engineering model to reduce risks in the experimental phase.

During the development, evaluation of components and circuit techniques was performed to optimize for weight and efficiency. Based on these results, a choice of designs was made for regulation, pulse width modulation techniques, and filtering. The resulting designs were breadboarded and tested to verify results. The overall system package was designed to provide structural and thermal compatibility with a deep space mission.

The breadboard final weight was 39.11 pounds, as opposed to the 28 pound weight goal for the experiment systems. The unit measures 36 x 30 x 3.75 inches overall, including a mesh cover over the component side to protect against mercury contamination. The unit is substantially flat in construction with module plates fastened to an I-beam frame. Components are mounted to one side of the plate with the other side acting as a direct thermal radiating surface. The module concept was shown to be superior to lumped power modules by direct comparison analysis. The electrical performance was tested by operation with a 20 cm oxide cathode thruster for over 1300 hours, during which many thruster high voltage arcs occurred. The total power output capability is 2950 watts over an input line voltage variation of 40 to 80 volts.

A thruster design change to utilize the hollow cathode required a modification of the breadboard system. The resulting increase in discharge power and addition of two supplies pushed the maximum allowable weight to 30 pounds. No effort was made to reduce the weight of the modified breadboard, since analysis showed that the weight of the experimental system would meet the 30 pound limit. Modification of the breadboard was accomplished and integration testing was successful after additional circuit protection was provided. The input line variation was decreased to 53 to 80 volts to avoid a redesign of the arc supply. The unit efficiency is estimated to approximately 86 percent at 67 volts line.

The experimental system final weight was 29.97 pounds. The efficiency, as measured in a calorimeter, was 89.7 percent at 80 volt line and 89.9 percent at 57.6 volt line when delivering 2590 watts. The unit weight was reduced by decreasing material thicknesses in the frame and module plates and by using simplified component mounting techniques. Additional weight savings were achieved through the use of TO-61 isolated collector transistors and the control of conformal coating. Preliminary integration tests indicate that the experimental units operate satisfactorily with the thruster. Additional tests, including long-term operation in thermal vacuum, are planned.

2. SYSTEM SPECIFICATIONS AND DESIGN APPROACHES

SPECIFICATIONS

The power conditioner system specifications as imposed by oxide cathode mercury ion thruster requirements are summarized below. Table 2-1 and Table 2-2 detail the exact power conditioning output requirements of the contract

1) The power conditioner shall be designed to operate with a JPL ion thruster

2) The power conditioner shall be compatible with a spacecraft solar cell array power source.

3) The beam current shall be controlled by analog command of 0 to +5 volts representing 0.5 to 1.0 amperes. The arc current shall be controlled as a predetermined function of beam current.

4) Power conditioner on/off and sequencing commands shall be a nominal 28 volt pulse of 50 ms duration.

5) All outputs must be capable of permanent shorts from any output terminal to another (except remote transformer terminals at power conditioner) without damage to the power conditioner.

6) The power conditioner must be space or high vacuum compatible and provide its own radiating surface. The unit must also operate at ambient pressures.

7) The unit must be capable of meeting launch phase vibration and shock.

8) The unit shall be capable of operating in the near proximity to other electronic equipment without adverse effect to itself or the other equipment.

9) The power conditioner shall not be required to operate below 0 °F.

TABLE 2-1. POWER CONDITIONING OUTPUT REQUIREMENTS (OXIDE CATHODE)

Group	Supply No.	Supply Name	Type	Output[1]	Maximum Ratings			Nominal Ratings					Range of Control[5]	Frequency	
					E	I	I_{LIM}[2]	E	I	P	Regul.	Peak Ripple		Output	Ripple
					V	A	A	V	A	W	Percent	Percent	A	kHz	kHz
I	1	Magnet Manifold Heater	DC	F	19	0.85	0.9	15	0.67	10.5	1.0(I)	5	--	--	10
	3	Cathode Heater	AC	V	5	40	45	4.5	35	160	Loop	--	10 - 40	5	--
	7	Neutral Heater	AC	V	12	3.4	4	12	2 8	35	Loop	--	0.3 - 3.4	5	--
	8	Neutral Keeper	DC	F	300V 5ma	20ma 30v	0.55	10	0.50	5	1.0(E)	2 at 30V 5 at 10V	0.02 - 0.5	--	10
II	2	Vaporizer	AC	V	10	2	2.05	5.5	1.1	6	Loop	--	0.5 - 1.2	5	--
	4	Arc	DC	V	150V 20ma[4]	7 at 36V	8	34.5	6	210	1.0(E)	2	2 - 7	--	30
	5	Beam	DC	V	2050	1.0	1.05	2000V	1.0	2kw	1.0(E)	5	0.5 - 1.0	--	30
	6	Accelerometer	DC	F	2050	0.1[3]	0.105	2000V	0 01	20	1.0(E)	5 at 0.15	--	--	30

1) Output: V = Variable, F = Fixed.

2) Current Limits or overload trips — exact values to be specified by the manufacturer.

3) Current stays at this level for less than 10 minutes at very low rep. rate.

4) Starting characteristics. (150V N_L to 36V at 20 ma.)

5) Current varies as function of engine loop control. See figures below.

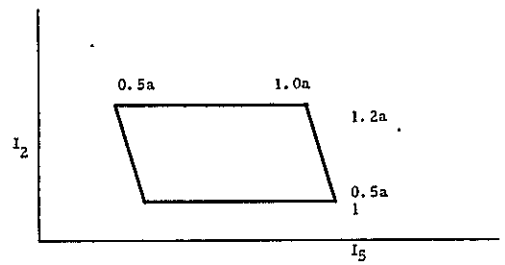

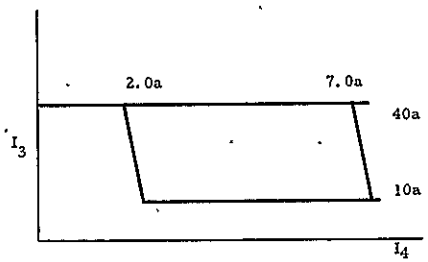

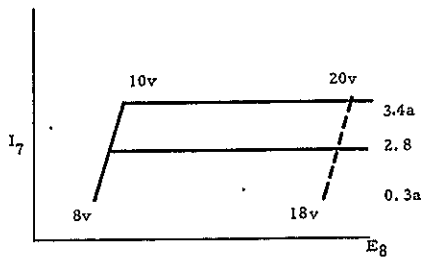

TABLE 2-2. TELEMETRY DATA AND SHUTDOWN LEVELS

Supply No.	Name	Telemetry				Shutdown Levels
		0 to 5 volt Telemetry Range		High Accuracy Part of Telemetry Range		
		Current, amperes	Voltage, volts	Current, amperes	Voltage, volts	
1	Magnet	0.3 to 0.9	----	0.65 to 0.75	----	
2	Vaporizer	0 to 3	----	----	----	
3	Cathode Heater	10 to 45	----	----	----	
4	Arc	0 to 7	30 to 40	2 to 7	34 to 36	
5	Beam	0 to 1	1700 to 2100	0.5 to 1	1950 to 2050	
6	Accelerometer	0 to 20	1700 to 2100	----	1950 to 2050	
7	Neutral Heater	0 to 4	----	----	----	
8	Neutral Keeper	0 to 0.55	0 to 30	----	----	
	Neutral Emission	0 to 1	----	----	----	
	Arcings					10 arcmin

10) The experimental unit weight shall not exceed 23.51 pounds.

11) The unit efficiency shall be greater than 91 percent at 40 volts input and 92 percent at 80 volts input.

12) The calculated reliability for 10,000 hours shall be greater than 0.96

Breadboard Unit

The basic electrical requirements the breadboard unit were those of Tables 2-1 and 2-2. Items in the summary list concerning structural or environmental requirements do not apply although the unit was fabricated as a prototype of the experimental system. As a result of the breadboard final weight of 39 pounds, the maximum allowable weight was raised to 28 pounds for the oxide cathode system.

Modified Breadboard and Experimental Units

The thruster design was changed to the hollow cathode configuration and the electrical requirements were modified to those specified in Tables 2-3 and 2-4. The changes are the deletion of the cathode supply and the addition of the cathode heater, cathode keeper, and cathode vaporizer supplies. The general specification for the weight of the experimental units was increased to 30 pounds to accommodate the addition of the two supplies.

DESIGN APPROACHES

The broad system design objective was to meet all requirements imposed electrically by the thruster as well as survive the mechanical thermal and vacuum environment of a spacecraft. These objectives, and those described in the previous section, require a light but durable structur capable of radiating internally generated heat into deep space. The electronics must be efficient and capable of withstanding a high transient environment caused by thruster noise and arcing.

The modular design approach was taken, requiring no single supply to provide more than 300 watts. This approach had been used by Hughes in previous thruster power conditioners and was found to be significant in providing a minimum weight design (Reference 1). The configuration chosen utilizes the reverse side of the radiating surface for component mounting, which provides a short heat path. This construction technique results in a low weight, rigid structure with easy access to circuit components. The open construction reduces the danger of high voltage arcing and provides an ideal structure for gas desorption. Both the breadboard and experimental units were fabricated using this technique.

TABLE 2-3. POWER CONDITIONER, POWER REQUIREMENTS – HOLLOW CATHODE, 20 cm THRUSTER

PS No.	Supply Name	Type	Maximum Rating			Nominal Rating						Remarks
			E	I	P	E	I	P	Regulation	Peak Ripple	Range of Control	
			V	A	W	V	A	W		Percent	A	
1	Magnet Manifold	dc	19	0.85	16	13	0.6	8	I (1)	5	Const Current	Preset within 0.5 to 0.85 amp
7	Neutral Heaters	ac	12	3.4	40	5.2	1.5	8	Loop or 5 (I)	-	0.3 - 3.4	Set I_7 ref. within 2.8 to 3.4 amp
8	Neutral Keeper	dc	300V[1] at 5ma	0.6 amp[2] at 0V	5	10	0.5[2]	5	Loop or Fig. 5	2	0.1 - 0.5	Set E_S ref. within 10 to 20V
9	Cathode Heater	ac	8.5	4.8	40	8.5	4.8	40	5 (1)	-	On/Off	Manual control only
10	Cathode Keeper	dc	300V[1] at 5ma	0.6 amp[2] at 0V	5	10	0.5[2]	5	Fig. 5	2	-	Operates in open loop only
2	Vaporizer Main	ac	10	2	20	5.5	1.1	6	Loop or 5 (I)	-	0 - 2	Set I_2 ref. within 1.6 to 2 amp
3	Cathode Vaporizer	ac	10	2	20	5.5	1.1	6	Loop or 5 (I)	-	0 - 2	Set I_3 ref. within 1.6 to 2 amp
4	Arc	dc	60V at N. L.	37.5V at (9+1) amp	375	37	(8+1)	333	1 (1)	2	2 - 10	Set I_4 ref. within 2 to 9 amp
5	Beam	dc	2200[3]	1.05[4]	2100	2000	1.0	2000	1 (E)	5	0.5 - 1.0	
6	Accelerometer	dc	1100[3]	0.05[5]	50	1000	0.01	10	1 (E)	5	-	

NOTES:
1) 30 volts at 20ma.
2) Can be larger.
3) No load voltage.
4) 1.1 A trip.
5) 0.11 A trip.

GROUP I: PS-1, -7, -8, -9, -10;

GROUP II: PS-2, -3, -4, -5, -6.

TABLE 2-4. TELEMETRY DATA – HOLLOW CATHODE, 20 CM THRUSTER

Supply No.	Name	Telemetry			
		0 to 5 volt Range		High Accuracy Part of Telemetry Range	
		Current, amperes	Voltage, volts	Current, amperes	Voltage, volts
1	Magnet	0.3 to 0.9	----	0.50 to 0.75	----
2	Vaporizer main	0 to 2	----	----	----
3	Vaporizer cathode	0 to 2	----	----	----
4	Arc	0 to 9 [1)]	30 to 40	2 to 9 [1)]	34 to 36
5	Beam	0 to 1	1700 to 2100	0.5 to 1	1950 to 2050
6	Accelerometer	0 to 0.02	800 to 1200	----	950 to 1050
7	Neutral heater	0 to 4	----	----	----
8	Neutral keeper	0 to 0.8	0 to 30	----	----
9	Cathode heater	0 to 5	----	----	----
10	Cathode keeper	0 to 0.8	0 to 30	----	----
--	PC off	----	5		

NOTE: 1) Must indicate true arc current.

3. BREADBOARD

ELECTRICAL DESCRIPTION

All voltages delivered by the power conditioning system, shown in Table 2-1, are derived from inverters operating at two frequencies: 5 and 10 kHz. Individual inverters, as shown in Figure 3-1, deliver power in the range of 100 to 300 watts. Where higher power is required, such as the screen system at 2 kv and 1 ampere, total power is derived from the in-series output of eight 300 watt maximum converters. By restricting the maximum output per inverter module to 300 watts, it is possible to use high speed transistors to retain high efficiency at a reasonably high frequency of 10 kHz, permitting low weight, high efficiency transformers. Further advantages of modularization are adaptability to fractional redundancy for high reliability and adaptability to staggered phasing to minimize input and output ripple. The staggered phase technique also minimizes the peaking of the screen output filters at no load.

The 5 kHz inverter frequency is used for ac heater loads where a higher frequency would result in excessive line and load inductive impedance at the relatively high currents and low voltages required, (vaporizer heater, neutralizer heater, and cathode heater). It is also used for low power dc loads such as the magnet and neutralizer keeper to minimize circuit complexity.

Referring to Figure 3-1, regulated 35 volts from the line regulator, which regulates output voltage within 1 percent over the line voltage range of 40 to 80 volts, is used for accelerator and 5 kHz prime power and for all inverter base drive. The 5 kHz heater inverter supplies square-wave voltage to the magnet (PS1), vaporizer heater (PS2), neutralizer heater (PS7), and neutralizer keeper (PS8) supplies. Additionally, it supplies housekeeping dc voltages for logic and control functions.

The cathode, arc, and all screen inverters use pulse width modulated base drive for line and load regulation, with solar panel power derived from the 40 to 80 volt line. The accelerator inverter is driven by the 5 kHz heater inverter and the line regulator. The cathode, arc, and 5 kHz heater inverters are "double inverters", consisting of a prime and standby on each module, the standby being switched on in the event of a failure of prime inverter.

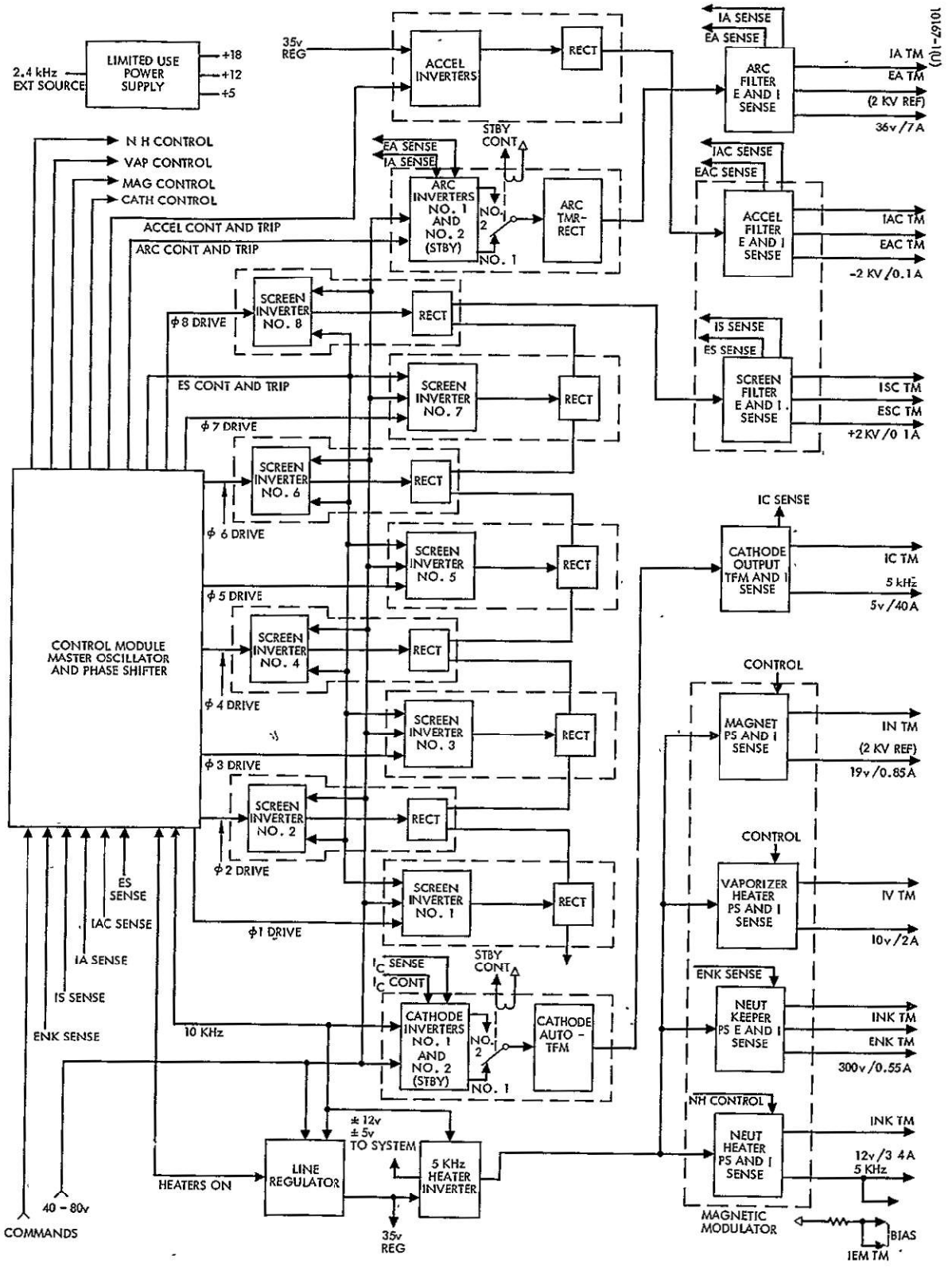

Figure 3-1. 3 kw Power Supply System Block Diagram

The control section provides the command and telemetry interface with the spacecraft, provides the required control link between interdependent supplies, provides the necessary automatic sequencing and time delays, monitors the system for overload trips, controls recycle time, senses inverter failures, and controls standby switching.

5 kHz Supplies

Magnet (PS1)

The magnet supply is required to furnish 16 watts of current regulated dc power to electromagnets mounted on the thruster. Since the electromagnets are tied to the +2000 volt screen supply (PS5), the output of the magnet supply is also referenced to the high voltage. The circuit for the magnet supply, Figure 3-2, except for the rectifier, is similar to the vaporizer (PS2) and neutralizer heater (PS7).

Drive power comes from the 5 kHz heater inverter as a constant amplitude square wave, thus providing line regulation for each supply. The circuit used here is that of a conventional "doubler" magnetic amplifier in the primary of the output transformer. Current is sensed by a current transformer with a peak sensitive ripple filter. Load inductance provides necessary filtering of the rectified pulse width modulated output current. Consequently, the output dc current is substantially constant, while the average ripple current varies with load impedance. While the primary current waveform is exponential rather than square wave, it has been determined experimentally that a peak current detector provides the necessary accuracy in current regulation, and is significantly less complex and more reliable than other devices that might be used when the output is floating at 2 kv. The circuit for the magnet supply will hold constant current into a short-circuited load. Fortunately, the exponential character of the output waveform, due to finite saturated inductance in the magnetic amplifier and leakage inductance in the transformer, results in a diminishing peak output voltage for small firing angles, and corresponding limited peak current into a short. This is desirable to prevent excessive loading of the 5 kHz drive source.

A control signal to the magnet supply from the control module can vary the output current from minimum to ON in a step or ramp function, depending on the desired thruster restart characteristics.

Vaporizer Heater (PS2)

The vaporizer supply provides a maximum 20 watts of current regulated ac power to the mercury vaporizer heater. The vaporizer circuit performs a dual function; i. e., rms current regulate for load changes in the absence of a control signal, and control output current when the screen current exceeds a desired set-point. Control interface is provided by the control module.

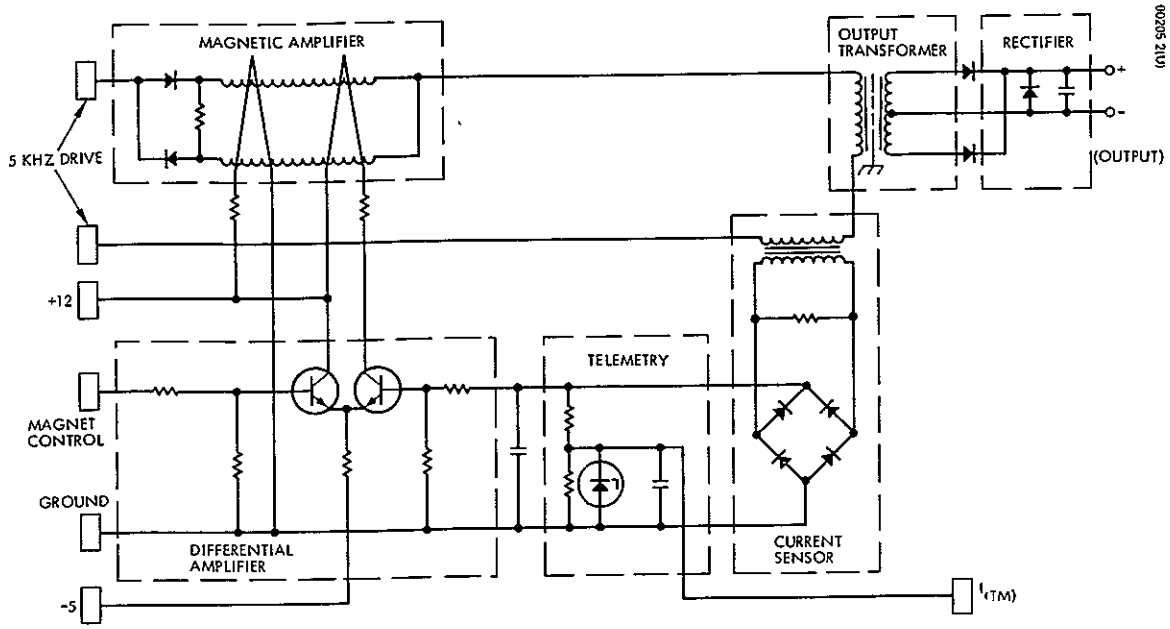

Figure 3-2. Magnet Supply Circuit

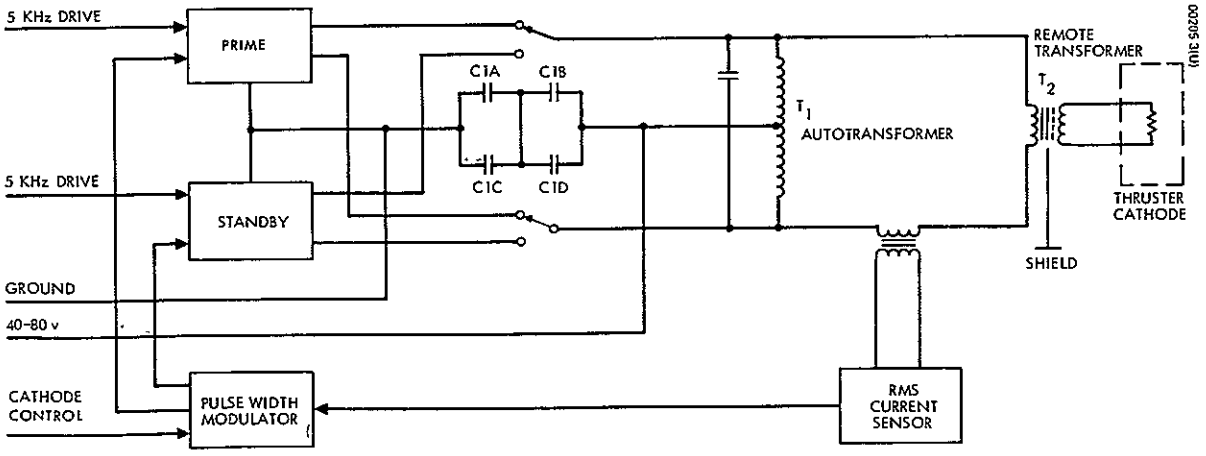

Figure 3-3. Cathode Supply Block Diagram

The magnetic amplifier regulation for the vaporizer supply is similar to that used in the magnet supply described above. However, the current sense filter is an rms approximation filter. The detection circuit chosen for rms control is an approximation circuit, rather than a "true rms" thermal sensing circuit, since it offers higher reliability, greater independence of ambient temperature, and faster response. An averaging filter would indicate current less than the rms value and a peak filter would indicate current greater than the rms value. Therefore, the circuit consists essentially of a hybrid peak/average filter on the rectified output of the current transformer. Since the line regulator will hold the input square wave voltage constant, the vaporizer supply must only regulate for load changes, including, however, a shorted output.

Cathode Supply (PS3)

This system uses the pulse width modulated double inverter (Figure 3-3) supplying a maximum of 200 watts of current regulated ac power to an oxide cathode at the thruster. The circuit described here is similar to the 10 kHz arc system except that the switching frequencies are different.

The 5 kHz output of either transistor inverter is switched to a single center tapped autotransformer and a remote transformer mounted on the thruster housing. A current transformer, in series with the primary of the remote transformer and its associated rms approximation filter, provides a current feedback signal, which is summed with a reference in the pulse width modulator (PWM) to produce a current regulated output. An isolated winding on the autotransformer supplies the ON sense signal, which will switch the standby inverter on if, after a delay following "HEATERS ON", the output is not present.

A remote step-down transformer is used to maintain short leads at the load to minimize the resistive and inductive drop in the load connection. The capacitor shunt across the autotransformer acts to partially tune out the effective inductance of the load and improve the IE switching envelope on the output transistors, thereby improving efficiency. Capacitors C1A, C1B, C1C, and C1D are line storage capacitors to supply power to switching transients within the inverter and to buffer the line against high di/dt and associated EMI.

Arc Supply (PS4)

The arc system delivers a maximum 288 watts of voltage regulated dc power to the thruster. As in the cathode circuit, the arc supply is a pulse width modulated double inverter, but the switching frequency has been increased to 10 kHz. As previously mentioned, choice of the higher switching frequency permits use of lightweight transformers and efficient filtering of the dc output voltage.

Both current and voltage feedback control pulse width modulation and the resulting output characteristic. A double function similar to the neutralizer keeper characteristic gives the arc output a starting boost of 150 volts

at no load, dropping to 36 volts at 20 ma, and regulated at 36 volts for line and load up to 8 amperes. The output is floating at the screen potential of +2000 volts.

Screen System (PS5)

The screen system delivers 2000 watts of voltage regulated dc power to the thruster. With all inverters operating, as shown in Figure 3-1, each inverter will deliver 300 watts for a line voltage ranging from 40 to 80 volts. The screen inverter circuit is typical of that shown in Figure 3-4 and the basic circuit is discussed later under Transistor Inverter Design.

Each inverter is phase shifted 1/8 of 1/2 cycle by the digital staggered phase generator (DSPG), resulting in efficient filtering of both the input and output lines. The line storage capacitors buffer the line from high speed switching currents and, when combined with the input line inductance, provide current ripple filtering and EMI suppression. The resulting composite current ripple on the power line is easily maintained at a maximum of 5 percent of the dc value with little cost in input line filter weight. Filtering of the sensed outputs is accomplished using an L-C filter. The output capacitor is sized to supply stored energy to extinguish an arc from screen to ground, thereby acting as a buffer to the inverters. In addition to filter considerations, the DSPG provides pulse width control of the filtered output voltage for regulation of 1 percent for line and load. In the event of an inverter failure, the DSPG will increase the duty cycle of each remaining screen inverter to maintain a regulated output.

Accelerator Supply (PS6)

The accelerator supply as shown in Figure 3-5, is a single converter delivering -2000 volts dc to the accelerator grid of the thruster. A steady state power level of 20 watts yields stress levels well within the component's reliable operating range, eliminating the need for a redundant inverter. No pulse width modulation or current/voltage feedback is necessary, since the inverter is driven with a regulated amplitude 5 kHz drive and prime power from the line regulator. The load regulation characteristic is within 1 percent of the 5 to 10 ma operating load range. Maximum power demands of approximately 200 watts can be supplied with derated performance for short-term transient periods such as occur during arcing of the thruster.

Neutralizer Heater Supply (PS7)

The neutralizer heater supply provides a maximum 41 watts of current regulated ac power to the neutralizer heater. The circuit used is identical, except in size of magnetic components, to that of the vaporizer supply. Like the vaporizer, the neutralizer heater provides a dual control function, i. e., rms current regulated for load and cutback output current when the neutralizer keeper voltage reaches a predetermined set point. Control interface is provided by the control module.

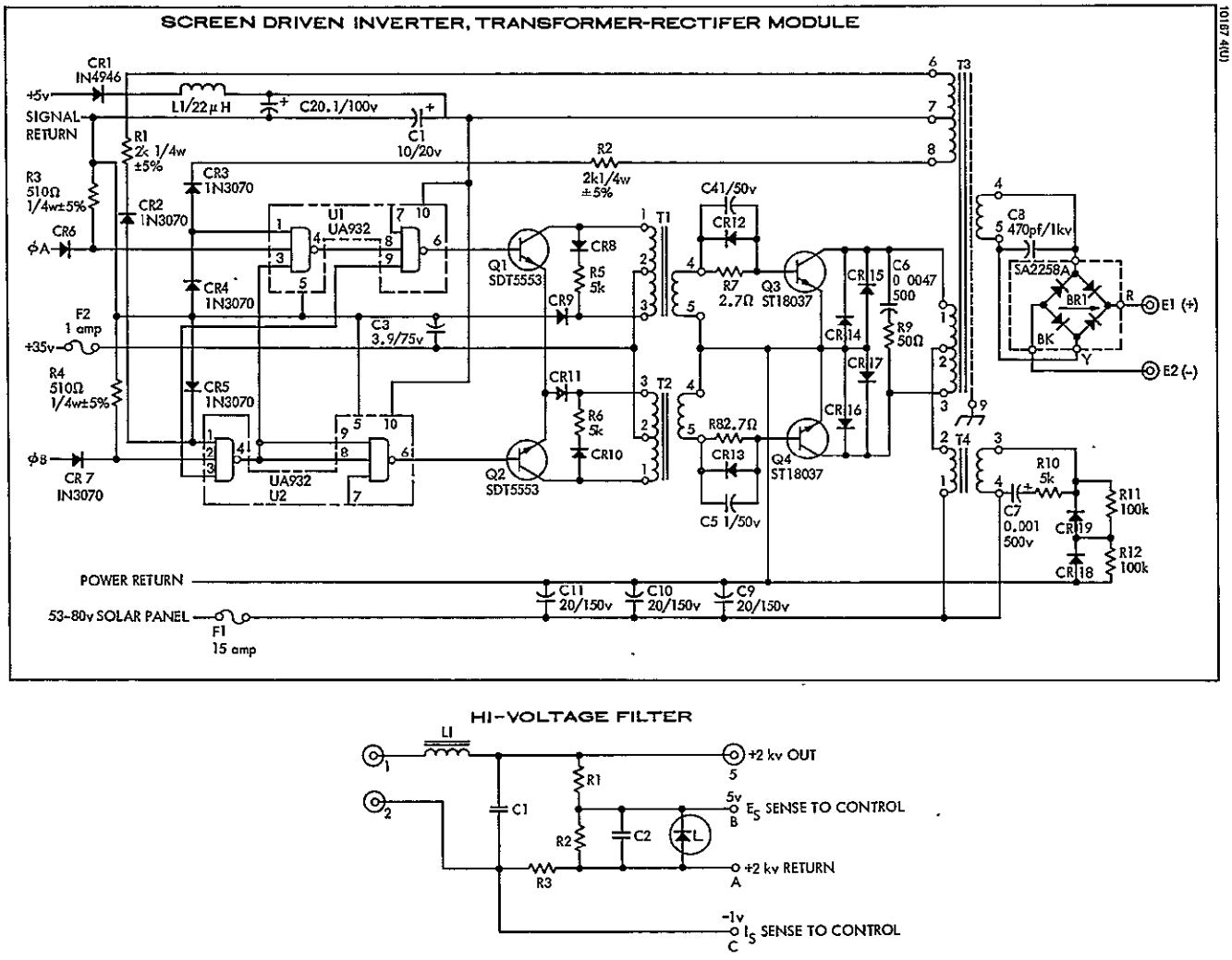

Figure 3-4. Screen Filter and Inverter Module

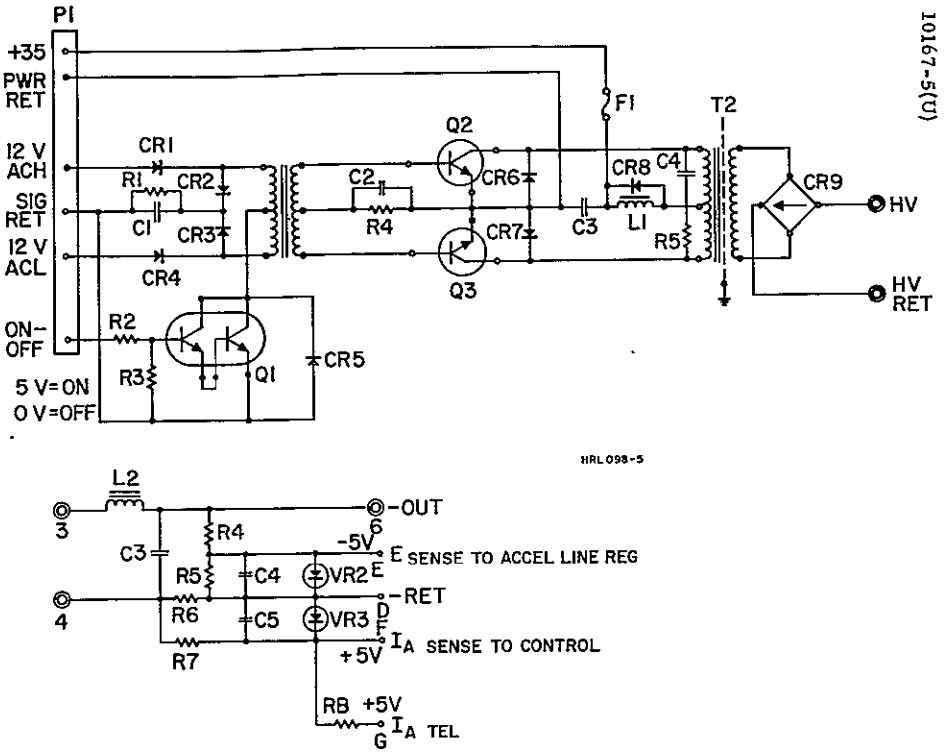

Figure 3-5. Accelerator Supply

Neutralizer Keeper Supply (PS8)

The neutralizer keeper supply, as shown in Figure 3-6, is designed to provide a maximum of 11 watts of unregulated dc power to the thruster. Since this is an unregulated supply, no magnetic amplifier control is required and there are no external control functions that modify the output characteristics. Instead, the double elliptic load characteristic to provide high starting voltage for igniting the neutralizer plasma is obtained by summing the outputs of two reactance limited supplies: one providing 270 volts at no load to 0 volt at 20 ma; the other providing 30 volts at no load to 0 volt at 550 ma, as seen in Figure 3-7.

Telemetry for neutralizer keeper current is sensed in the primary of the output transformer. An averaging filter on the output of the current sense transformer gives good tracking of the output current with, however, a scale change at the output break point. Under normal operation, the neutralizer keeper operates well within one scale range, thus eliminating the inconvenience of having dual scales. A differential amplifier is used for neutralizer keeper voltage telemetry, since the output voltage is floating above ground by the value of an external bias.

Line Regulator

The line regulator is a synchronized switching regulator. The circuit is shown in Figure 3-8. As a switching regulator, it converts the 40 to 80 volt solar panel voltage to a regulated or controlled nominal 35 volts dc with an efficiency of approximately 94 percent. A 10 kHz reference from the DSPG keeps the line regulator synchronized with the other systems, thereby eliminating possible beat frequencies between supplies. The regulated 35 volts provide approximately 160 watts of regulated power to the 5 kHz heater inverter, accelerator inverter, and base drive circuits of all inverters.

5 kHz Inverter

The 5 kHz inverter is shown in Figure 3-9. The total output power required of this inverter is 140 watts, 110 of which are provided as 5 kHz square wave drive power to magnetic regulators PS1, 2, 7 and 8, with the balance for accelerator converter base drive and housekeeping low power dc. The circuit is a driven inverter with the drive obtained from the 5 kHz output of the DSPG. Again, the double inverter concept provides a prime and standby power stage switched to a single output transformer.

The output transformer is connected as an autotransformer to supply the square wave 5 kHz to the magnetic regulators. Each magnetic regulator terminates in its own transformer, thus providing double transformation. Improved efficiency results from magnetic regulator gating at 70 volts, since outputs are characteristically low voltage. Use of double transformation reduces the number of isolated windings on the 5 kHz heater inverter autotransformer, thereby increasing the reliability of this component.

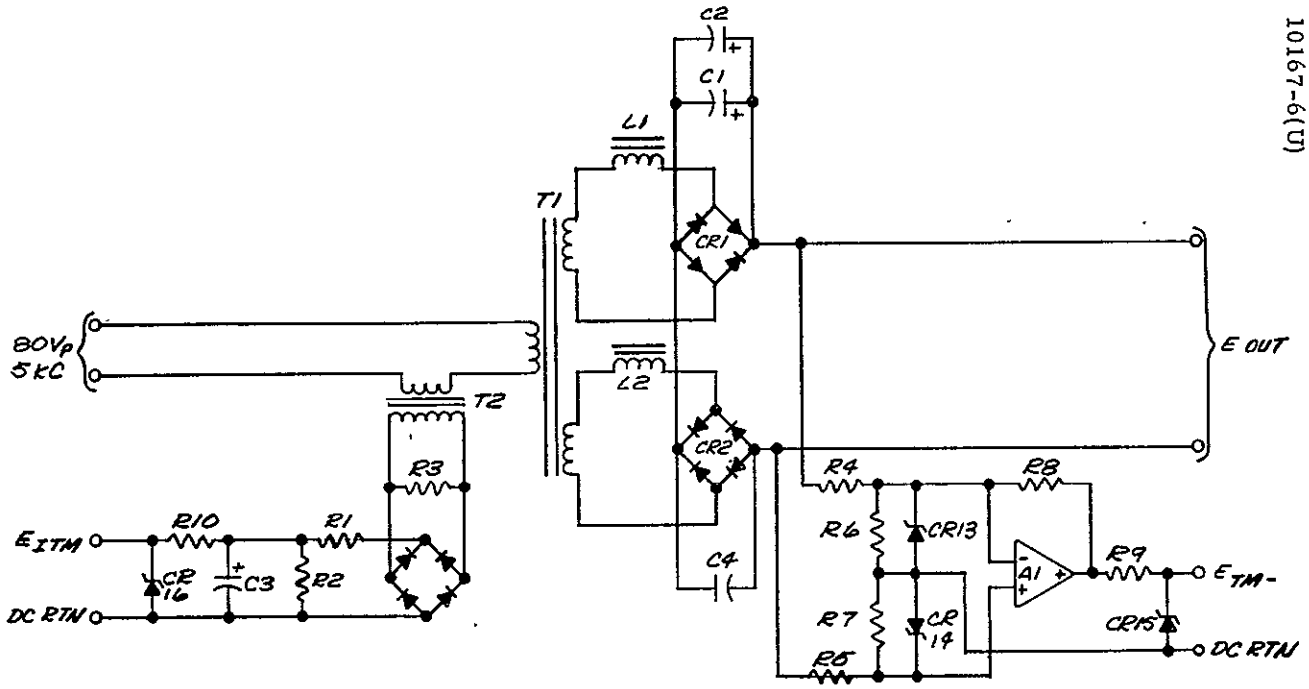

Figure 3-6. Neutralizer Keeper

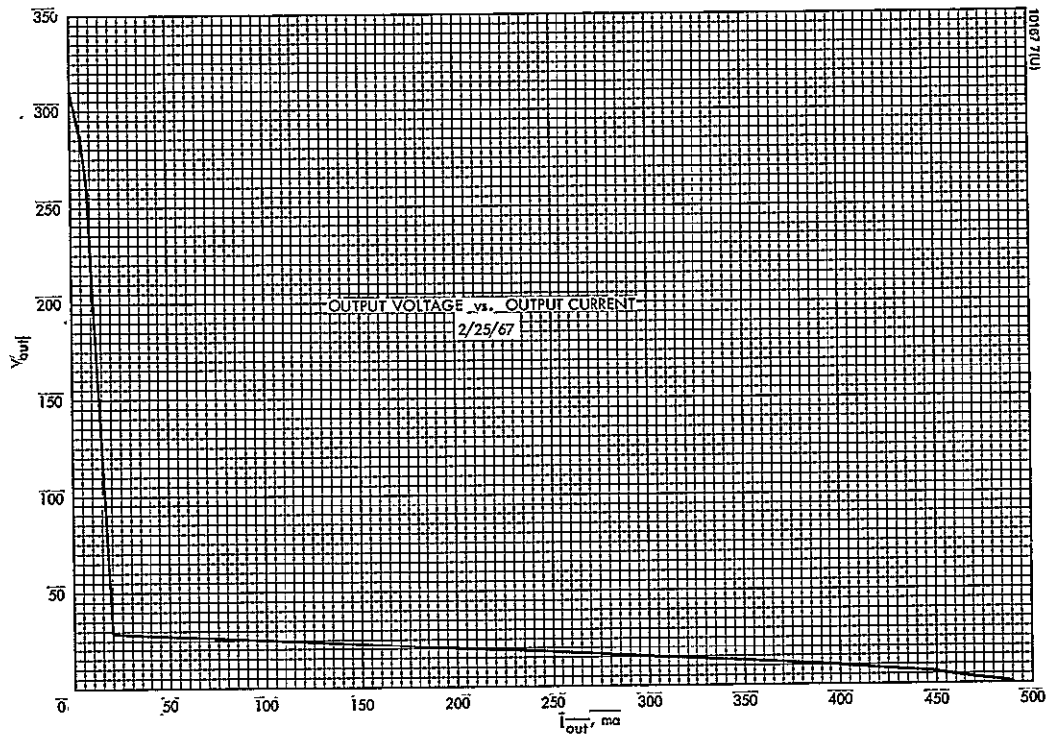

Figure 3-7. Neutralizer Keeper (Flight)

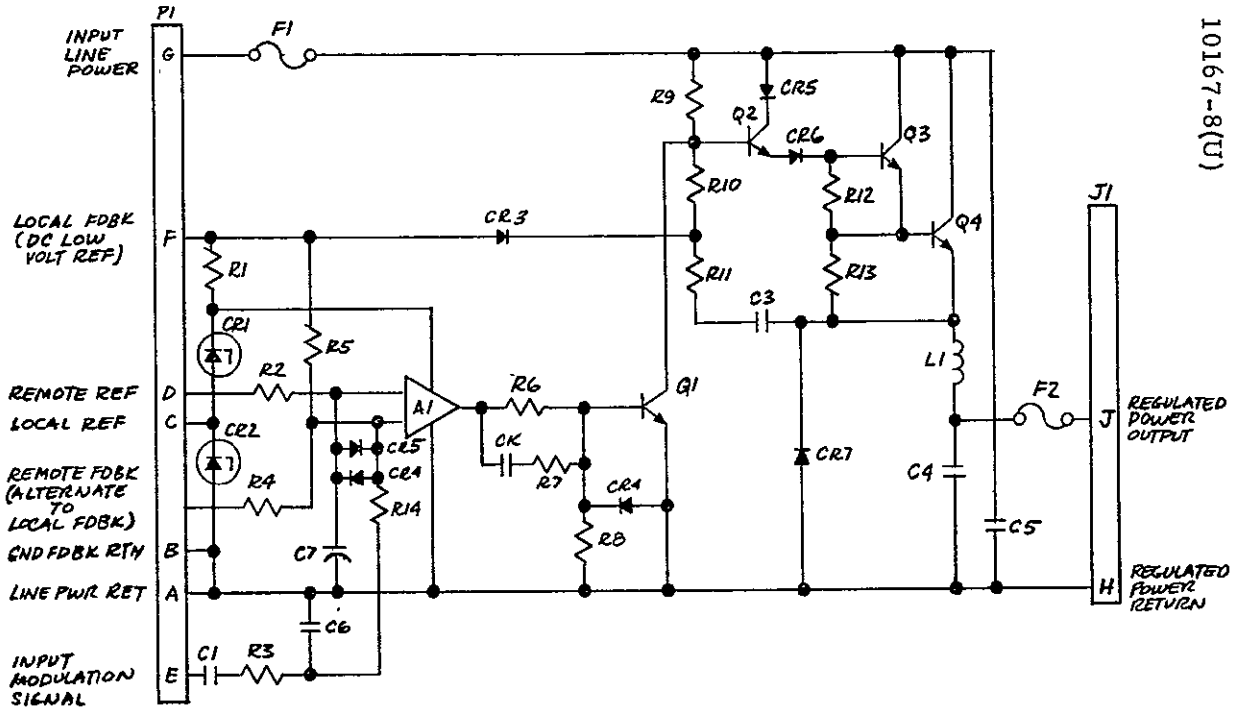

Figure 3-8. Line Regulator

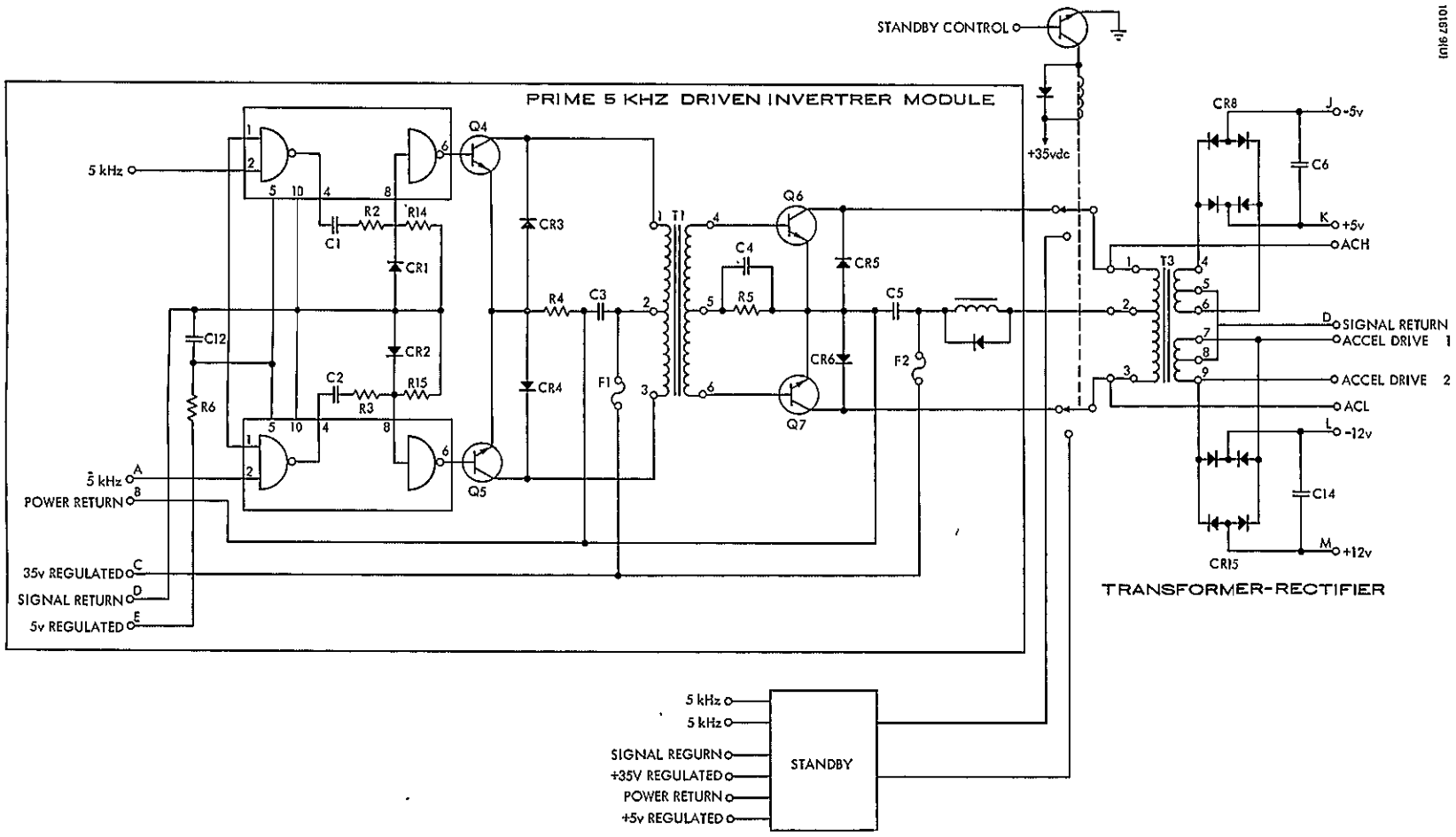

Figure 3-9. Kilohertz Converter

Transistor Inverter Design

In the conventional single transformer drive circuit for transistor switching inverters, a pulse is not transformed perfectly due to leakage inductance. Therefore, modifications were necessary to accommodate a high frequency pulse width modulated drive. The drive circuit chosen is essentially two energy storage converters, one driving each side of the inverter. Several advantages result from this configuration: use of low failure rate components such as signal transistors for base drive, low complexity, and power savings. The natural kickback of the transformer is useful in supplying the needed turnoff bias and, with separate transformers, does not affect the off transistor. The basic power drive stage for one-half the inverter is shown in Figure 3-10.

Application of power to the base of Q1 drops the collector voltage to near zero, impressing the supply voltage across the T1 primary. The voltage appearing at the secondary turns Q2 on. During the conduction period, the collector current increases. The initial step in current is the reflected base current. When base drive is removed from Q1, the stored energy in the transformer causes the voltages to reverse and CR1 clamps the primary. Since T1 is center tapped, the voltage developed at Q1 is twice the supply voltage and the voltage on the secondary is just the reverse of its previous value. The reverse base current is limited by CR2 and Q2 base impedances and, when measured, was found to be 2 amperes peak. The transistor is thus not subjected to high reverse base emitter voltages and a low impedance path is provided to remove the stored charge. Commutation or flyback current of 0.4 ampere at turnoff is large enough to supply the turnoff current for 100 percent duty cycle, and at 25 percent would be 0.15 ampere, which, when reflected to the secondary, would be 1.95 amperes. The system is designed to operate at no less than 50 percent duty cycle, thus adequate turnoff current is assured.

The drive pulse for Q1 is generated by a 932 gate. The two gates are ac coupled to prevent destruction of Q2 or Q4 due to loss of drive signal.

The storage time of output transistors Q2 and Q4 requires that there be a compensation scheme when full-on to prevent overlap of output transistors with resultant output current spikes and high switching dissipation. A compensation winding on the output transformer supplies a "hold-off" bias such that the drive on the "on-coming" transistor is held off until the current in the "off-going" transistor starts to collapse.

Control Module

The control module provides a centralized control point for supplies that are interrelated and a control interface with the vehicle. Techniques have been incorporated in the control system as a result of previously reported power conditioner and thruster integration tests (References 1 and 2).

The control module contains all of the system timing functions, analog control circuits, and some of the failure control logic. System timing is accomplished by a digital clock consisting of an oscillator, digital counters, and logic gates. Pulses from the digital clock are used to control the off times of various supplies after shutdown due to overloads. Thus function is performed using integrated circuit (IC) flip-flops and gates.

The analog portion of the control module contains IC operational amplifiers and sense amplifiers. Operational amplifiers are used to close three major control loops around the thruster, as shown in Figure 3-11. The first major loop controls engine thrust. Propellant flow (and thus engine thrust) is adjusted by varying the current to the vaporizer. The beam current varies as a function of propellant flow rate. Beam current is sensed in the control module and compared to an external reference signal by a vaporizer control amplifier. The control amplifier gain is such that a 1 percent change in beam current changes the vaporizer current from maximum to minimum.

A second major loop controls the power to the arc. The external reference signal used in the first loop is preconditioned by a function generator, which produces a voltage that has a functional relationship to the beam current as determined by thruster tests. The functionally related reference voltage is compared with arc current by a cathode control amplifier. The amplifier controls the cathode current to hold the arc current constant.

Finally, the neutralizer heater current is controlled by an operational amplifier that senses neutralizer keeper voltage and reduces the neutralizer heater temperature to form the third control loop.

The unit was constructed to be easily modified for greater flexibility in logic and control requirements of the thruster. During integration testing, additional circuitry was added to provide functions necessary for compatible operation of the thruster with a power conditioner. Thruster operation with laboratory type power supplies masks the difficulties found when operating with a power conditioner since laboratory supplies have greater transient capacity than a power conditioner that is optimized for a particular application.

Figure 3-12 shows the construction of the module prior to mounting components. The cards were hardwired to the module via service loops so that they might be easily removed from the card guides holding them in place. The finished cards are shown in Figure 3-13 prior to being wired into the unit. Each epoxy-fiberglass card has a heat sink and a ground plane strip down the center over which the components are mounted. Heat generated by the components is removed through the strips and out to the chassis by clips at each end of the cards.

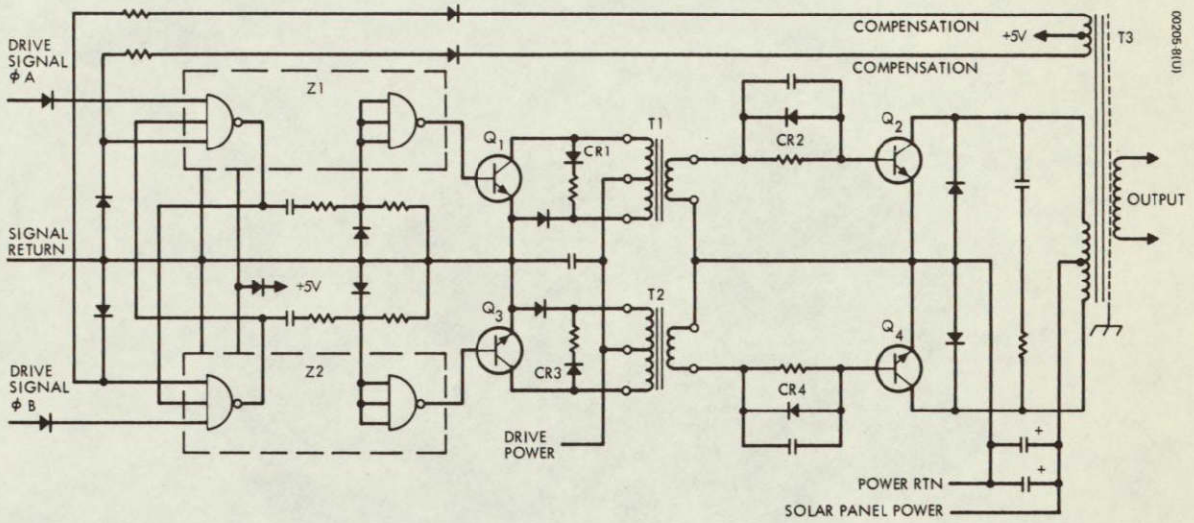

Figure 3-10. Basic Inverter Design

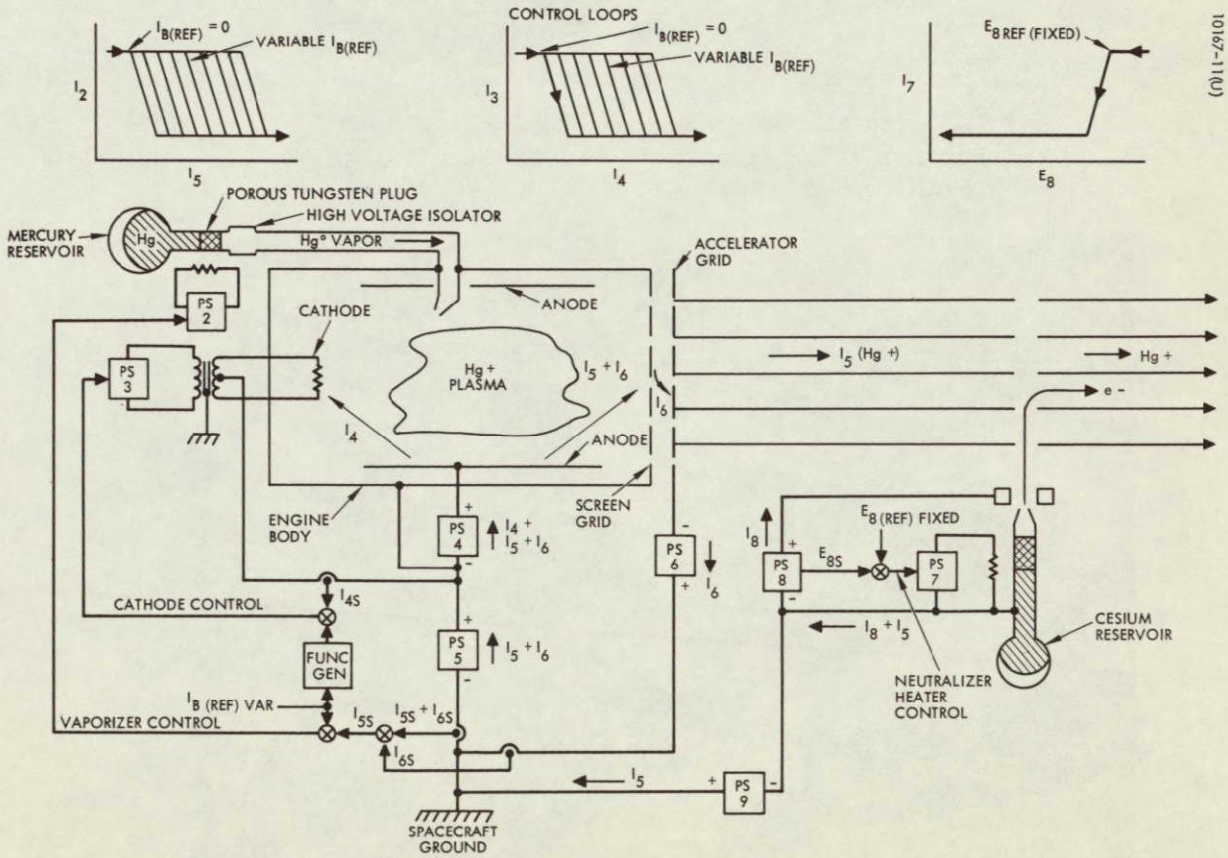

Figure 3-11. Control Block Diagram

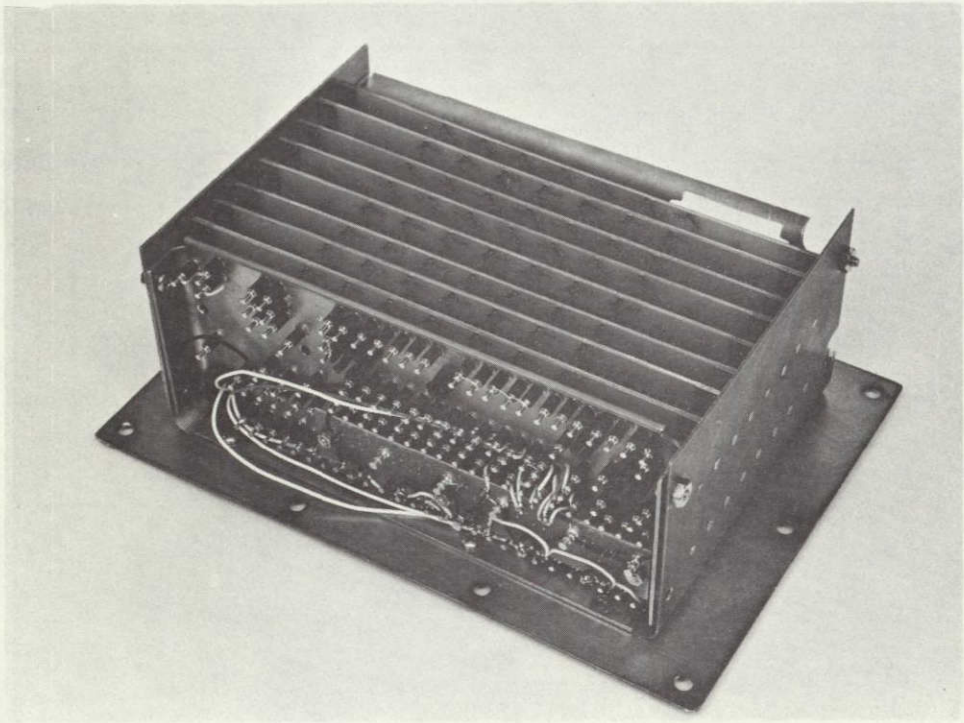

Figure 3-12. Control Module Assembly
(Photo ES 23702)

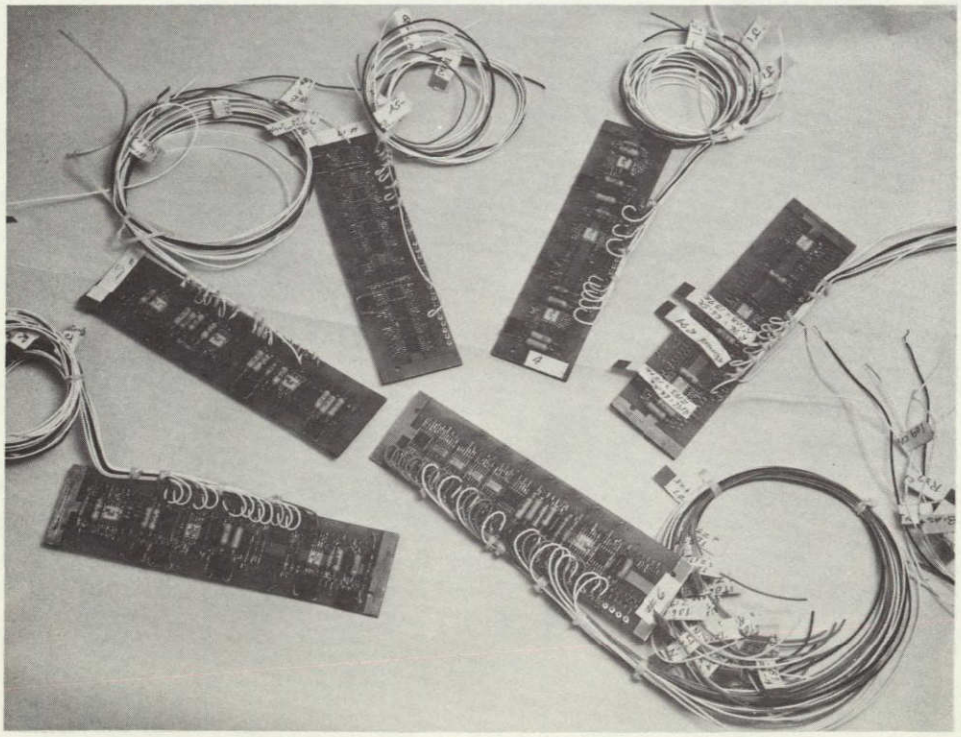

Figure 3-13. Control Module Component Assembly
(Photo ES 23701)

Master Oscillator and Phase Shifter

Largest of the power supplies is the screen, which must provide 1 ampere at 2 kv, efficiently and to within 1 percent for both line and load variations. Since the supply is modularized, it was convenient to modulate each of the eight inverters making up the supply in such a way as to form a 16 phase system. The advantages of doing this are twofold: 1) the input ripple current is considerably lower and 2) the amount of output ripple is decreased by a factor of 16 for a given size of filter.

To provide the 16 phase shifted, pulse width modulated signals, the digital modulator shown in Figure 3-14 was designed. The circuit is basically an analog-to-digital converter in that the pulsewidth is varied only in discrete increments of 1 percent, as will be explained. Also, at the time the slave counter is reset, the digital word difference between the master and slave counter is a representation of the pulse-width. A simplified description of the circuit is presented in the following paragraphs.

The digital staggered phase generator is designed to provide two sets of 10 kHz square waves. Each set consists of eight separate square waves separated by exactly 1/8 of 1/2 cycle. The two sets of staggered square waves are then logically combined to produce 16 modulated pulses that are buffered to provide current drive for the inverter transistors.

The slave channel is a duplicate of the master channel. The slave channel counters are reset at the trailing edge of the pulse width modulator output. The PWM is a standard triangle wave zero crossing. The output of the master channel counter is integrated to obtain the triangle waveform. The ramp compared with the control voltage produces the PWM waveform shown.

By resetting the slave counters at the end of the PWM pulse, the count is effectively delayed by one-half the PWM pulsewidth. By "anding" the two shift register outputs, a delayed pulse equal in width to the PWM pulse is obtained for each phase of the system.

Since the counters change state only on the fall of the clock pulse, the phase difference between the two counters, and hence the shift registers, can only be increments of 1 clock pulse. This determines the accuracy to which the pulse width can be controlled. To achieve 1 percent regulation, the clock rate must be at least 200 times the inverter frequency since each half cycle must be controlled to within 1 percent. Since integer powers of two are available from binary counters, a factor of 256 is used. The oscillator frequency is thus 2.56 MHz.

The 10 kHz staggered square waves are produced by shifting a 10 kHz square wave through a 7 bit shift register at a 160 kHz clock rate. The 160 kHz square wave is given for reference. The 10 kHz waveform is the output from the second 16 bit counter in the master channel. The slave channel is the delayed channel. The outputs from the first 4 bits of the shift register in the master are shown as 2A, 3A, and 4A.

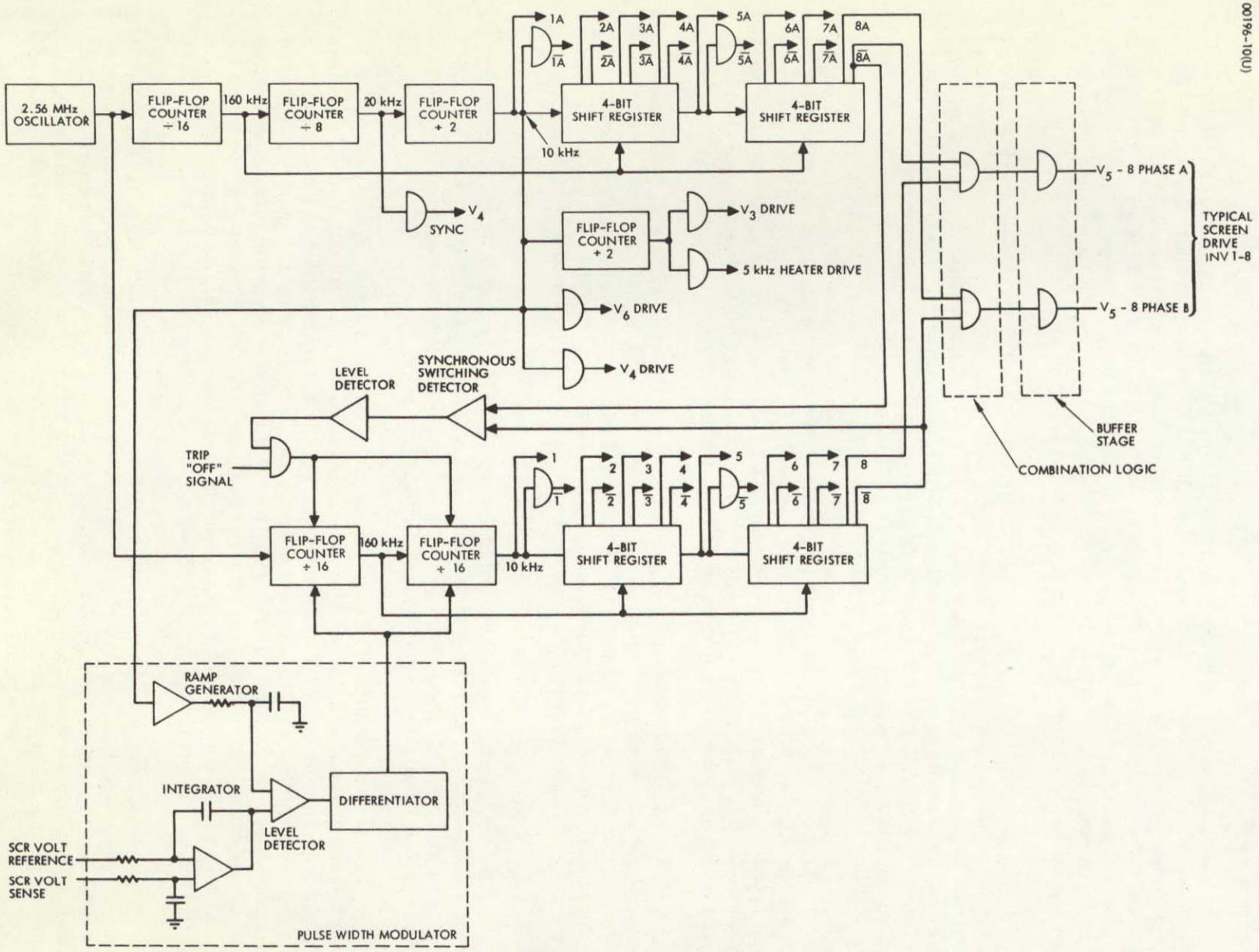

Figure 3-14. Digital Staggered Phase Generator Block Diagram

The square wave outputs of the phase shifter are "anded" on the inputs of the screen inverter buffer gates to produce the controlled pulse-width. The buffers, mounted in the DSPG module, provide isolation from noise transient, introduced on the lines between the module and the screen inverters. They also protect the successive stages of the shift register against catastrophic failures on output lines.

The module was constructed using integrated circuit logic. Figure 3-15 is a photograph of the unit. The cards were mounted to expose the circuits for easy repair.

Several problems were encountered in development of the modulator because the screen supply was required to operate at no-load condition. The minimum pulse width required by manufacturer's specifications for flip-flop reset time determined the minimum pulse width that could be generated by the modulator. The pulse width is enlarged by the storage time of the output transistors and thus caused the output voltage to rise at no-load as a result of filter peaking. The solution was to delay each of the eight output pairs a slightly different amount but always greater than the minimum pulse width generated. This allowed the inverters to be phased on in sequence and provide no-load voltages that were within tolerable levels. It was also found that one manufacturer's ICs allowed the clock pulse to appear at all outputs during the reset pulse, causing false inputs to the shift register. This IC type was not used further.

The master counter output of 10 kHz is divided by two to produce the required 5 kHz for the heater inverter. Other higher frequency outputs are used for the line regulator, arc inverter, and cathode inverter.

PHYSICAL DESCRIPTION

The system is designed for mounting from four edges of the assembly, with one support point in the center of the rear face. The cover is removable from the back without dismounting the assembly, making accessible the components and circuit connections, which are located on the rear face of the individual module plates. The outside dimensions are 36 x 30 x 3.78 inches (see Figure 3-16). The system consists of an assembly of 20 modules, mounted on an "egg-crate" structure. Individual modules are removable from the front after disconnecting them from harness connectors on the rear face. All external connections are made at connectors located at one end of the assembly, with all low voltage connections, in one corner, made with space approved subminiature, rectangular connectors. All high voltage connections are made at the other corner to high voltage standoffs, with screw terminals. These connections are made behind a removable, small connection cover.

The radiating surface of the assembly is electrically "dead" with protruding power transistor studs and nuts covered by epoxy conformal coating. All other components and connections are behind module plates.

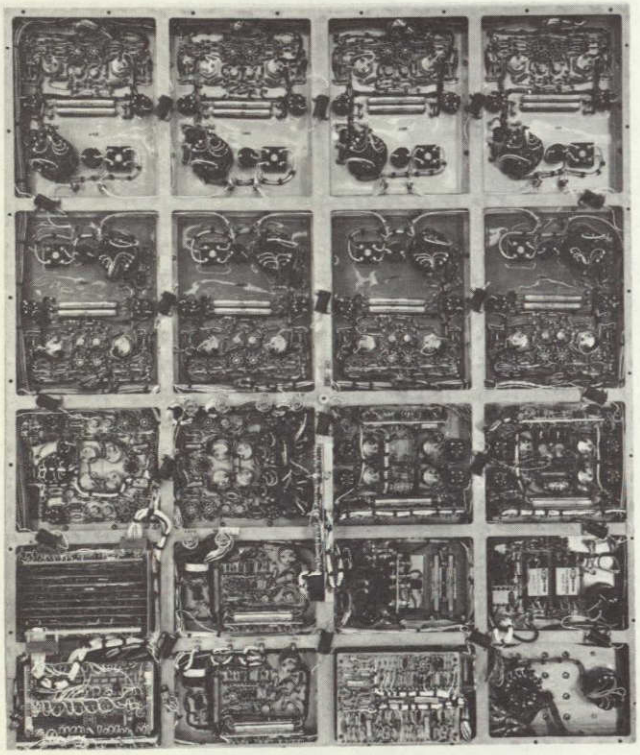

a) Component Side (Photo ES 24250)

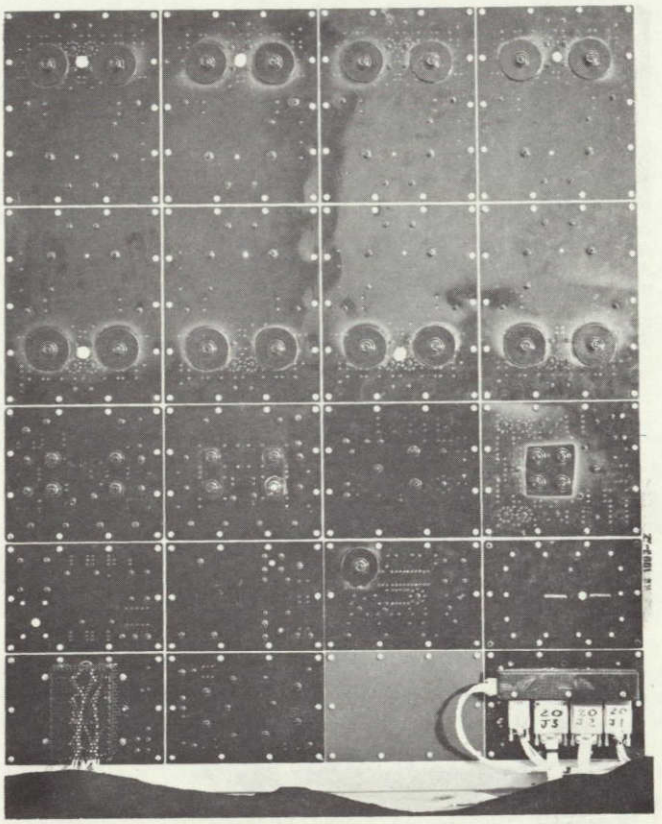

b) Radiating Side (Photo ES 27296)

Figure 3-15. Breadboard

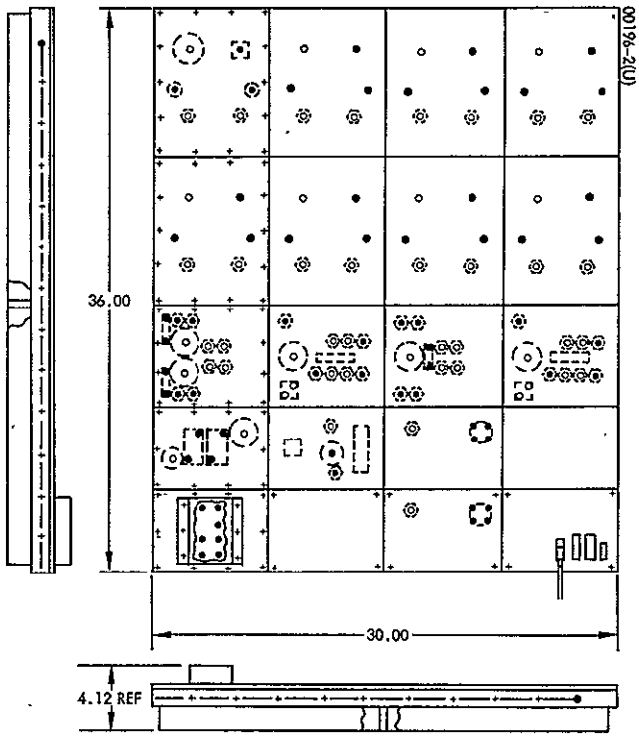

Figure 3-16. Power Conditioner Outline

Thus, the assembly, with its cover, is totally enclosed to provide EMI shielding and freedom from high voltage hazard during testing. The clear front surface, facing space in a vehicle, provides shielding from incident radiation. Since in a typical vehicle installation, the rear of the assembly would be shielded from radiation by the vehicle structure, and other power conditioning assemblies, the back cover is perforated to reduce weight, and permit free outgassing, thereby preventing pressure buildup and transition to regions of voltage breakdown (Paschen's curve). All materials were selected for low outgassing.

The various modules used in the system are sized in frontal area, for a worst case thermal radiation of 0.3 watt per square inch from the front face, assuming radiation from the rear face. This is a conservative assumption, since in a typical vehicle, the vehicle structure to the rear is expected to be at a lower temperature than the power conditioner with some radiation from the rear. At this level of radiation with no solar incidence, a worst case plate temperature of 35°C may be expected, providing high reliability operation of components, which, with few exceptions, are mounted on the module plates. With the design philosophy of low watts/square inch, each module is thermally self-sufficient and will not require conduction to structure and sharing of radiation area between modules. Thus, hot spots are minimized. Since high reliability is obtained by extensive use of redundant, or standby, circuits, the thermal design philosophy has resulted in packaging of redundant circuits on the same module plate with operating circuits, intermixing the components on the plate to obtain uniform thermal density regardless of which circuit is operating.

Support Structure

This supporting frame forms an egg crate structure with a web, or I-beam, running between all modules, and a channel section forming the edges. Holes, located in I-beam webs reduce weight, without significantly reducing the section modulus. In order to provide a flat surface for module mounting, the structure is formed by assembling front and back plates, with module cutouts, with webs interlaced in egg-crate fashion, the whole being dip-brazed. Material is 0.040 inch aluminum, 6061T4, chosen rather than lighter magnesium, to permit dip brazing of thin sections. A riveted magnesium structure of the same strength would be heavier.

A stress analysis has been made of the structure using conservative simplifying assumptions of no contribution to strength from attached module plates, and no reduction of stress due to interlacing of beams. This analysis shows that structure is more than adequate to survive vibration at launch phase. Module mounting screws fit into steel Pem nuts, riveted to the frame, providing a lightweight fastening that will permit frequent replacing of screws without damage to threads. The 240 screws provided will result in significant damping of the structure in vibration, as well as permitting ready replacement of modules during test or service. Riveted Pem nuts are also used along edges of structure for mounting.

Module Assemblies

Screen Inverter

As indicated previously, modules are sized for a thermal radiation of 1/3 watt per square inch. Since the screen inverter will dissipate 21.8 watts for 300 watts out in worst case of one module failed out of eight, or 19.0 watts for normal operation, an area of 70.5 in^2 will result in 0.27 watts/in^2, or 25°C, normally, or 0.31 watts/in^2 maximum, with a maximum operating plate temperature of 35°C. Principal sources of dissipation have been separated in the assembly to minimize local hot spots; i.e., power transistors, output transformer and output rectifiers. The large area available permits mounting all components on base plate, which is 0.050 inch sheet magnesium for low weight, and maximum thermal conductivity per weight.

To obtain good thermal conductivity, yet conservative insulation of components, the area used by small components is convered with a 3 mil sheet of epoxy glass bonded to plate with epoxy adhesive. Thus, the component may be placed against the plate, and when conformally coated with epoxy, will be thermally intimate with the plate, solidly anchored against vibration, and sealed against moisture, with a minimum of weight.

To provide good thermal interface and security from vibration, transformers, transistors, and output rectifiers are bonded with a thin layer of RTV, in addition to mounting screws. Use of RTV for bond will permit ready replacement of a component, if necessary, during tests.

Low voltage connections are made through a subminiature rectangular connector shown at the bottom edge. High voltage connections are made at the top to two standoff screw terminals.

High Voltage Filter

This assembly consists of the screen and accelerator output filters and the bleeder resistors with voltage and current sensing networks. Since the screen output is at +2000 volts, special attention must be given to voltage isolation.

The bleeder resistors are potted in epoxy in a plastic case. The cases therefore provide a convenient mounting for the mica capacitors which are shunted across the bleeder. Cases provide a positive thermal path for losses in the capacitors, which are flat with a good interface, and also provide a secure mounting for vibration. Low voltage components are mounted in the fashion described for the screen inverter. High voltage input and output connections are made at standoff screw terminals, with low voltage connections through a rectangular, subminiature connector. Magnetic components and bleeder resistor assemblies are bonded to chassis for good thermal interface and resistance to vibration.

The loss on this assembly will be approximately 5 watts. Thus, with an area of 38.6 in^2, and 0.135 watts/in^2, temperature will be between 0°C for a free body and 25°C of adjacent modules.

5 kHz Heater Inverter

This assembly is typical of design of inverters with standby circuits, where the operating and standby inverters are packaged on the same plate, making the thermal radiation area available equally to either circuit. In this case, a common output transformer is switched between inverter circuits. With a dissipation of 9 watts expected, and an area of 47.5 in^2, or 0.19 watts/in^2, a plate temperature of 5°C would result for a free body, or close to average system temperature of 20°C when mounted. Mounting of small components, power transistors, and magnetic components is similar to that described for the screen inverter.

Accelerator Inverter

This chassis is similar to the 5 kHz inverter, except for two output transformers and two output rectifiers. High voltage outputs are brought out to two standoff, screw terminals. To share the radiation area equally between the operate and standby conditions, active components are staggered. In a transient mode, at system turnon, dissipation will be 14 watts, whereas steady-state dissipation will be less than 3 watts. At 42.9 in^2, therefore, and 14 watts, or 0.29 watts/in^2, final value temperature would be 35°C, a safe value. However, since transient should not last more than 15 minutes, and thermal time constant will be about one hour, expected rise in 15 minutes is 15/60 x 0.63 x (35 - 0) = 5.5°C rise above assumed 0°C starting conditions, free body. At 3 watts or 0.078 watts/in^2, a final temperature of -50°C would be expected for a free body, or close to the average temperature of the system (about 20°C).

Line Regulator

This assembly is identical in layout for the 5 kHz and accelerator applications. At a loss of 10.5 watts worst case, steady state, for the 5 kHz applications, and an area of 38.6 in^2, or 0.27 watts/in^2, temperature will be 25°C free body, or somewhat higher when mounted in a system with an average temperature of 30°C. Components are mounted with techniques similar to those described above.

Arc Inverter and Cathode Inverter

These inverters are similar in layout, differing in only the few small components associated with output telemetry and feedback. Techniques are similar to those described above for the 5 kHz and accelerator inverters, where radiating area is shared between operating and standby inverters.

Dissipation will be approximately 12 watts for the cathode inverter and 15 watts for the arc inverter. With 47.9 in^2 of radiation, or 0.25 and

0.31 watts/in^2, respectively, free body temperatures would be 20°C and 35°C, respectively.

Arc Rectifier and Filter

This module is a unique case of mounting relatively high dissipation components at high voltage. This applies in particular to the output rectifiers, which dissipate 7 watts while floating, at a potential of 2 kv. To accomplish the firm objective of good thermal conductivity and good insulation, the rectifiers are mounted on an aluminum bracket, which is bonded to an epoxy-glass insulator, in turn bonded to the chassis. By providing a liberal interface area of 3 in^2 between bracket and insulator, a temperature rise across interface of 6°C will result, quite acceptable for the components with a plate temperature of 25°C. The latter results from a total dissipation of 10 watts, with an area of 38.6 in^2, or 0.26 watts/in^2.

The output filter choke is a source of about 3 watts, and is a core directly heat-sunk to chassis with high voltage insulation internally. The filter capacitor is a tantalum type which will dissipate about 1 watt due to high-frequency ripple losses. It is mounted in a fashion similar to that used for rectifiers. A 1/2 inch creepage path is maintained between high voltage elements and chassis, a desirable minimum to prevent flash-over. Except as noted, other techniques are similar to those described before.

Magnetic Modulator

This is an assembly of magnetically regulated supplies; i.e., vaporizer, neutralizer keeper, and magnet supplies. The only supply at high voltage is the magnet with its output at a reference of +2 kv. Estimated total dissipation is 4.8 watts, with a radiation area of 39.5 in^2, or 0.12 watts/in^2, thus an expected plate temperature of 10°C, free body, or closed to average temperature of 20°C mounted. The mounting area required by components is the limit in this case, rather than temperature. All magnetic components, the principal source of dissipation, are mounted on chassis, with small components mounted on a plate above the magnetics, with a thermal path to base plate through corner posts.

The components requiring high voltage insulation are the output diodes of the magnet supply. Using a technique similar to that described before for the arc rectifier, these diodes are heat-sunk to a small, magnesium plate, which is bonded to a 0.032 inch epoxy-glass insulator, in turn bonded to a supporting magnesium bracket, which conducts heat to main plate (approximately 1 watt). A 1/2 inch creepage path is provided between the diode heat sink and the bracket, across the epoxy-glass. A thin, 0.002 inch, H film layer insulates the diodes from the heat sink and, thus, from each other. The bracket also carries the high voltage, screw terminal standoffs for the magnet output.

Techniques for mounting magnetics and small, low voltage components are similar to those described for other assemblies.

Control Module

This module is an assembly of low power components, both discrete and microcircuit. Nevertheless, all components are mounted to heat sinks, with defined conductive paths to the base plate radiator. Total power dissipated is estimated at approximately 5 watts maximum, thus the temperature of the assembly will be controlled primarily by heat conduction from adjacent modules, and should be close to the average temperature of the system; i. e., about 20°C.

Discrete components are mounted on a 1/32 inch epoxy-glass terminal board, bonded to a magnesium heat sink. All components will rest on the terminal board and will be conformally coated with low outgassing epoxy to improve heat transfer, seal against moisture, and secure against vibration during launch. Microcircuits used here will be of the flat pack type, and will be mounted on a printed circuit board with an etched copper heat sink for a good thermal path to the main heat sink.

Low Voltage Connection Module

This module holds all low voltage connectors interfacing with vehicle connectors; i. e., control and telemetry, low voltage loads, and input power. Connectors are all of the subminiature rectangular type, rated at 5 amperes contact. All internal connections will be made at the rear of the assembly and all external connections on the front face. Each connector used is a different size from adjacent connectors, to prevent interchange of connectors. Harness connectors are provided with side access covers for maximum convenience in routing vehicle harness from the edge of the assembly.

High Voltage Connection Module

This module mounts all high voltage connections to vehicle harness. Connections used are high voltage standoff, screw terminal type for minimum weight compatible with high voltage insulation. A protective cover will be provided for personnel protection during tests.

Miscellaneous Considerations

Thermal

System thermal design philosophy was discussed above, and detail thermal design was discussed under each module discussion. For overall assummations Figure 3-1 gives heat loads for each module, watts/in^2, and expected temperatures. Although not indicated in the drawings, an array of power resistors will be arranged throughout the frame, to be powered from vehicle control to preheat assembly to -20°C before starting the system, and to ensure a minimum temperature of -40°C at any time.

Choice of Materials

Two criteria have been used in selection of materials, over and above the usual criteria of strength, insulation, etc. These are: 1) low outgassing, and 2) compatibility with Freon to be used in calorimeter test. Choice of materials for the first criterion are based on extensive data collected by Hughes Materials Laboratory. Choice of materials for the second criterion has been made on the basis of tests for 24 hours immersion in Freon at 45 °C (expected operating temperature) and previous experience with surveyor batteries in Freon calorimeters. These tests indicate that RTV is incompatible, hence must be sealed with epoxy (only hairline joints must be sealed). Nylon, adhesive mylar film, teflon, and epoxy have been verified as compatible insulations.

WEIGHT ANALYSIS

The final weight of the breadboard was 39. 11 pounds. The weight goal of 23. 51 pounds was based on a very much simplified system with no line regulation required for the screen, accelerator, arc, and vaporizer supplies. There was no load regulation required for the magnet, vaporizer, cathode, and neutralizer heater supplies. The system proposed did not contain the separate arc and accelerator supplies that eventually were necessary to satisfy requirements that changed as the knowledge of thruster operational characteristics grew. It should also be noted that, although the unit was fabricated as a prototype for the experimental units, the effort to hold weight down was at best minimized while the effort to satisfy the electrical requirements was maximized.

From the breadboard weights, a reduction study was made to attain the overall weight goal of 28 pounds, which was raised as the unit complexity grew. Breadboard unit weights are totalized in Table 3-1, showing the contribution of each module and other support members. A comparison of the breadboard weight and experimental units actually fabricated is difficult since the types of thrusters for which they were designed are different. The comparison is made wherever possible in Table 3-1. The experimental weight will be discussed in detail later.

EFFICIENCY

Reference 2 presents a good definition of the various efficiencies usable for power conditioners. They are repeated below:

1) Thermal efficiency is based on heat dissipation: the ratio of PC output power to output power plus dissipation. In principle, the dissipation can be accurately measured in a calorimeter. The use of output power in both numerator and denominator reduces the effect of output power measurement errors.

TABLE 3-1. SUMMARY OF BREADBOARD UNIT WEIGHTS

Item	No.	Unit	Unit Weight	Total Weight Pounds	EX-1	Reduction	Increase
1	8	Screen inverters	1.505	12.04	10.00	2.04	
2	1	Accel. inverter	1.98	1.98	0.65	0.33	
3	1	5 kc inverter	1.30	1.30	1.02	0.28	
4	1	Cathode inverter	2.00	2.00	—	—	
5	1	Arc inverter	1.67	1.67	1.54	0.13	
6	1	Arc rectifier filter	1.26	1.26	—	—	
7	1	High voltage filter	1.11	1.11	1.25	—	0.14
8	1	High voltage module	1.28	1.28	—		
9	1	Magnetic modulator	2.06	2.06	—		
10	1	Control Module	1.53	1.53	1.07	0.46	
11	1	Master oscillator and phase shift	1.10	1.10	0.71	0.39	
12	2	Line regulators	0.75	1.50	1.34	0.16	
13	1	Limited use PS assembly	0.50	0.50	0.24	0.26	
14	1	Low voltage modulator plate and connector assembly	0.30	0.30	—		
15	25	Harness connectors	6 grm	0.33	—		
16		Connector solder	70 grm	0.15	—		
17	1	Frame	3.74	3.74	2.72	1.02	
18	240	Screws and washers	0.84 grm	0.45	0.23	0.22	
19	1	Cover and screws	1.85	1.85	1.93	—	0.08
20		Shielded wire, 8 cond.		0.88	—		
21		Power wire, dual 20 gauge		1.05	—		
22		Miscellaneous wire, 24 gauge		1.03	—		
23		Heaters, wiring, thermostat, additional 5 thermistors and wiring		(0.69)	—		
				39.11			

2. Average volt-ampere efficiency is based on the ratio of average power out to average power in. In this case, the "average" is based on average reading dc meters for dc input and output and on rms meters for ac outputs. If the ac component (ripple) imposed on the dc values is reasonably small, and if the ripple current and voltage are in phase (nonreactive), this average E-I efficiency is identical with that in type 1.

3) Effective volt-ampere unit efficiency is based on the maximum required input volt-amperes, including ripple and average output power. This definition results from the fact that the power source must supply peak power, up to certain frequency limits, while thrust depends only upon average power. The difference between this efficiency and type 2 depends upon the input ripple frequency and the power source (solar array) frequency response characteristics. In addition, the solar array response depends upon power loading. Near the maximum power point, ripple below about 50 kHz will affect the array. Thus, the "maximum required input" is the power the solar array must supply, including the amount of ripple to which the array responds.

4) Effective volt-ampere overall efficiency is an extension of type 3 to include power dissipation in cabling and connections. In total system analyses, particularly mission calculations and solar array sizing, a single efficiency (from array output to thruster input) is generally used. This value must obviously include any significant losses. Later in this section, cabling will be discussed to indicate that a 1 to 2 percent power loss can be expected.

The calculated thermal efficiency is 92 percent, while the indicated average volt-ampere efficiency is approximately 86 percent. A summary of the breadboard efficiency calculation is given in Appendix A and Table 3-2. Several factors contribute to the discrepancy between calculated and measured results, but some of the following must remain as speculation until detailed tests and analysis verify that they are correct. The transistor switching speed used for calculation purposes was 0.5 microsecond, while the average unit was greater than 1.0 microsecond in turnoff time. The switching envelope is inductive while the assumed switching envelope was assumed to be resistive. The transistors (Solitron SDT8805) did not fall into hard saturation as assumed in the analysis. There are possible losses associated with series connection of inverters that are not accounted for in the calculations. Losses in the transformer copper may be higher than calculated due to skin effects at 10 kHz.

Due to transistor performance, the transistors were purchased from another manufacturer for the experimental systems. Comparative results from breadboard tests indicate an improvement of 3 to 4 percent in system efficiency with the new faster transistors. The results of efficiency testing using a calorimeter will be discussed in the experimental system efficiency section. These tests did confirm an improvement in the order of that

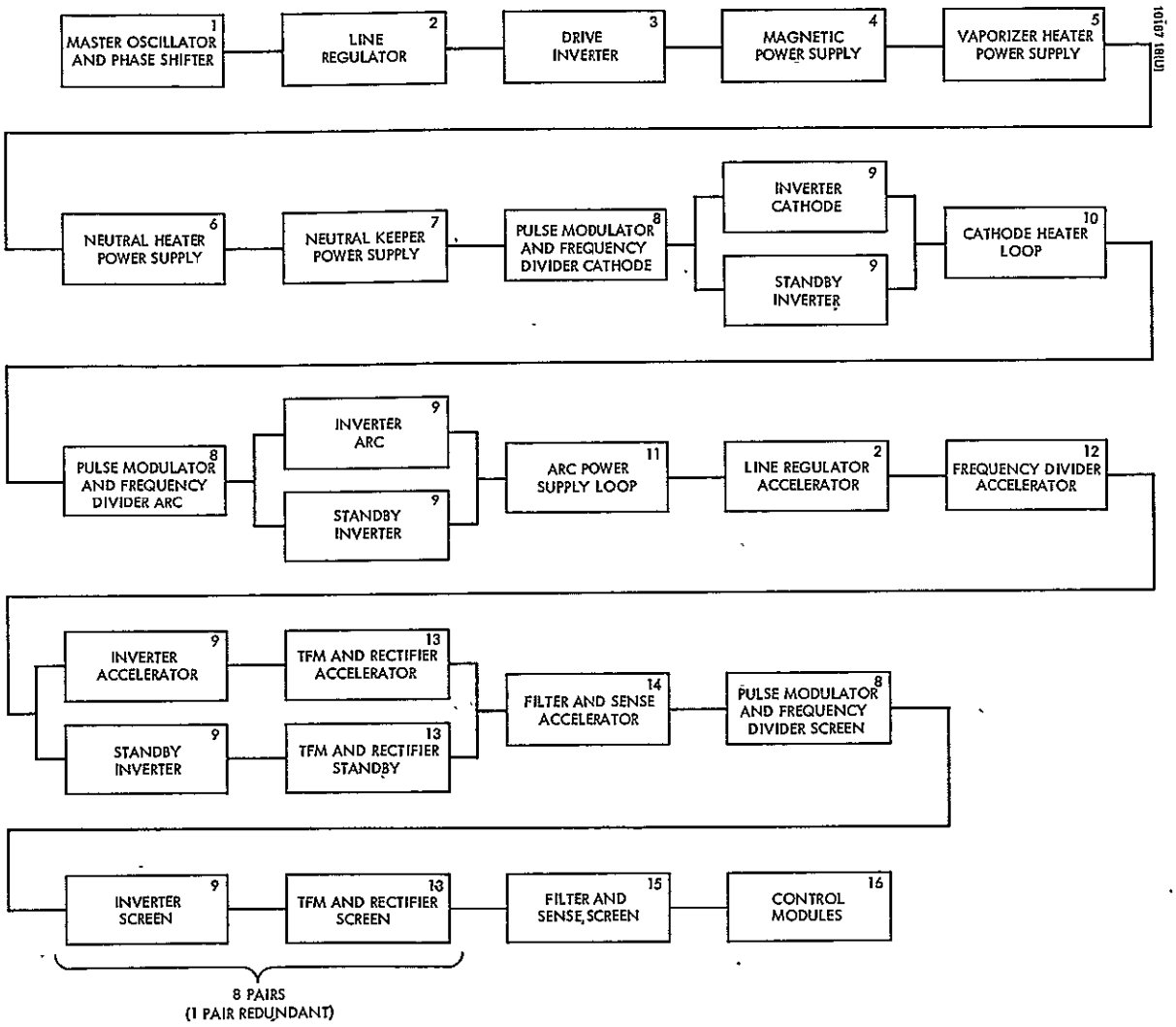

Figure 3-17. Reliability Block Diagram

TABLE 3-2. CALCULATED EFFICIENCY SUMMARY

Item	Power Out, watts	System Power, percent	#/kW	Losses, watts	Total Loss, percent	Efficiency
Screen supply	2000	77	6.72	150	67	93
Arc supply	280	10.9	12.00	30	13.4	90
Accelerator supply	20	0.8	90.00	6	2.7	77
Cathode supply	200	7.7	12.00	13	5.7	94
Low voltage supplies	92	3.6	40.00	20	9.0	82
Total power circuits	2592	100	9.50	219	97.8	92
Digital control	---	---	---	3	1.3	--
Analog control	---	---	---	2	0.9	--
Total system	2592	100	10.80[2]	224	100	92
Screen supply	2000	77	6.72	150	67	93
All other supplies and controls	592	23	24.5	74	33	89

mentioned above. This is one area in the design of the electric thruster power conditioning that requires additional study.

RELIABILITY

Reliability Analysis

$R_M^{(t)}$, mission reliability, calculated to be 0.9458, where $R_M^{(t)} = \pi R_i$ and mission time is 10,000 hours. The reliability block diagram (Figure 3-17) displays the complete system with all involved subsystems or units. The reliability for each of the units was determined by the relationship $R = e^{-\lambda t}$, except for those units where redundancy practices were followed (these math models are noted below). The set of failure rates utilized for the analysis

effort were developed by utilization of Hughes Document R22-100DC. After determination, the subsystem failure rates were then modified by use of an E-factor, the Hughes experience factor. The set of utilized failure rates and a rationale justifying use of these failure rates together with the E factor are attached. The resultant failure rate (λ) of each unit, modified by the E factor (0.6). The experience factor has changed to 0.475 and the failure rates have dropped since this analysis was performed. The resultant calculated reliability would be somewhat higher.

Cathode and Arc Inverters

The reliability for the cathode, arc, and accelerator inverters was determined by the formula

$$R_S = R_{ON}\ 1 + \frac{\lambda_{ON}}{\lambda_{OFF}}\ (1 - R_{OFF})$$

Screen Inverters

For the purpose of this analysis, the overall mission time of $(10)^4$ hours was broken into three intervals:

Interval	Time, hours
1	0 to 2,500
2	2,500 to 5,000
3	5,000 to 10,000

At the start of flight, seven (of the eight active) inverters are required. At the end of each interval, the requirement drops as follows:

Interval	Inverters Required at End of Interval
1	7
2	6
3	5

The reliability probability of meeting these requirements for each interval was determined from the formula:

$$R_{Redund} = \sum_{i=c}^{n} \binom{n}{i} R_{10}^{i}\ (1 - R_{10})^{n-i}$$

where

n = operating inverters

c = inverters required at end of each interval

$R_{10} = e^{-\lambda 10t}$, λ = failure rate

t = interval time

The redundant screen inverter reliability calculated to >0.999. Since the entire power conditioner will be inoperative if one of the output transformers of the accelerator and the screen inverters fails in failure mode short to ground, and since each transformer is exposed to seven failure modes, a failure rate of 3×10^{-9}) has been placed in series with the other elements for each of those transformers.

Where those transformers are part of the redundant or standby circuitry, the failure rate has been accordingly modified from $20 \times ^{-9}$ to 17×10^{-9} hours, to account for the 6/7 of total failure modes inside the redundant portion of the circuit.

External Environment

The space environment to be encountered by the system in flight is considered to be gentler than that experienced by the presently operating Hughes space synchronous satellites. The only large consideration is exposure to radiation from the Van Allen belt. The effect is judged to be very minor for the subject system, whereas the Hughes synchronous satellites see the radiation for several days while in transfer orbits. Even though this system could encounter solar flares in flight, these are not considered as potentially harmful as the Van Allen belt radiation.

Part Selection

The component parts used in the subject system are high reliability parts selected from a JPL preferred Parts List. The specifications for these parts have extensive and stringent reliability proof test requirements, which appear satisfactory to assure procurement of high reliability parts for the program.

The reliability proof tests include among others: 1) qualification tests, such as soaking at temperature extremes, humidity, shock, hermetic seal plus a high temperature test to demonstrate with 60 percent assurance that a tested lot's failure rate is less than 1 percent per 1000 hours and 2) quality assurance tests, such as life stability, environmental plus final visual and electrical tests.

Conclusions

The computed reliability of 0.9458 for 10,000 hours is somewhat lower than the design objective of 0.96 and significantly lower than the proposal estimate of 0.9826.

The significant drop from the proposal estimate is substantially due to increased complexity resulting from much tighter regulation requirements introduced by JPL during negotiation phase, for screen and accelerator supplies (no line regulation originally required, and 5 to 10 percent load regulation required, respectively; now ±1.0 percent for line and load). A small drop in reliability is due to somewhat higher temperature stresses than originally assumed in analysis for purposes of simplified analysis.

The calculation results presented represent the effect of failure rates available in 1968. Since that time, a very large amount of component hours has been compiled and failure rates in 1970 reflect that experience. This is true since no matter what failure rate was chosen for a component, the rate will asymptotically approach the true failure rate as the number of component hours increases. This assumes that the original failure rate was chosen higher than true failure rates.

Rationale for Use of Selected Failure Rates

The component part failure rates utilized for the program are based on failure rates taken from the high reliability Minuteman ballistic missile program, somewhat modified by Hughes, using engineering judgment. These failure rates (detailed in Hughes Document R22-100DC) were originally set up for the Hughes space satellite systems. They are utilized for this program as basic rates, modified as necessary to allow for the estimated environmental stresses (temperature, electrical, etc.) that the system is expected to encounter in flight. These basic failure rates are then adjusted as a set by the Hughes experience factor (E-factor) described below. Failure rates are shown in Tables 3-3 and 3-4.

E-Factor Usage

It is Hughes practice to modify the basic set of failure rates by a prediction factor

$$E = \frac{k}{\Sigma \lambda i t i} = \frac{\text{Observed failures}}{\text{Expected failures}}$$

based on flight experience of Hughes Satellite Systems (Syncom II, Syncom III, HS-303, Intelsat II, F-2, Intelsat II, F-3 and ATS, F-1). Multiplication of the basic set of failure rates by the E-factor in effect will correct any optimistic or pessimistic bias in the basic rates. This utilization of the E-factor, when significant differences between the flight experience rates and the basic rates are observed, will cause the basic failure rates to

TABLE 3-3. FAILURE RATES FOR POWER CONDITIONER

Part Type	Failure Rate x 10^{-9} hours	
	Active	Dormant
Diode, Switching and General Purpose	2.4	1.0
Zener	24.0	2.0
Power	60.0	6.0
Transistor, Switching	6.0	1.0
General Purpose	12.0	1.0
Power	120.0	10.0
Integrated Circuits, DTL (932, 946, 948, etc.)	20.0	5.0
μA709	84.0	
Resistor, Carbon Composition (RC)	1.7	0.1
Metal Film (RN60)	2.4	0.02
Power (RW)	6.0	0.01
Capacitor, Ceramic, etc.	5.0	0.02
Tantalum	24.0	1.0
Magnetics, Transformer, Choke	20.0	0.5
Magnetic Amplifier	30.0	
Relay	100.0	

converge to true values. The technique is asymptotically unbiased regardless of the validity of the originally assumed basic failure rates. The data from the Hughes space satellites are considered applicable to the subject program as the mission environments are similar and long time service and essentially free-fall operation are also involved here. The Hughes satellites to date have accumulated over 400 million operational component hours and over 250 million component hours in the dormant stage. The current value of the E-factor is 0.6.

Internal Temperature

Based on design considerations and calculations, which were confirmed by experimental tests in a vacuum chamber, the component mounting base plate temperature will be at +38 °C and the junction temperature of semiconductors at +50 °C ±5 °C. The utilized failure rates were subjected

TABLE 3-4. COMPONENT FAILURE RATES

No.	Title	Failure Rate, $X10^{-9}$ Hr		Reliability	Number of Units	Total Failure Rate	Total Reliability
R1	Master Oscillator and Phase	584 10		0 9942	1	584.10	0.9942
R2	Line Regulator	464.50		0 9954	2	929.00	0.9907
R3	Drive Inverter	514.14		0.9949	1	514.14	0.9949
R4	Magnetic Power Supply	98.10		0.9990	1	98.10	0 9990
R5	Vaporizer Heater Power Supply	108.24		0.9989	1	108.24	0 9989
R6	Neut. Heater Power Supply	128.38		0.9987	1	128 28	0.9987
R7	Neut. Keeper Power Supply	234.36		0 9977	1	234.36	0.9977
R8	Pulse Mod. and Frequency Divider	74.5		0.9993	6	447.00	0.9955
R10	Cathode Heater Loop	290.16		0.9971	1	290.16	0.9971
R11	Arc Power Supply Loop	463.02		0.9954	1	463.02	0.9954
R12	Frequency Divider, Accelerometer	12 00		0 9999	1	12.00	0.9999
R14	Arc Power Supply System Loop	164.04.		0.9984	1	164.04	0.9984
R15	Filter and Sensor Screen	63.24		0.9994	1	63.24	0.9994
R16	Control Modules	1497 54		0 9851	1	1497.54	0.9851
		$\lambda_{ON(X10^{-9})}$	$\lambda_{OFF(X10^{-9})}$				
R9	Inverter	191 40	20.33				
R13	TFM and Rect:						
	Accelerometer	127.44	26.82				
	Screen	81.36	76.20				

Single Units Total Failure Rate	5533.22
Circuits with active redundant unit: Screen Inverter	
Equivalent Failure Rate <	10.00
Circuits with dormant standby unit:	
Cathode, Arc and Accelerometer Inverters	
Equivalent Failure Rate < 10 each	
Total <	30.00
Total Failure Rate	5573 22 $X10^{-9}$ Hours
Reliability = 0.9458	

to (and modified by) derating curves in the aforementioned Hughes Document R22-100DC. In order to assure stability of these temperatures, the system is designed so that the solar panels will always face the sun, while the power unit is always facing away from the sun.

Breadboard Integration Testing

During normal operation of an ion thruster, it is common for arcs or temporary shorts to occur. The energy stored in the screen power supply filter capacitor is dumped into the short, producing current pulses greater than 300 amperes. As expected, very large electromagnetic pulses were generated throughout the system, which produced voltage spikes on all unprotected lines including returns. After taking normal precautions with all power lines, transients of 15 volts were seen on 5 volt logic buses. Additional L-C filtering was added in the control module to reduce these transients to levels felt to be safe. These filters were added directly to each card to distribute the filter and thus increase its effectivity while holding down the size.

The grounding system used prior to thruster integration tied the high voltage return to the signal return at the power conditioner so that telemetry signals generated in the high voltage filter would be referenced to signal return. The high current pulses generated during thruster arcs caused large voltage transients in the power conditioner ground line and raised the power conditioner above ground to voltages in excess of 200 volts. To eliminate this problem, all screen and accelerator telemetry amplifiers were reconnected to differentially sense the telemetry signals. One additional amplifier was added for accelerator current which previously did not require buffering. This change allowed the screen and accelerator return line to be connected to the thruster test vacuum tank. The ground transients dropped to below 30 volts.

The noise caused by arcing disturbed the digital circuits, forcing addition of capacitors on clock and reset lines. The type of circuits were sensitive to fast transients, but were used because of packaging constraints. At the time the system was designed, only dual TTL flip-flops were available in a single flat package. It would have been more desirable to use the slower DTL dual flip-flops which are now available. It was found that binary counters are much too noise-sensitive for this system environment because of their high speed. Recently, digital circuits have been developed which are designed for high noise environments and have noise margins exceeding 10 volts, but are not packaged in materials suitable for high vacuum application. The desirability of this type of circuit is obvious from the noise viewpoint, but another, less obvious, advantage is its operation from a voltage close to that used by IC operational amplifiers.

After filtering was added and during a subsequent 500 hour continuous operation life test during which over 10,000 engine arcs occurred, no loss of ICs or circuit malfunctions took place.

Circuit modifications required to permit a recovery from overloads such as arcing which did not exceed the power conditioning capabilities was added. A delay in turn-on of the vaporizer was added to prevent excess mercury in the thruster upon restart which causes high surge currents in the beam current upon turn-on. If the surge currents exceeds the trip level, the supply will continue to recycle while the condition worsens without the delay.

4. BREADBOARD MODIFICATION

SYSTEM DESCRIPTION

The breadboard system, described in the previous section, was modified to provide power to a 20 cm hollow cathode electric thruster. The general system specifications were revised to reflect this change by increasing the weight allowance to 30 pounds. The detailed specifications, as given in Table 3-1, contain the requirements for the additional supplies and the changes in the cathode supply. The ground rules used for the modifications were that no physical or electrical changes would be made unless they were required to meet the electrical specification. Weight, efficiency, and reliability were not specifically considered except in those cases where the supply would be used directly in the experimental systems.

The system block diagram is shown in Figure 4-1 and the module positions in the system are shown in Figure 4-2. The modules modified were the arc inverter, control module, line regulator, 5 kHz inverter, and accelerator inverter. The changes in these modules were required basically to accommodate higher power delivered by the arc supply which raised the lower limit of input line voltage from 40 to 53 volts. The line regulator, 5 kHz inverter, and accelerator inverter changed as a direct result of this increase to test the changes prior to their incorporation into the experimental models. The details of the changes will be described in the modified breadboard electrical description. The arc inverter was modified to convert the supply to a constant current source. Control module changes were required to add a third control loop shown as the arc voltage-cathode vaporizer loop in Figure 4-3. A new module was fabricated to house the three cathode supplies.

The physical construction did not significantly change and thus the description given in Section 3 will suffice. The cathode modulator was fabricated using the techniques employed for the magnetic modulator shown in Figure 4-4. Photographs of all modules used in the experimental systems will be presented in the subsection describing the physical layout of those units.

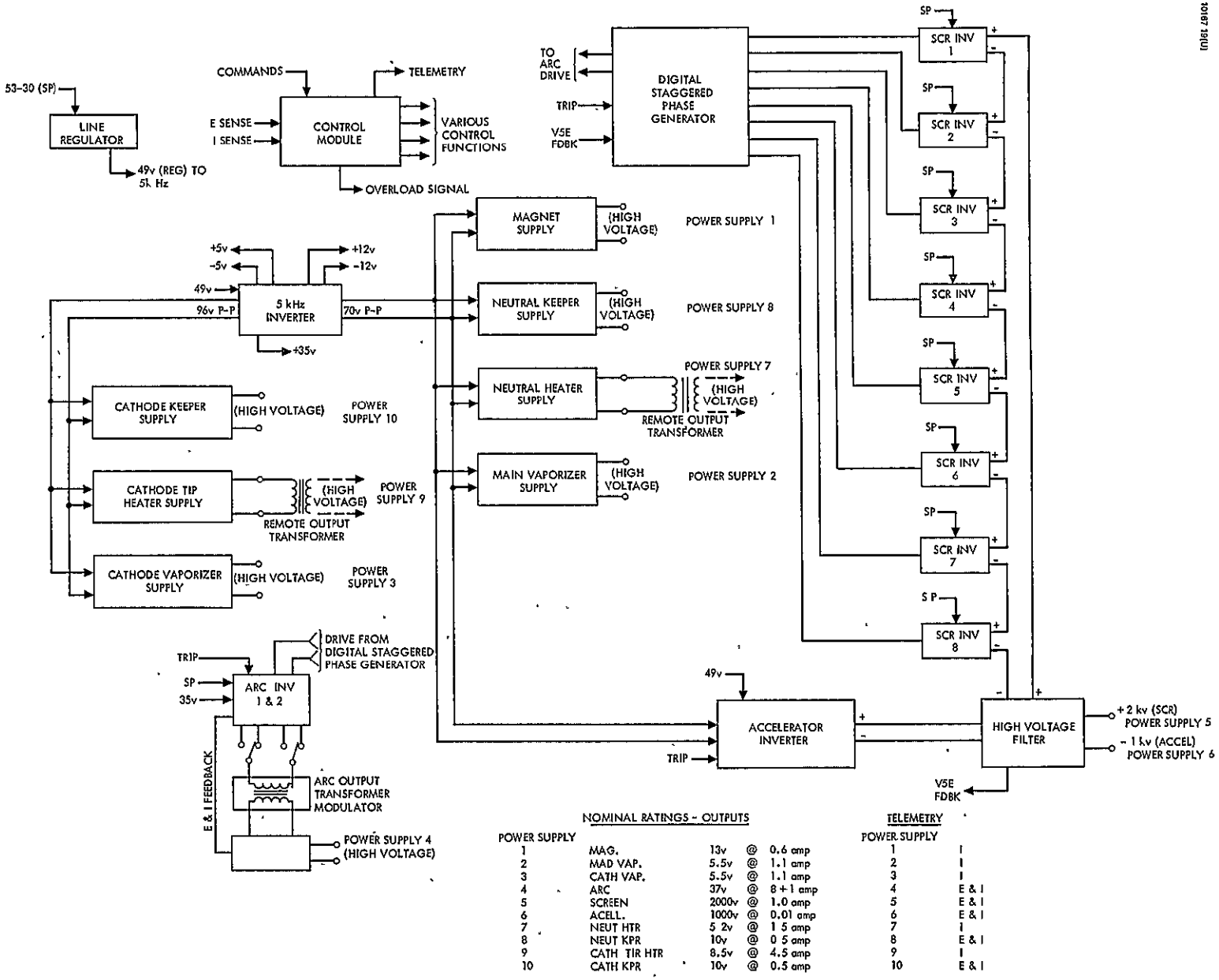

NOMINAL RATINGS - OUTPUTS

POWER SUPPLY					TELEMETRY POWER SUPPLY	
1	MAG.	13v	@	0.6 amp	1	I
2	MAD VAP.	5.5v	@	1.1 amp	2	I
3	CATH VAP.	5.5v	@	1.1 amp	3	I
4	ARC	37v	@	8 + 1 amp	4	E & I
5	SCREEN	2000v	@	1.0 amp	5	E & I
6	ACELL.	1000v	@	0.01 amp	6	E & I
7	NEUT HTR	5 2v	@	1 5 amp	7	I
8	NEUT KPR	10v	@	0 5 amp	8	E & I
9	CATH TIR HTR	8.5v	@	4.5 amp	9	I
10	CATH KPR	10v	@	0.5 amp	10	E & I

Figure 4-1. Functional Block Diagram

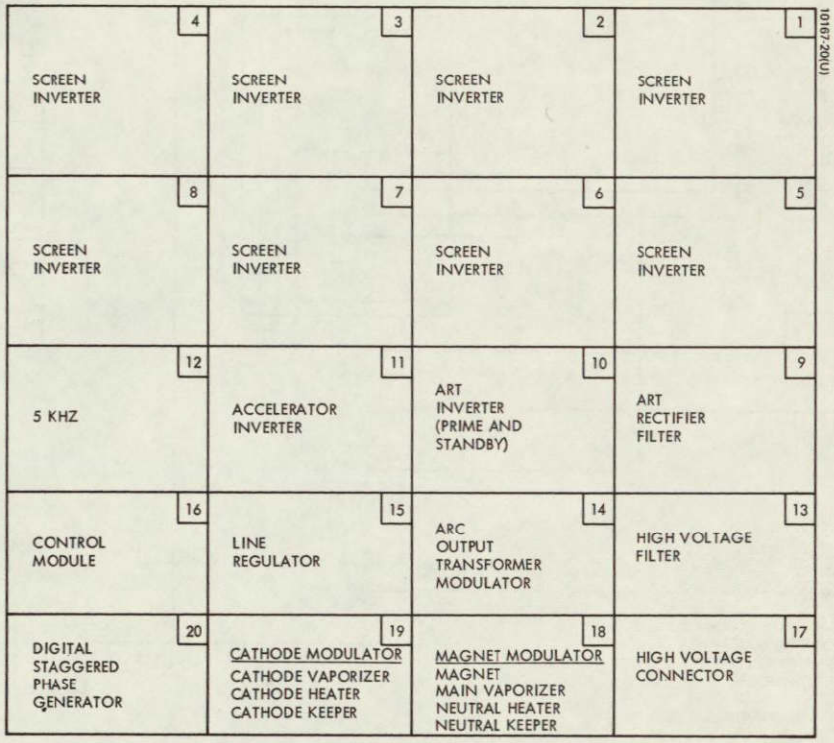

Figure 4-2. Backside View of BB-1/M-1 System Layout

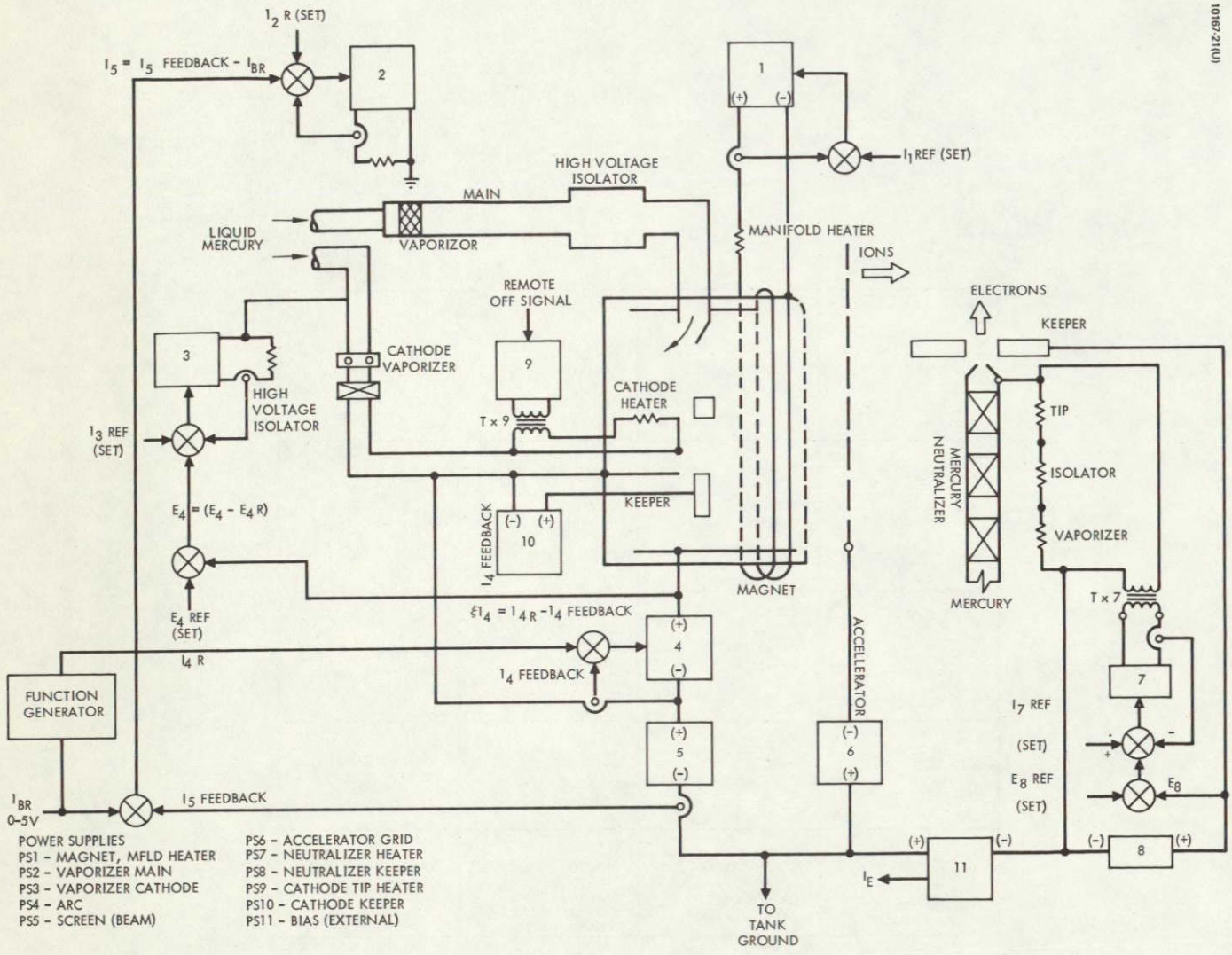

Figure 4-3. 20 cm Thruster Hollow Cathode PC Control Loop

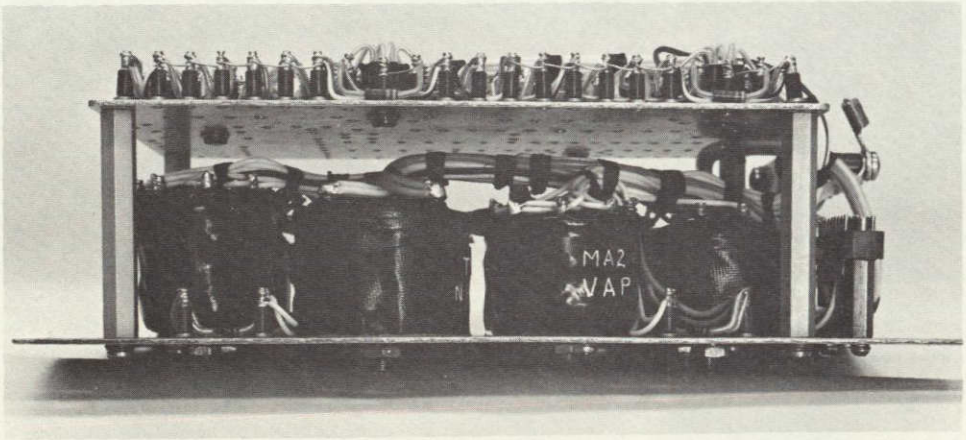

Figure 4-4. Mag-Modulator
(Photo ES 23712)

ELECTRICAL DESCRIPTION

With the increase in line voltage minimum to 53 volts, a number of changes resulted. The line regulator output voltage was raised to decrease the load current caused by increased power delivered by the 5 kHz inverter. As a result, a source for 35 volts used for base drive in all the other inverters was added to the 5 kHz inverter. The old magnetic modulator and accelerator still require 70 volts rms square wave for operation, so taps were added to the 5 kHz inverter output transformer while the cathode modulator obtains its drive directly from the collector-to-collector voltage. Some additional filtering was added in the 5 kHz inverter low voltage supplies. The accelerator output transformer was redesigned to operate at 49 volts input and 1 kv output. The arc supply output transformer and filter were modified to the new requirements.

The test console loads are being modified in a fashion similar to the test console No. 1.

The physical layout of the modules in the frame is shown in Figure 4-2. The arc rectifier filter has been moved to the position previously occupied by the cathode inverter. The arc output transformer is mounted in the space where the arc rectifier filter was and the cathode modulator replaces the accelerator line regulator. This arrangement physically locates the arc output transformer close to the inverter and rectifier filter module.

Arc Supply (PS-4)

The inverter was modified to provide current limit by the addition of an amplifier that overrides the voltage regulator circuitry when the preset current is exceeded. The amplifier is connected to the anode of the reference zener (negative reference voltage) which sets the output voltage. As the output current, as sensed in the rectifier-filter module, reaches the control signal, the amplifier starts to raise the reference signal toward zero, thus reducing the pulse width which holds the current constant for varying load resistance.

The amplifier gain was chosen to hold the output current to within 1 percent of full scale. The control signals were preset to 2.0 ± 0.09 amperes at 0 volts and 9.0 ± 0.09 amperes at + 5 volts in. The Figure 4-5 gives load regulation curves for various input command voltages.

The rectifier-filter module was rebuilt to handle the higher current by changing the diodes to 20 ampere units and adding a new choke. The output transformer was also redesigned to take advantage of the higher input line voltages. By decreasing the turns ratio, the pulse width can be increased at low line and thus reduce the switching losses.

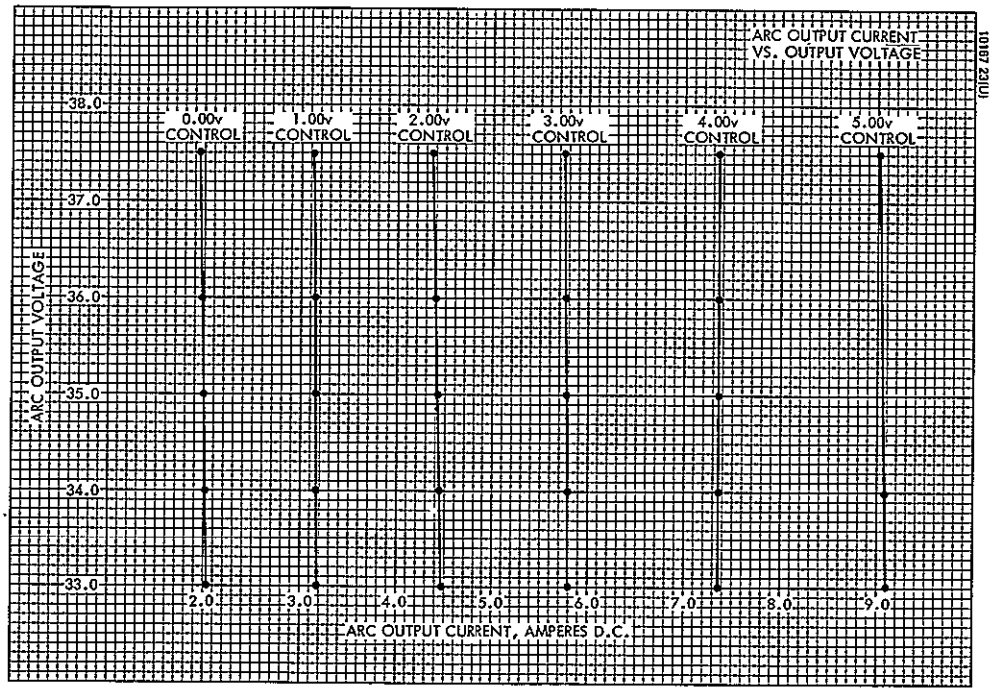

Figure 4-5. Arc Output Current Versus Output Voltage

The current telemetry curve is given in Figure 4-6, and Figure 4-7 shows the output current at a fixed 35 volts output for various input currents. The nonlinearity is due to the current sensor as can be seen in Figure 4-6.

Line Regulator

The basic 5 kHz line regulator required minor modifications for use in BB-1/M-1. Only the regulated output voltage was changed. Since system requirements now allow a minimum solar panel voltage of 53 volts, the regulated output voltage was changed from 35 to 49 volts. The voltage feedback resistor was reselected for a 49 volt output voltage. Functionally, the line regulator supplies prime power to the accelerator inverter and to the 5 kHz inverter. Maximum steady state load on the line regulator under this configuration is estimated to be 185 watts.

Section 4 - 5 kHz Inverter

The 5 kHz inverter as used in BB-1/M-1 is a single inverter with prime and drive power supplied by the line regulator. The basic inverter is similar to that used before; however, the output configuration has changed. The primary of the output transformer has taps on each side of the center tap, resulting in an autotransformer configuration. The taps provide 5 kHz drive power to the magnetic modulator and accelerator inverter at 70 volts peak. The primary winding provides drive power to the cathode modulator at 96 volts peak. A second winding supplies ac excitation to the arc current sense circuit. Three additional windings and their associated rectifier/filters provide the various dc housekeeping voltages. The ± 12 volts and ± 5 volt supplies are basically unmodified except LC filters have replaced capacitors on the outputs. A new winding has been added to the output transformer which, when combined with its rectifier/filter, provides 35 volts dc. The output of this supply is connected to the + 35 volts distribution ring, thereby replacing the line regulator as a source of regulated 35 volt power.

Cathode Modulator (PS-3,9,10)

The three new cathode supplies are being packaged into a separate module called the cathode modulator, which will contain all the control circuitry and magnetics except the remote transformer for the cathode tip heater. The input power comes from the collector-to-collector voltage in the 5 kHz inverter at 96 volts peak.

The cathode tip heater is controlled by a digital one or zero supplied by external command. The + 5 volt one signal turns a transistor on holding the reference signal at ground, which sets the output at minimum current. The output current does not go precisely to zero due to magnetizing current in the magamps. The output current is, however, held to less than 15 ohm amperes. The regulator circuitry is almost identical to the magamp regulators in the magnetic modulator except for use of the orthonal material for magamp cores and the compensation networks. Orthonal has a much higher permeability per unit volume than the HY-Mu 80 used previously, thus the weight and volume are reduced.

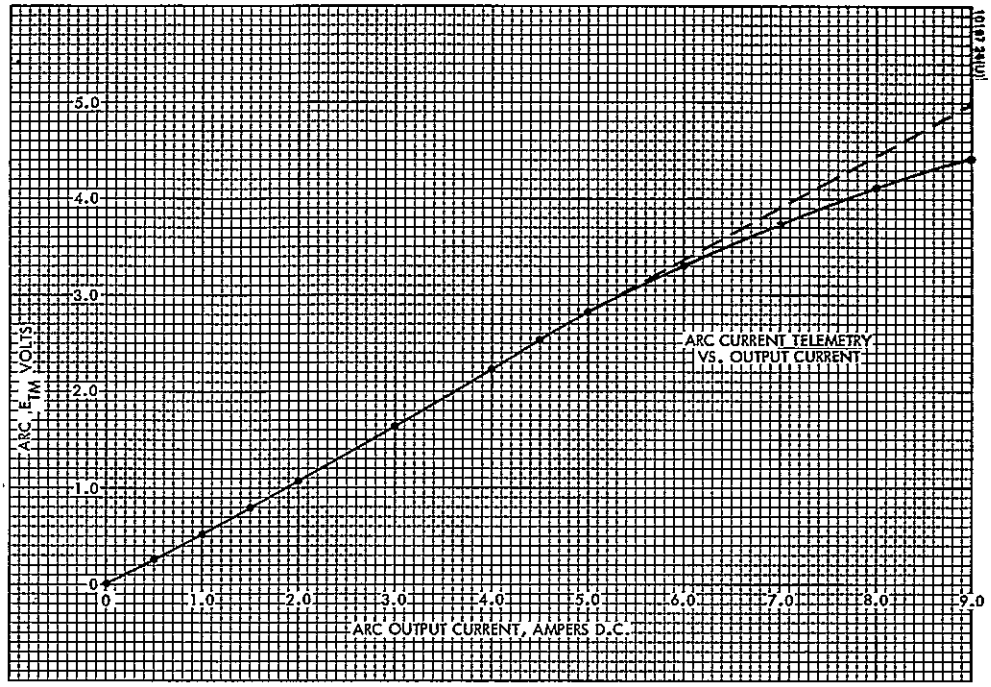

Figure 4-6. Arc Current Telemetry Versus Output Current

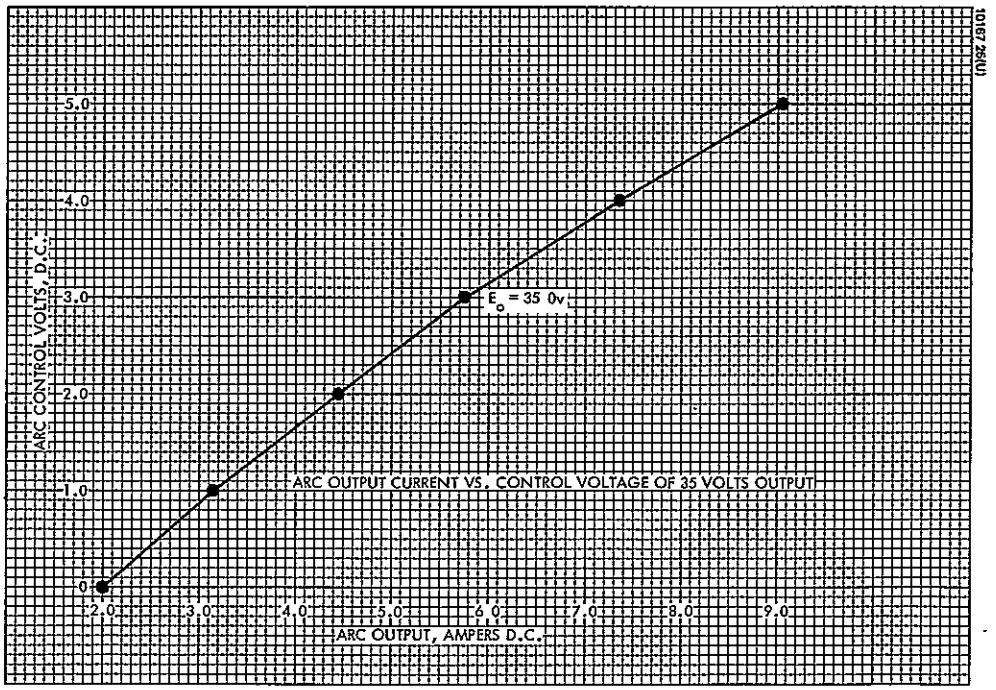

Figure 4-7. Arc Output Current Versus Control Voltage of 35 Volts Output

The cathode keeper voltage telemetry is provided in a manner different from that provided in the neutralizer keeper due to the high voltage. A small, high voltage insulated transformer senses the ac voltage after the choke in the low voltage leg of the supply. The output is not linear due to the drops in the output rectifier.

Accelerator Supply (PS-6)

The output transformer was changed to change the output voltage from -2000 to -1000 volts.

Control Module

The amplifier, which was formerly used to control the cathode power, was modified to provide the control function necessary to meet specification requirements. The amplifier compares two input signals. One is the arc voltage reference, the other arc voltage is represented by a 0 to + 5 volt signal for 30 to 40 volt arc voltage. The feedback signal thus represents 1/2 volt per volt of arc voltage. The amplifier output controls the vaporizer controller, which has a gain of 2 amperes for 5 volts input change. In order for the $\Delta I3/\Delta I4$ gain to be 6 ampere/volt, the amplifier gain must therefore be 30 volts per volt:

$$A_{amp} = \frac{\text{Slope}}{A_{cont} \cdot A_{TM}} = \frac{6\ A/V}{\frac{2}{5}\frac{A}{V} \cdot \frac{1}{2}\frac{V}{V}} = 30$$

A bias voltage is then applied to the noninverting side of the amplifier so that the cathode vaporizer current is not reduced until a preset level is greater than the feedback voltage.

The accelerator voltage telemetry amplifier was modified to have the same gain but different bias point. The old requirement was a 0 to + 5 volt signal for 1700 to 2100 volts, whereas the new requirement is 800 to 1200 volts. In both cases the ΔE is 400 volts.

The arc voltage telemetry amplifier required modification due to the deletion of the arc current compensation in the arc inverter, which was removed in converting the circuit to a current limited supply. The unmodified amplifier was current compensated to take out the compensation added to the signal in the arc inverter. The new amplifier must now compensate in the opposite sense due to the drop in output voltage caused by losses in the output filter.

A switch previously switched the arc reference, which was fed into the cathode control amplifier, from an external source to the function generator. The switch now selects the same two inputs but feeds this signal to the arc power supply that contains the control amplifier.

BREADBOARD INTEGRATION

The breadboard, modified for operation with a hollow cathode thruster, was integrated with the thruster at JPL's Electric Propulsion System Laboratory. Circuits that had previously survived engine arcing failed or performed erratically with the hollow cathode system. The apparent problem appeared to be the higher intensity of arcs, in that additional filtering was required to reduce transients seen on low level circuitry supply lines. The thrusters used also generated high level noise from an instability in the arc which draws approximately sinusiodal current at 25 to 30 kHz. This noise is also impressed on the beam supply since the beam originates in the arc.

Following the addition of sufficient circuit protection, the breadboard and thruster were operated together for many hours without power conditioner failure.

5. EXPERIMENTAL SYSTEM

SYSTEM SPECIFICATIONS

The general specifications for the oxide cathode system apply except for system weight and input line voltage. Unit weight was set at 30 pounds maximum, and the input line voltage minimum was increased to 53 volts as discussed in Section 4.

ELECTRICAL DESCRIPTION

A functional block diagram of the experimental system is given in Figure 5-1. It differs from the modified breadboard system only in the grouping of power supplies in module construction. The circuit mechanizations, while similar, have some notable differences which will be discussed below.

Screen Inverter

In an effort to reduce losses and thereby increase efficiency, an additional line capacitor was used, a line choke with an energy return winding was added, capacitor turning was employed on the primary and secondary of the output transformer, and the output transformer was designed to take advantage of the reduced input line voltage swing. The ac coupling between the input control gates was removed since its inclusion was to protect the inverters during system development against accidents.

5KHz Inverter

The output transformer was redesigned to directly provide drive to the two vaporizers at the output voltage since the vaporizer magamps are no longer in the primary but directly in series with the load. A winding was added to provide excitation to the magnet current sensor. Windings were provided to supply the high and low voltage segments of the keeper supply, which were previously derived from a separate transformer. The circuitry associated with the standby inverter was deleted and the ac coupling in the gating circuitry was removed.

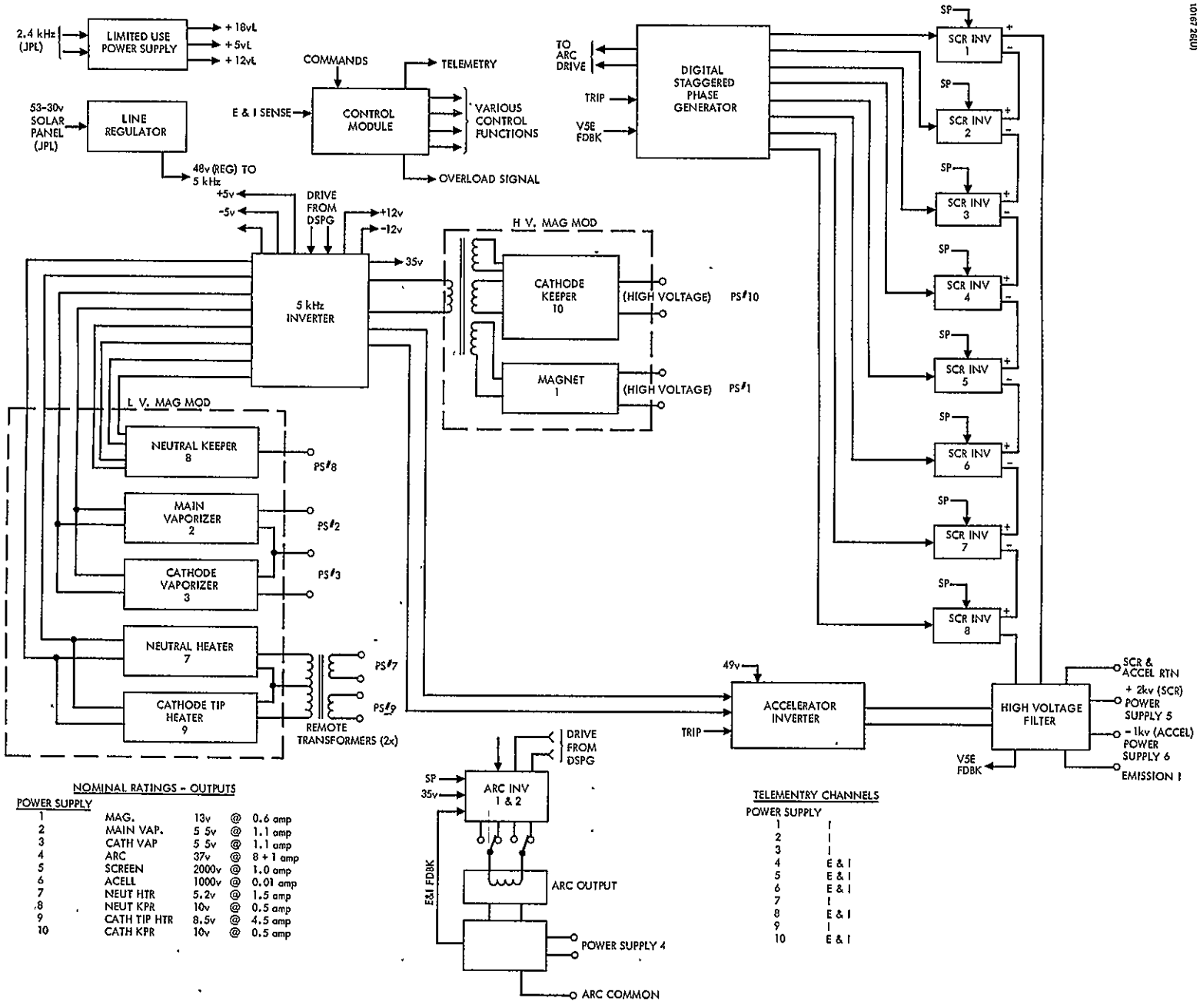

Figure 5-1. Functional Block Diagram – Experimental System

Low Voltage Modulator

The low output power supplies were all repackaged in order to separate the supplies operating at ground potential and those floating at + 2 kv or with remote transformers. The new low voltage modulator contains the two vaporizer supplies, the neutralizer and cathode heaters, and the neutralizer keeper supply. The cathode heaters output is at + 2 kv, and a remote transformer is employed so that no high voltage is present in the module.

The typical magamp circuit is shown in Figure 5-2. The magamp core material used is orthonal to reduce weight. The ac drive for the vaporizers is approximately 13 volts peak with the output feeding directly to the load. The advantage of this configuration is to reduce the number and thus weight of magnetic components. The neutralizer and cathode heater circuits are fed with 96 volt peak ac and have remote transformers to reduce transmission line losses. The network consisting of R_8, R_9, C_1, C_2, CR1 provides rms compensation for the feedback signal.

The neutralizer keeper circuit is similar to the circuit shown in Figure 3-6 except that the ac drive power is not fed from a separate transformer as shown. This drive comes from the 5 kHz output transformer.

High Voltage Modulator

This module contains the magnet and cathode keeper supplies. The magnet regulator is similar to the vaporizer circuit except that the magamp gate windings are separated and the drive signal is provided by a center tap winding. The circuit thus forms a push-pull control circuit better known as a dc magamp. The cathode keeper supply differs from the neutralizer keeper supply in that the voltage telemetry is provided by a transformer that senses the ac provided for the low side of the output volt-ampere curve. The module is provided with its own drive transformer to easily facilitate high voltage isolation. The transformer is driven from the collectors of the 5 kHz inverter.

Arc Inverter

Additional line capacitors were added to the inverter to reduce the capacitor losses.

EXPERIMENTAL SYSTEM EFFICIENCY

An analysis of the experimental system efficiency is included in Appendix B. This analysis is somewhat modified from the breadboard calculation in an attempt to account for increased losses due to the inductive switching envelope seen by the output power transistors. The analysis used worst case saturation voltages and switching speeds in order to determine the least efficiency expected.

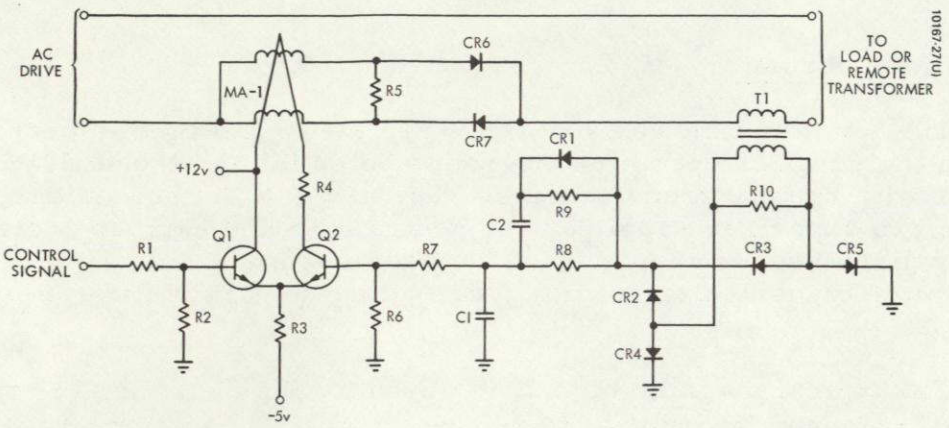

Figure 5-2. Magamp Controller

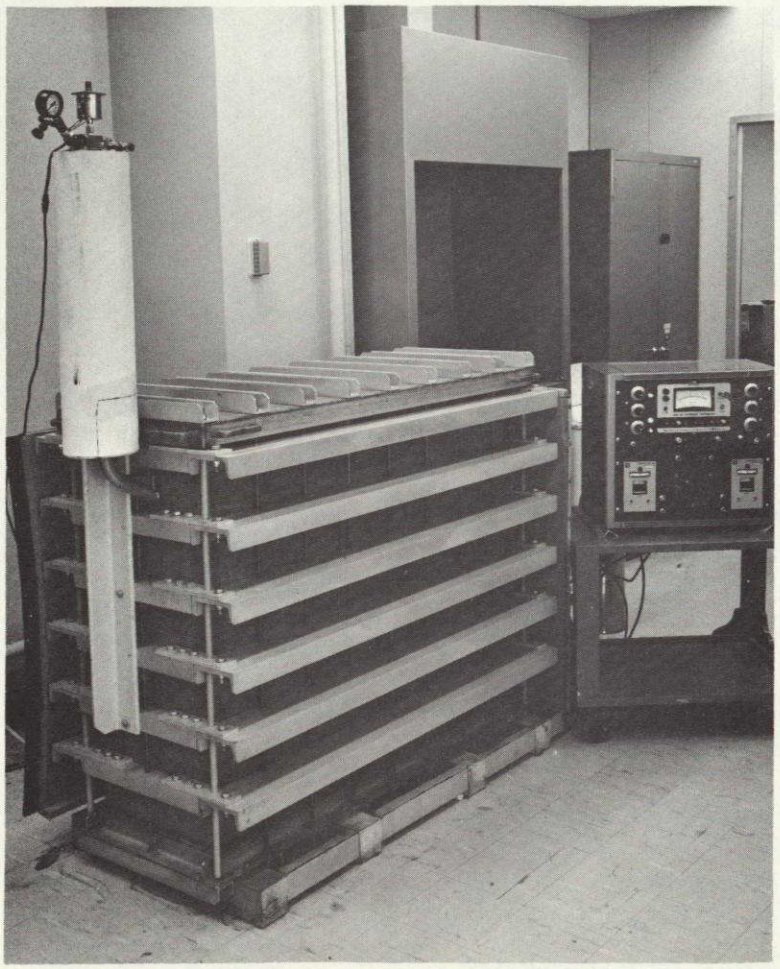

Figure 5-3. Calirometer (Photo ES 23694)

A test using the calorimeter shown in Figure 5-3 was performed on EX-1 in order to measure the power lost when the unit was operating at full power. Although there is some reservation as to the accuracy of the results, due to difficulties with the calorimeter, the results are interesting in that they confirmed the relative analytical comparison at high and low input line voltage. The absolute values of efficiency were disappointing in that they did not meet expectations. Several possible explanations for this discrepancy exist.

The calorimeter might be considered as being an error source, although recent test results, summarized in Appendix B, indicate that the results are reasonable. The unit operates as an isothermal system with constant differential pressure being maintained between a chamber containing the test specimen and an outer chamber enclosing the smaller chamber. Heat dissipated by the test specimen evaporates Freon from the inner chamber, forcing vapor through a fixed orifice. The outer chamber utilizes a condenser to keep the outer tub pressure constant. Keeping the outer chamber pressure constant was a prime problem in that the transducer was much coarser than desirable to hold a fixed pressure to the accuracy required. The dissipation in the inner chamber is measured by holding the total inner chamber dissipation constant using a calibration heater and the test specimen. As the test specimen dissipation increases, the calibration heater is turned down. If the outer tub pressure changes, it invalidates the calibration.

Also a second source of difficulty was the condenser, which was too small for the total heat input. To compensate for this inadequacy, the top insulator was removed, which exposed the outer chamber to changing air currents.

Another consideration is the geometry of the heat source. It was found that with various types of test specimen shapes, radically different results were obtained. This indicates that the calibration heater must resemble, to a high degree of accuracy, the thermal profile of the test specimen. A detailed explanation of the calorimeter operation theory is given in Appendix B.

The results did show that the expected increase of about 4 percent over the breadboard performance was probably experienced, but left in doubt the absolute value to within an uncertainty of ±1 percent. The experiment unit efficiency could probably be raised by 1/2 to 2/3 of 1 percent by lowering the overall system operating frequency by 10 percent. This is possible because operating frequency was about 10.5 kHz instead of the planned 10 kHz. The additional 500 Hz would not push the transformers into an unsafe region of operation. It is thus expected that the unit efficiency can be as high as 91 percent. The test results, summarized in Appendix C, show that, at the present operating point, the power efficiency is 89.9 percent at 57.6 volts input and 89.7 percent at 80 volts input.

Results of individual inverter sections are also tabularized and show that the inverter efficiency does not meet the calculated values. Additional testing will provide sufficient information to allow a possible tradeoff of weight for increased efficiency.

Experimental Physical Description

The overall physical dimensions and mounting surfaces did not change from the breadboard configuration. The basic differences in the two unit types is in the frame design, choice of plate materials, choice of components and hardware, and component mounting techniques, all of which were changed to reduce unit weight.

Module placement was changed from the breadboard configuration to reduce wiring path lengths and thus weight. Table 5-1 shows the module placement as seen from the radiating side. Solar panel power is introduced at the low voltage connection module and flows down the center of the unit branching out to the inverters. The position of the 5 kHz inverter allows low power flow paths up the center of the unit to each using module. The harness was fabricated on a wiring jig and is tied along the top of the frame web as can be seen in Figure 5-4a.

TABLE 5-1. MODULE PLACEMENT – RADIATING SIDE

Line Regulator	Low Voltage Connection Module	Stag. Phase Gen.	Control Module
Screen Inv.	Screen Inv.	Screen Inv.	Screen Inv.
Screen Inv.	Screen Inv.	Screen Inv.	Screen Inv.
ARC Rectifier Filter	ARC Inv.	5 kHz Inverter	Low Voltage Modulator
High Voltage Filter	ARC Output Transformer	Accel Inv.	High Voltage Modulator

Weight Reduction

The breadboard, upon completion, was measured and found to weigh 39 pounds as compared to a 23.5 pound weight goal for the experimental system. A weight reduction study was undertaken with various alternatives in regulation allowances and reliability tradeoffs. As a result, the predicted weight of an oxide cathode-compatible power conditioner was 25 to 30 pounds, depending on the options chosen. With the design change to the oxide cathode system, a weight goal of 28 pounds was set, with 30 pounds being acceptable.

The frame was reduced in weight by reducing the thickness and total amount of material used. The total weight saved by the reductions amounted to 0.75 pounds at a calculated increase of 0.03 inches in deflection undervibration.

Figure 5-4b shows the radiating side of the experimental unit. Careful inspection will indicate that the screen inverter module plates were chemically milled to reduce the material thickness from 0.05 to 0.03 inches where heat dissipation was low. The size of unmilled area is calculated so that the temperature drop is minimized between the component and the surrounding heat sink. The module plates are fabricated from 99.5 percent pure magnesium for good thermal conductivity per unit weight.

Figures 5-5 through 5-20 show the fabrication techniques of each of the modules in the system. Capacitors are bonded directly to the chassis, thereby eliminating the clips used on the breadboard system. This technique was also used on TO-5 and TO-18 transistor and integrated circuit packages. Small fiberglass washers were used as insulators when needed. A minimum of epoxy was used to filet around components for heat removal and mechanical strength. The normal conformal coating was eliminated by the use of Dow 17 on the magnesium plates and spot conformal coating high voltage terminals. The power transistors used were of the isolated type to TO-61 case. This faciliated mounting and heat removal as well as reducing weight over the larger TO-63 case.

The control module and staggered phase generator were fabricated using perforated fiberglass boards and small push-in terminals as seen in Figures 5-6 through 5-8. The wiring on the backside used was solderable magnet wire. The insulation of this wire flows back at approximately 700°F, allowing use of the wire without stripping prior to wrapping the terminals. Upon application of a soldering iron, a good connection is made. The wiring is shown in Figure 5-9. The assembled unit forms a very lightweight circuit board system, which can be easily modified.

The magnetic modulators were fabricated using the component bracket rather than the two layer system used on the breadboard. This type of construction provided easy access to all components for repair or modification.

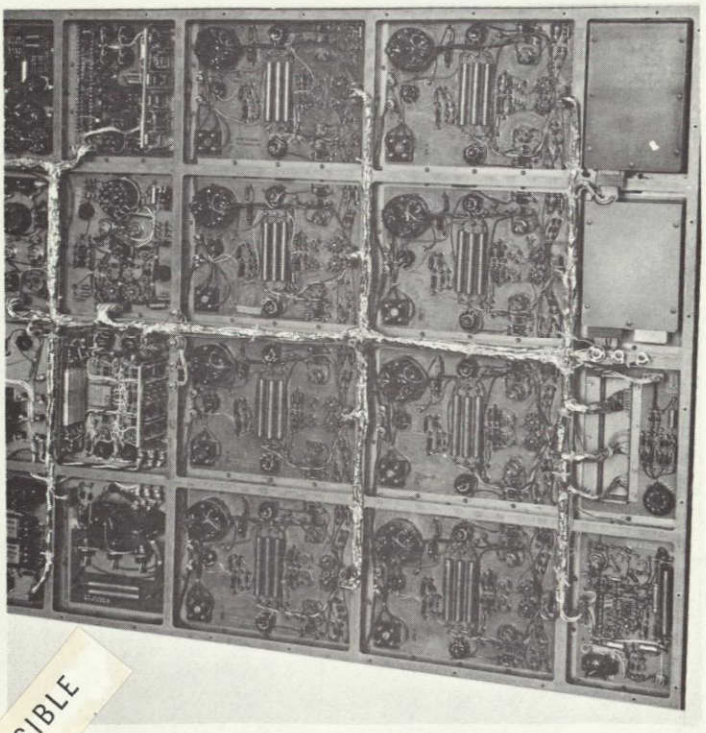

a) Component Side (Photo ES 30053)

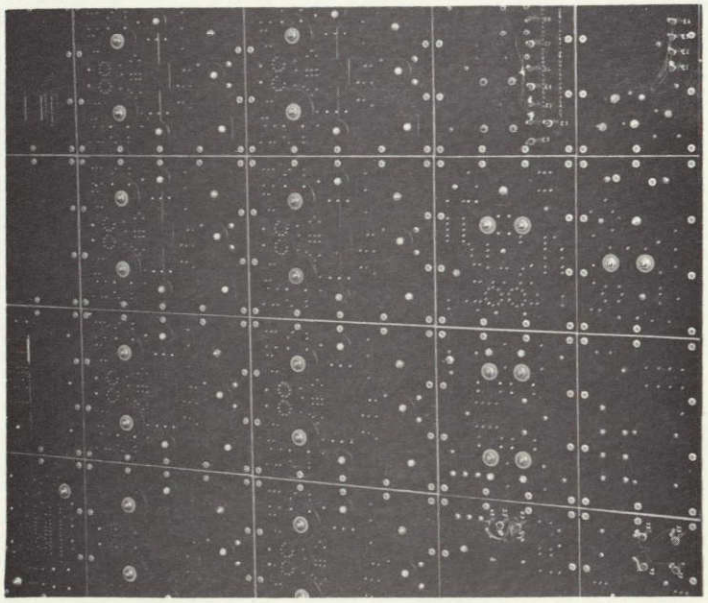

b) Radiating Side (Photo ES 30054)

Figure 5-4. Experimental System

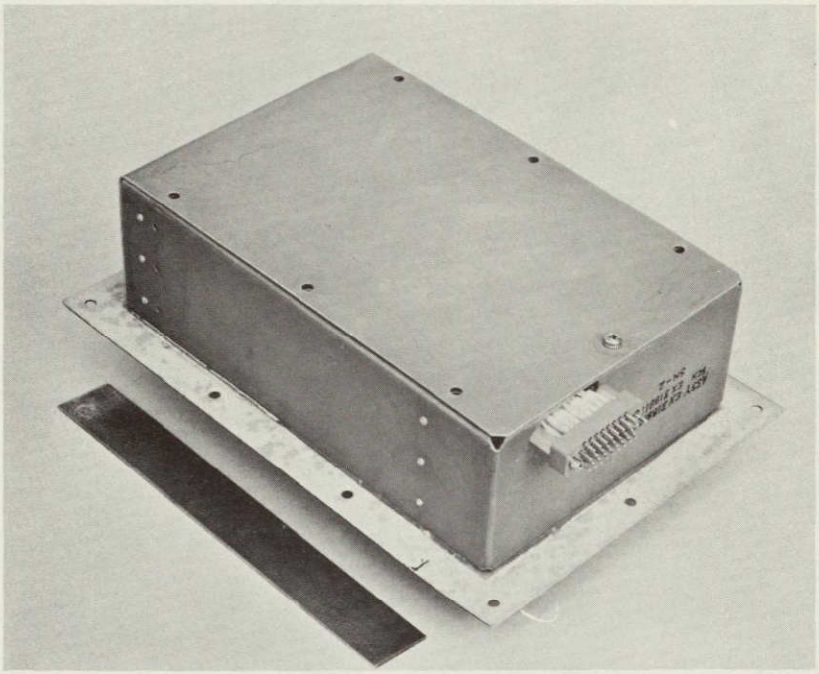

Figure 5-5. Control Module (Photo ES 29997)

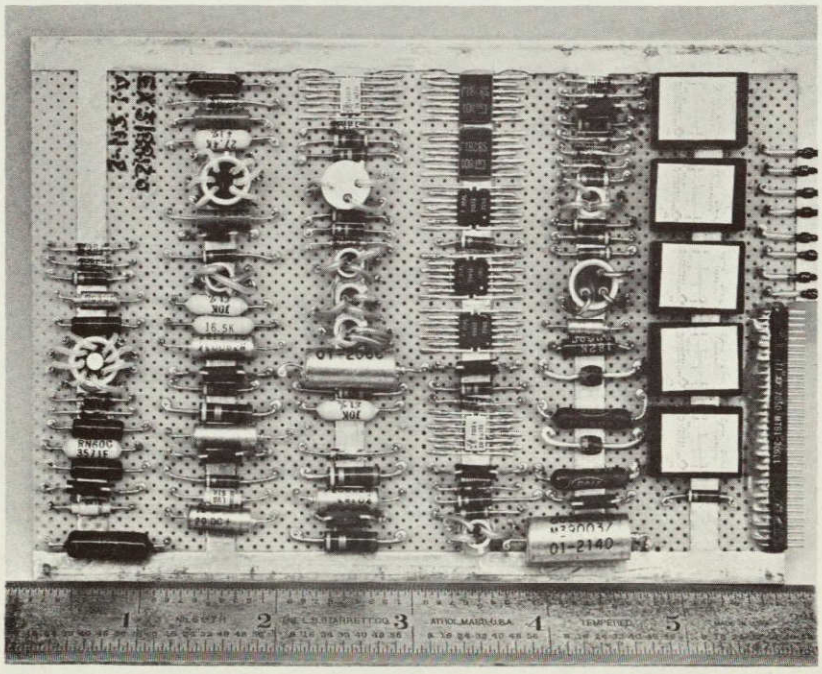

Figure 5-6. One Control Module Board (Photo ES 30003)

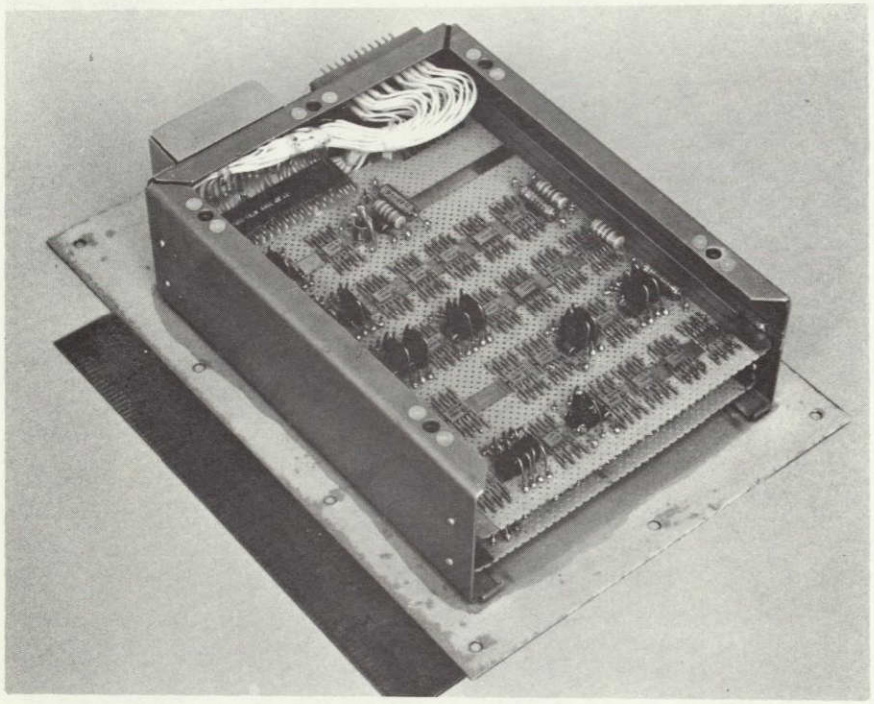

Figure 5-7. Digital Staggered Phase Generator (Photo ES 29983)

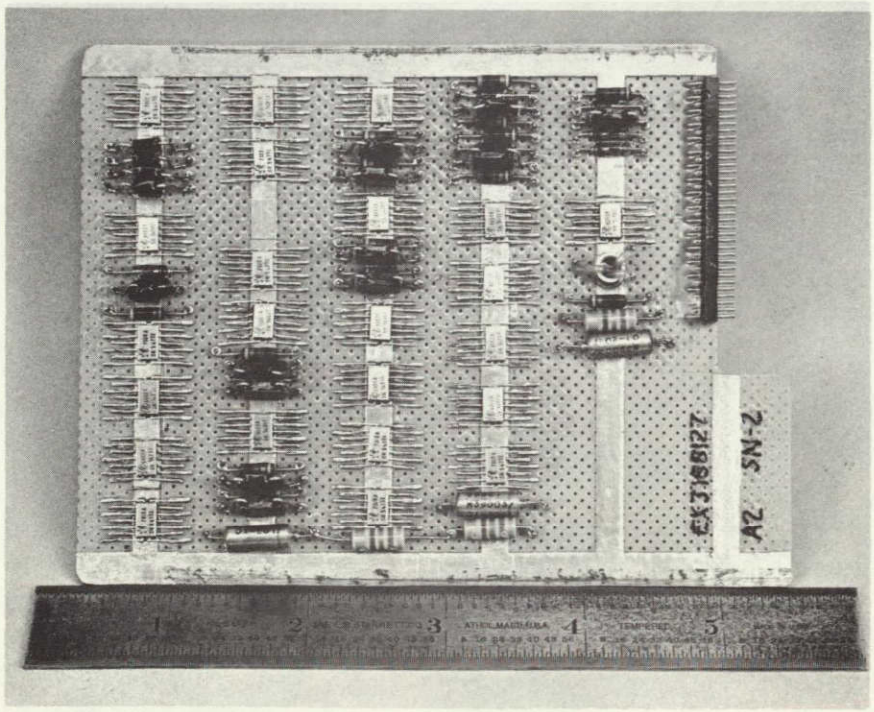

Figure 5-8. One Digital Staggered Phase Generator Card (Photo ES 30002)

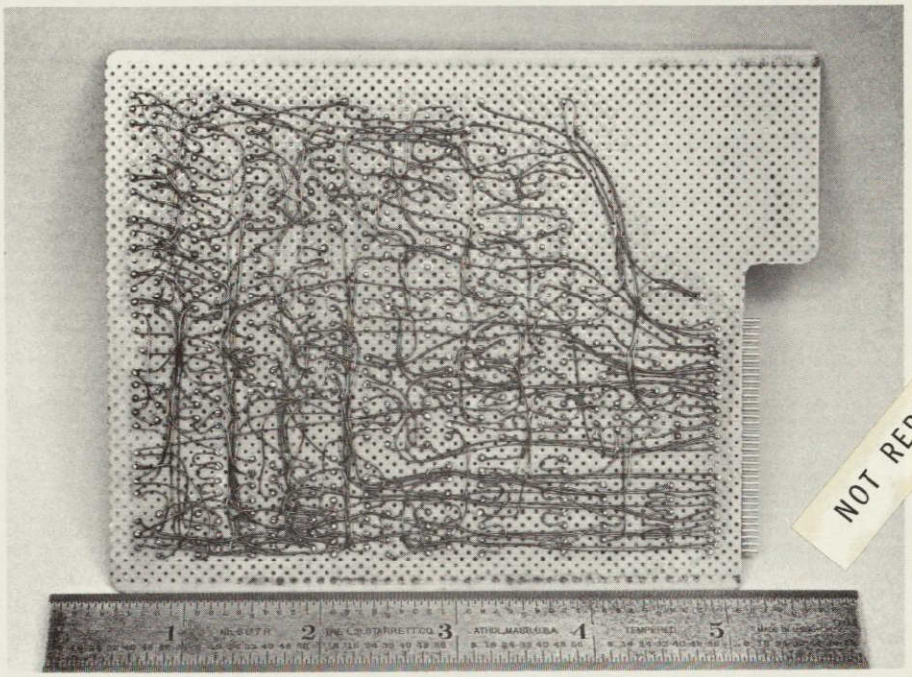

Figure 5-9. Wiring on Backside of Module Cards (Photo ES 29985)

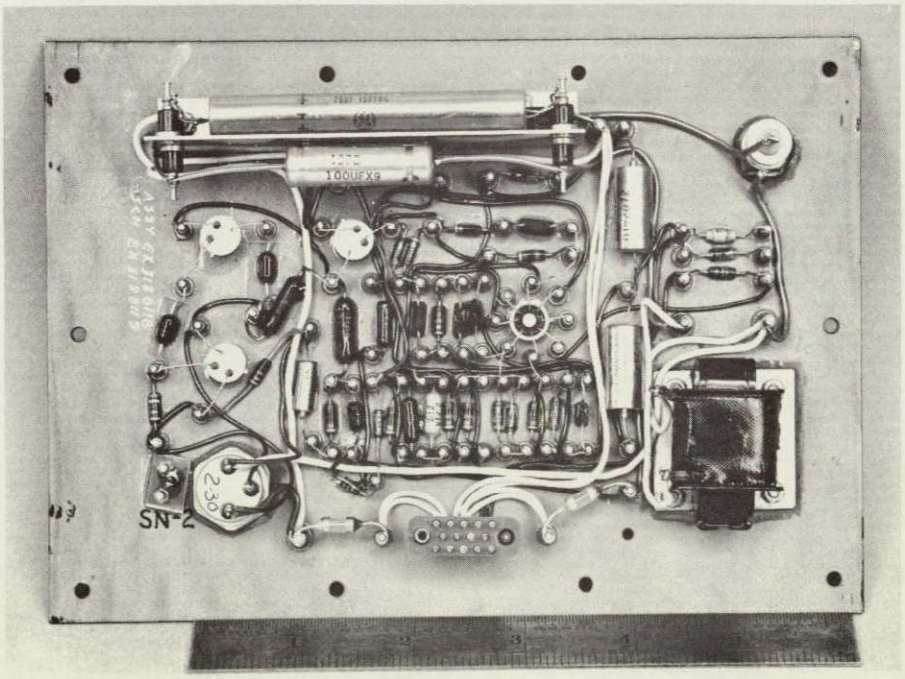

Figure 5-10. Line Regulator (Photo ES 29992)

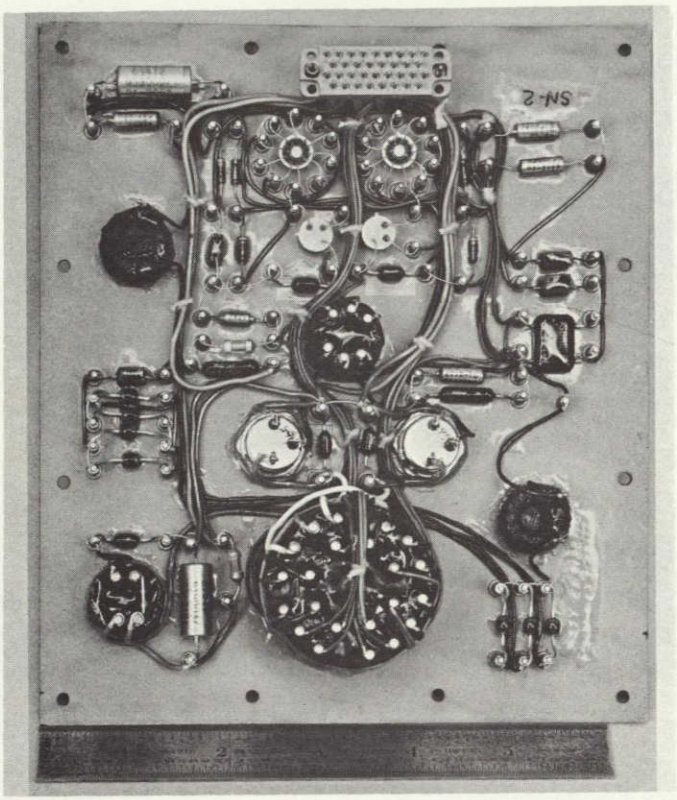

Figure 5-11. 5 kHz Inverter (Photo ES 29987)

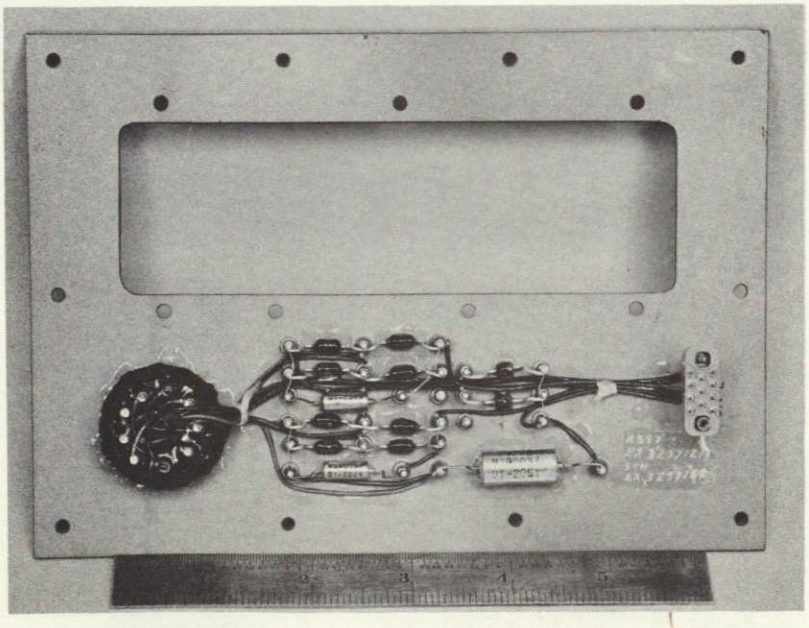

Figure 5-12. Limited Use Power Supply (Photo ES 29993)

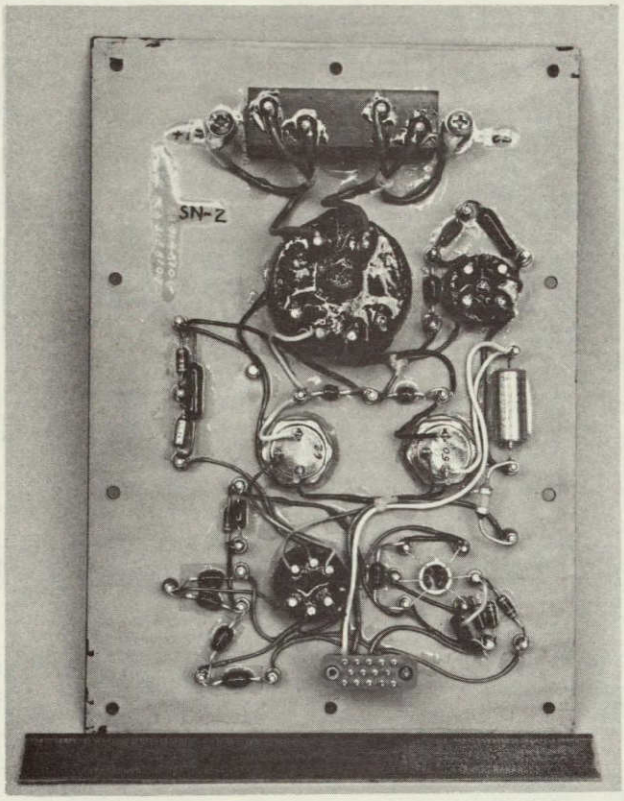

Figure 5-13. Accelerator Inverter (Photo ES 29982)

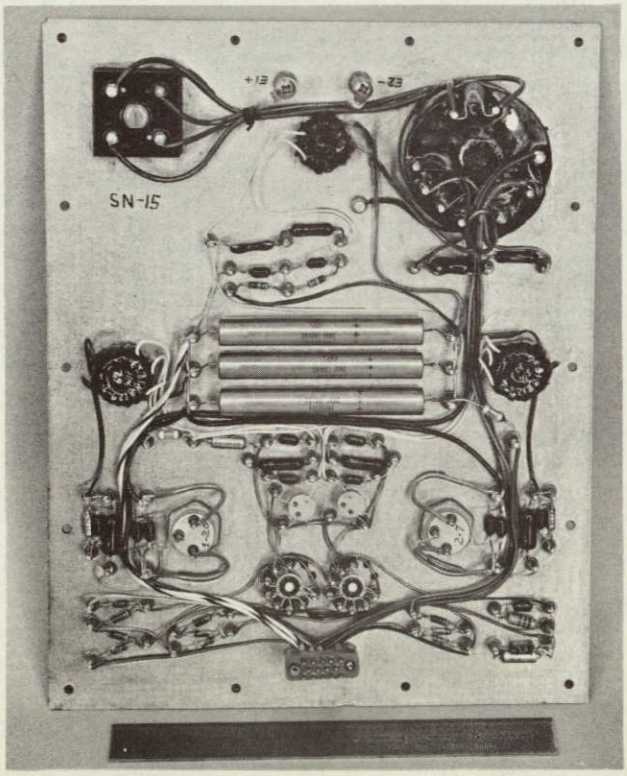

Figure 5-14. Screen Inverter (ES 29986)

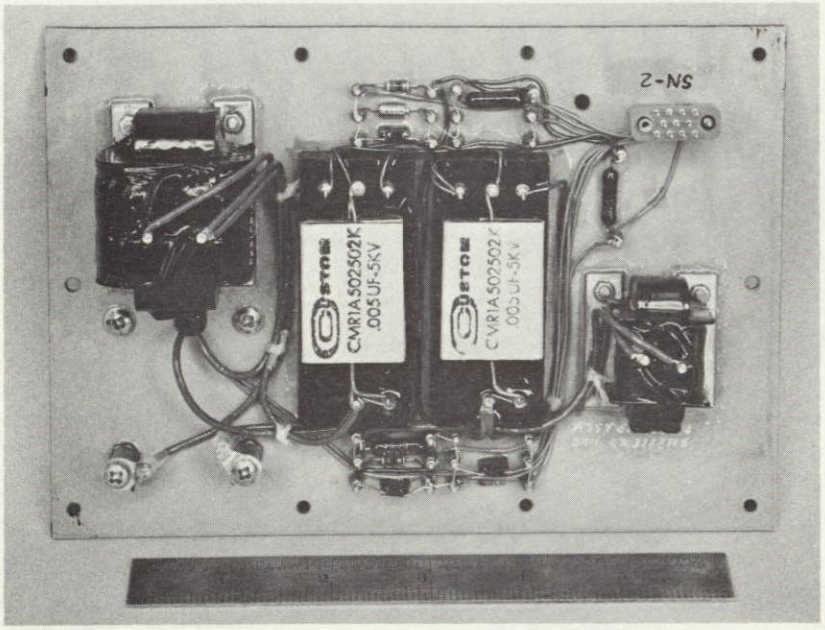

Figure 5-15. High Voltage Filter (Photo ES 29995)

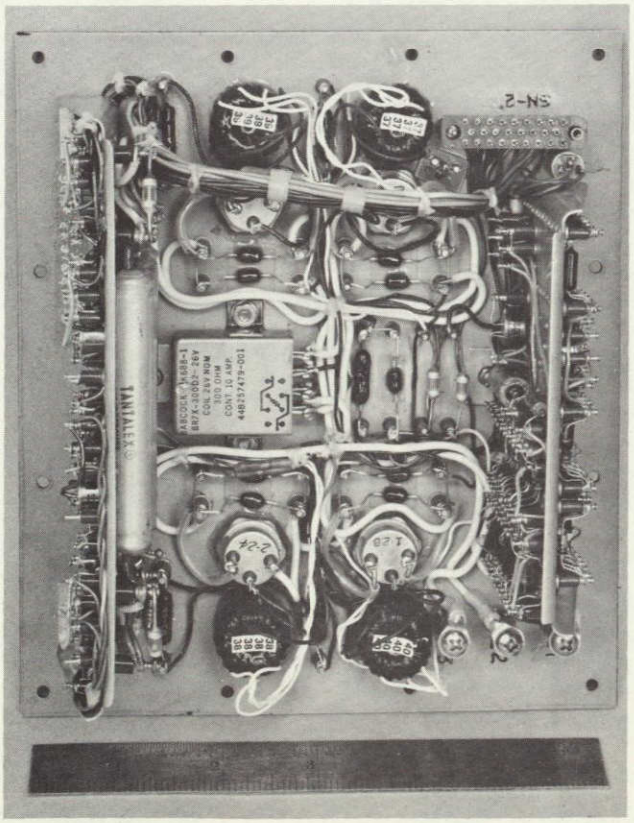

Figure 5-16. Arc Inverter (Photo ES 29994)

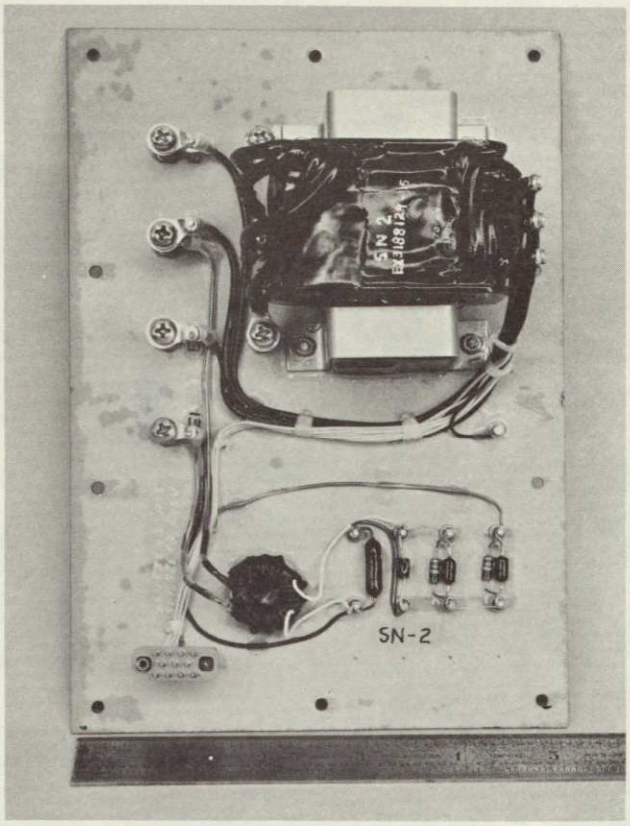

Figure 5-17. Arc Transformer
(Photo ES 30001)

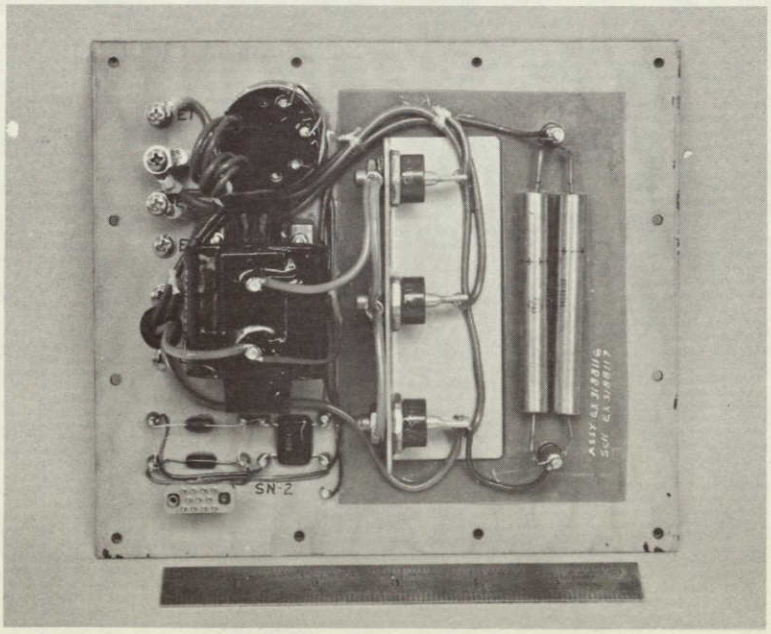

Figure 5-18. Arc Rectifier-Filter (Photo ES 29996)

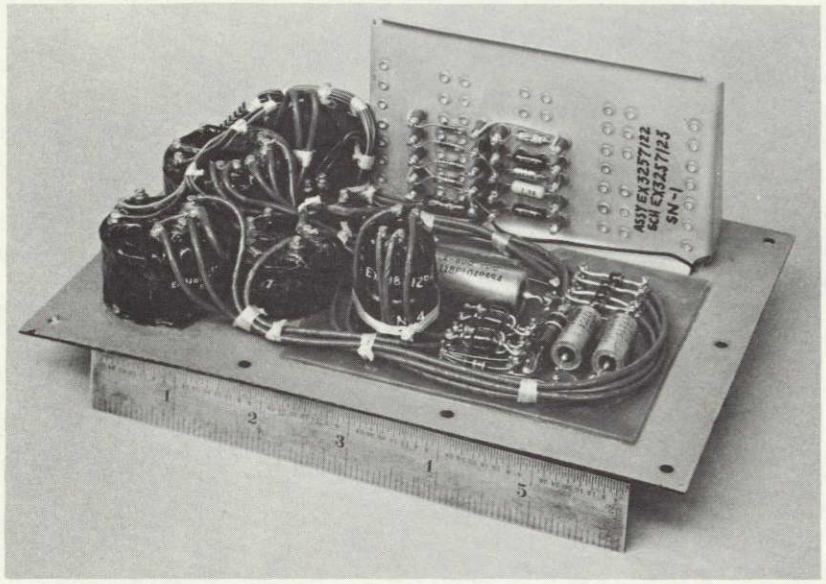

Figure 5-19. High Voltage Magnetic Modulator
(Photo ES 29981)

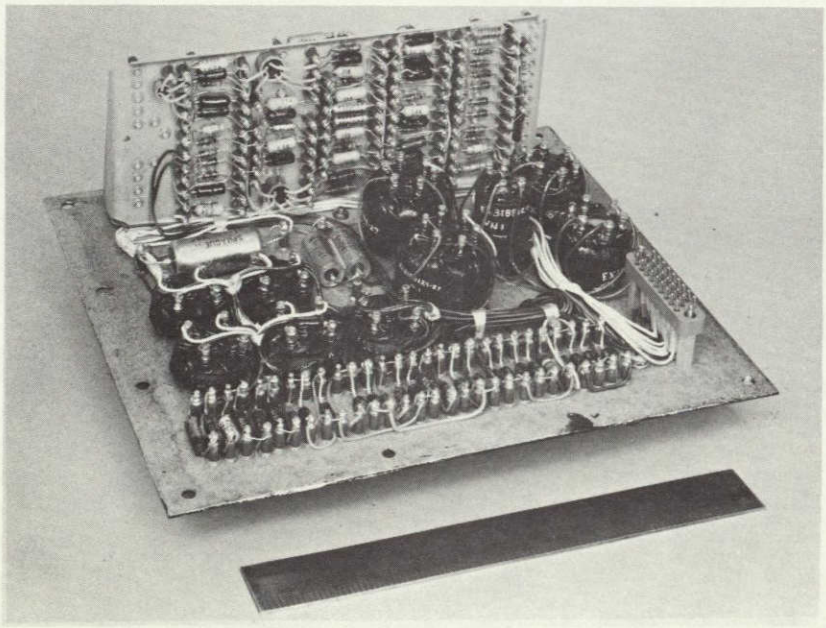

Figure 5-20. Low Voltage Magnetic Modulator
(Photo ES 29991)

A summary of the system weight by module and structure is given in Table 5-2. Included is a listing of the estimated weight for each item. The original weight estimate mistakenly listed the 5 kHz inverter at 213 grams, which put the estimated weight under 30 pounds.

TABLE 5-2. SYSTEM WEIGHT SUMMARY

	Estimate	Actual
Line regulator	213	299
Low voltage connection module	100	106
Staggered phase generator	600	314
Control module	400	476
Screen inverter X8	4,424	4,544
Arc rectifier filter	841	822
Arc inverter	696	687
5 kHz inverter	522	465
Low voltage magnetic modulator	540	590
High voltage filter	452	556
Arc output transformer module	621	704
Accelerator inverter	311	294
High voltage magnetic modulator	409	498
Frame	1,240	1,236.5
Harness	1,035	738
Cover	875	875
Screws	120	126
Remote transformers	198	200
Shielding tape	45	62
Total weight	13,682 grams	13,593 grams

EMI Considerations

Since the power conditioner is the prime load on the array, conducted interference caused by other sources was not considered a problem. Conducted and radiated interference generated by the power conditioner was considered. To this end, construction techniques were implemented which reduce EMI. The guide for suppression and measurement of EMI was TOR-1001(2307)-4 for space systems, which states that each and every instance shall be considered in light of the rest of the system and action taken accordingly.

Test results from cursory examination of the breadboard unit under nonideal conditions show that the cables and power conditioner radiate at somewhat higher levels than those limits specified as a guide in TOR-1001(2307)-4. These data are plotted in Figure 5-21. The test setup is shown in Figure 5-22. It is suspected that the test cables were the prime source of radiation, since they were not shielded and power and return lines were not twisted. The data should therefore be disregarded, and new data taken using a screenroom and techniques that will indicate true radiation levels.

Steps taken on the experimental systems to reduce EMI were generally those used on any power system to reduce radiation. All of the input power leads and all output ac leads are twisted pairs. The power leads are are dressed together and wrapped with aluminum foil tape. Additionally, all low level cabling was grouped together and wrapped as a bundle using the aluminum tape. With the tape grounded to the chassis, the EMI leakage from the wiring is reduced to a minimum. The component side is enclosed by a cover. The use of isolated collector power transistors also helped to reduce EMI in that the case acts as a shield. The studs of the electrically hot cases of transistors protruded through the radiating surfaces on the breadboard and were thus EMI generators. Additional line storage capacitors on the screen and arc supplies help to reduce conducted noise which results in EMI.

Although the experimental systems were not tested, it is felt that the levels will be lower than those measured on the breadboard. Final evaluation must be accomplished by cut and try modifications to circuits to reduce any residual EMI to acceptable levels.

EXPERIMENTAL SYSTEM RELIABILITY

The reliability calculations were carried out using the same rationale and equations as used on the breadboard. A reliability block diagram is shown in Figure 5-23. The reliability block diagram for the experimental system is different from that given for the breadboard system because the standby for 5 kHz and accelerator inverter were dropped, and the reliability numbers for components have been considerably increased. A summary of failure rates are given in Table 5-3. The module failure rates are given in Table 5-4.

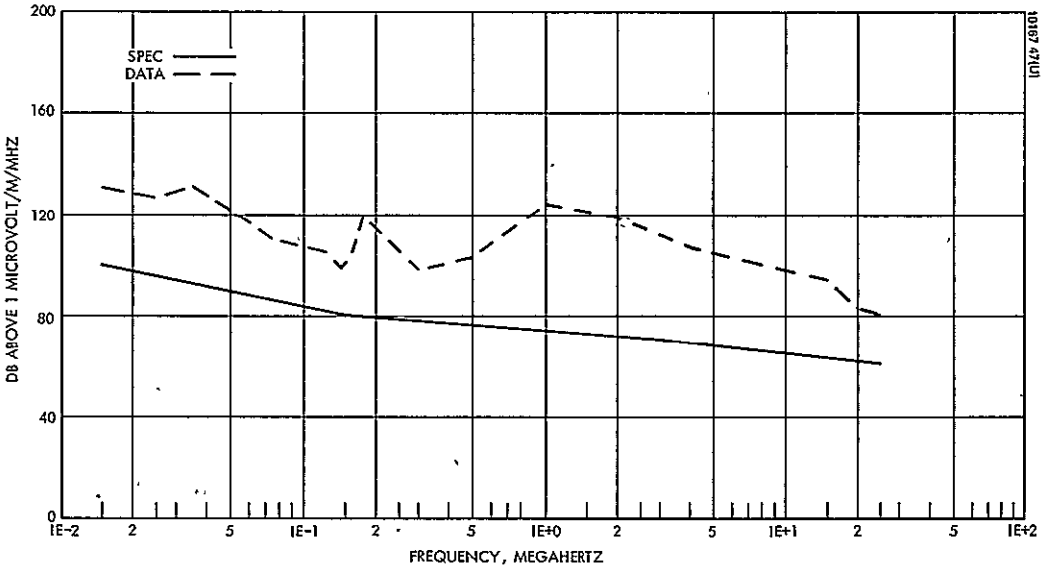

Figure 5-21. Program-Elect Thrust Test Item — Power Conditioner

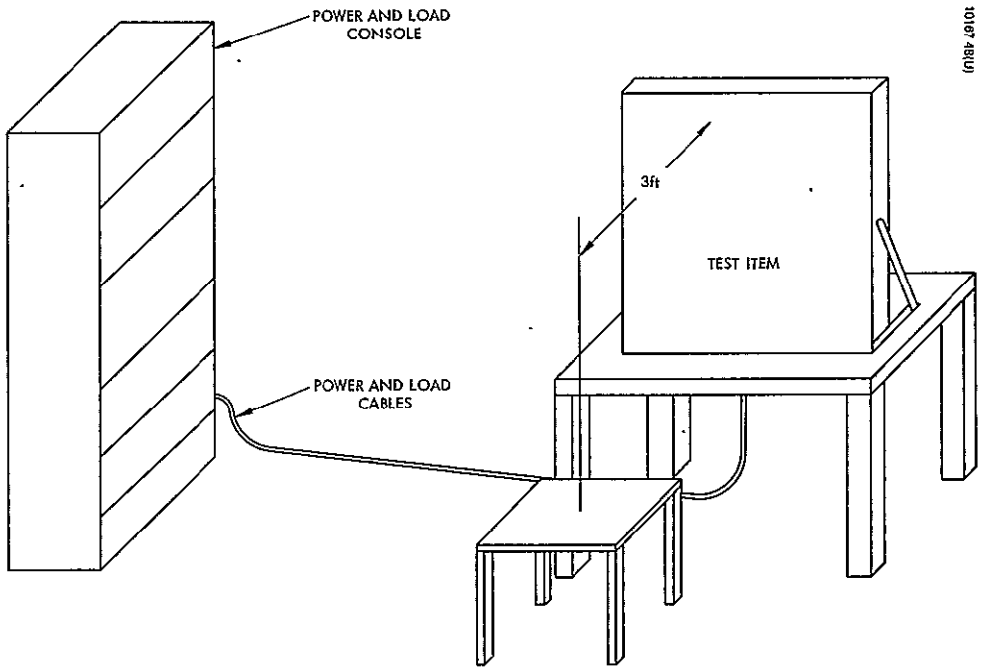

Figure 5-22. EMI Test Setup

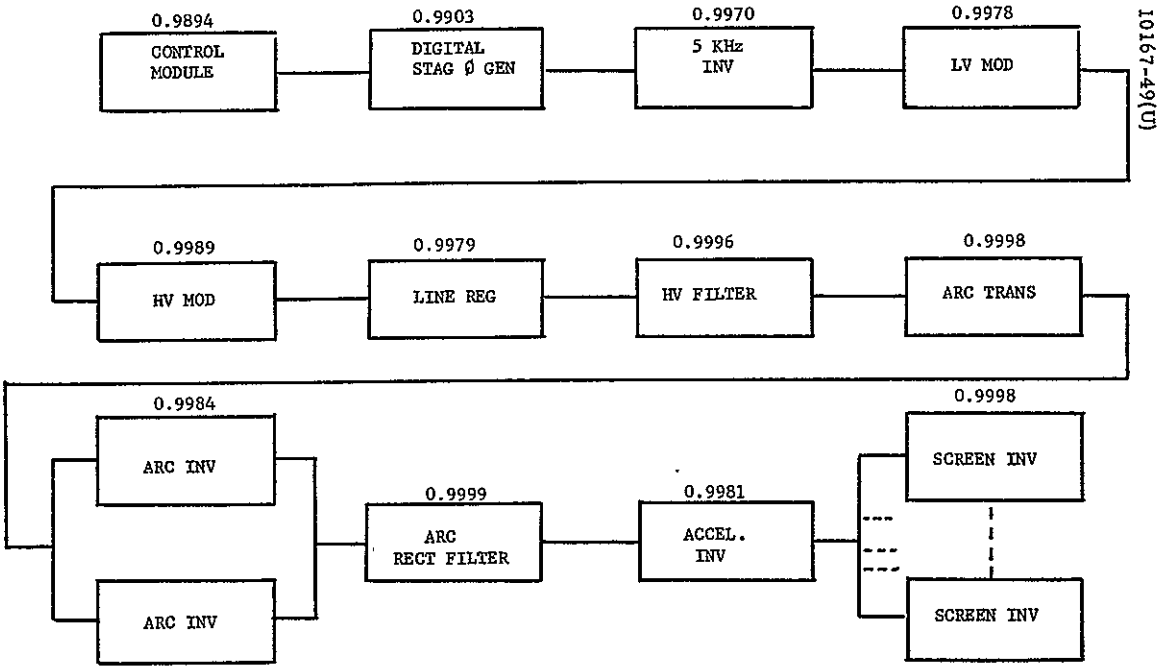

Figure 5-23. Reliability Block Diagram

TABLE 5.3.1A FAILURE RATE SUMMARY

Component	Failure Rate x 10^{-9}/Hour
Module	0.32
Control module	10.7
Digital stag @ gen	0.05
5 kHz inverter	0.1
LV modulator	0.3
HV modulator	0.45
Line regulator	4.1
HV filter	3.1
4 kHz inverter	14.0
Arc transformer	21.0
Arc rectifier filter	14.
Accelerator inverter	3.1
Screen inverters	10.
	7.0
	17
	2.7
	349.
	75.
Integrated circuit, linear switching	45
Integrated circuit, linear	60
Integrated circuit, dual J-K flip-flop	45
Integrated circuit, counter	45
Integrated circuit, quadgate	30
Relays	100

TABLE 5-4. MODULE FAILURE RATES

Analysis Summary			
Module	FR x 10^{-9}	0.544 RF x 10^{-9}	R
Control module	1994.0	1072	0.9894
Digital stag Ø gen	1778.5	967	0.9903
5 kHz inverter	527.0	287	0.9970
LV modulator	402.3	219	0.9978
HV modulator	208.5	114	0.9989
Line regulator	389.1	212	0.9979
HV filter	66.4	36	0.9996
Arc inverter	296.1	161	0.9984
Arc transformer	35.3	19	0.9998
Arc rectifier filter	25.6	14	0.9999
Accelerator inverter	357.2	194	0.9981
	6080.0	3295	
Screen inverters	2424.0	20	0.9998
		3315 x 10^{-9}	0.96739
		495	
		3810 x 10^{-9}	0.96261

The computed reliability of 0.96261 for the 10,000 hours is higher than the design objective of 0.955. The increased reliability reflects the change in reliability numbers given in the latest Hughes Space Systems Division Product Effectiveness Handbook and the lowered experience factor of 0.544. This would indicate that it might be possible to eliminate the standby arc inverter and still meet the reliability goal.

TEST RESULTS – EXPERIMENTAL SYSTEM

Acceptance Test

A summary of the acceptance test data taken on EX-1 is given in Appendix D. The load regulation curves for the arc and cathode keeper supplies are given in Figures 5-24 and 5-25. A typical control characteristic is neutralizer heater-keeper curves shown in Figure 5-26.

The telemetry data taken on EX-1 were plotted and are included as Figures 5-27 through 5-42. These curves were very nearly duplicated by EX-2. The telemetry data are a calibrated signal that should lie within the specified lines shown on each curve. In practice, zero shifts can be tolerated due to the calibration accuracy of the signal. Any data processing performed using the telemetry signals can take into account the nonlinearities and zero offsets seen in the curves.

Integration Tests

Integration of EX-1 and EX-2 was accomplished easily when compared with the breadboard task. The experience gained on the breadboard and knowledge of the circuit protection required eliminated much of the time lost with the breadboard. The prime problems encountered were with the arc, accelerator, and screen supply.

During thruster testing, the arc output rectifiers shorted during arcing. This problem appeared to be caused by punch-through due to stored voltage on stray capacitances. Avalance rectifiers were placed in parallel with the output diodes and no further problems of this type occurred. It was later found that part of the system had been miswired and a laboratory power supply was connected to the arc supply in such a way as to bypass the current sensor. Although this error was corrected, the avalance diodes were not removed, in order to determine if the wiring error caused the original problem.

The accelerator inverter was experiencing shorted power transistors during thruster arcing. The circuits used in the experimental system had been slightly modified to reduce losses. When the configuration was restored to the successful breadboard configuration, no further failures occurred.

The thruster being tested passed through an unstable operating point at some cathode flow rate. As a result, a 1.5 kHz signal modulated the beam supply. The control system 0 dB point occurred very close to the disturbance frequency, and the disturbance was enhanced. AC voltages of up to 2 kv were seen on the beam supply. The voltage spikes above the 2 kv level caused the vaporizer isolator to flash over and shut the power supply down. The control loop was modified by halving the 0 dB point, and the system operated smoothly.

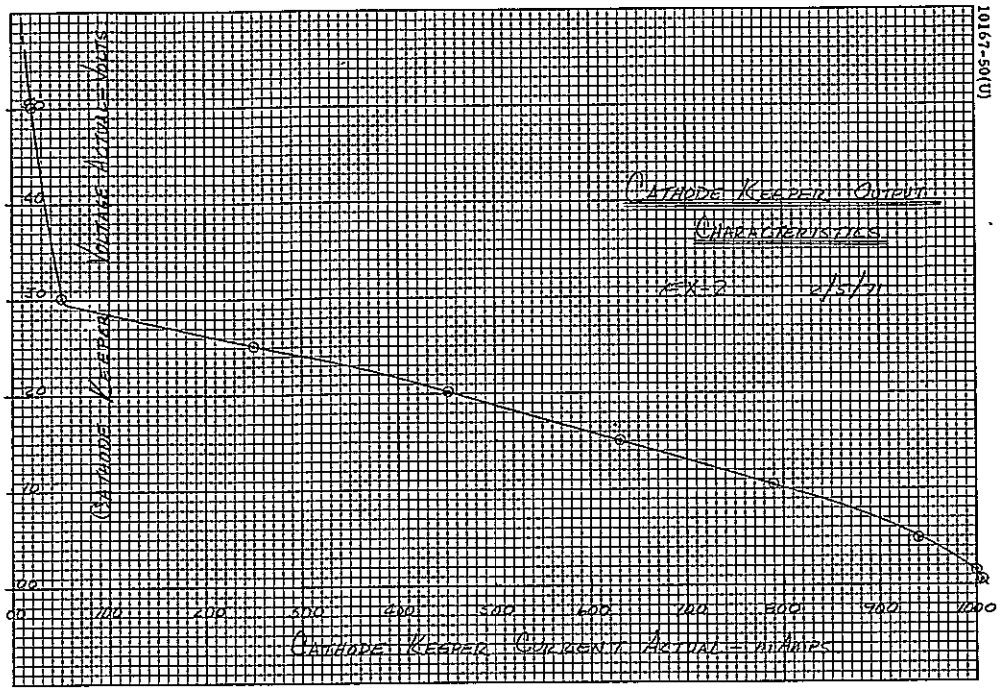

Figure 5-24. Cathode Keeper Output Characteristics

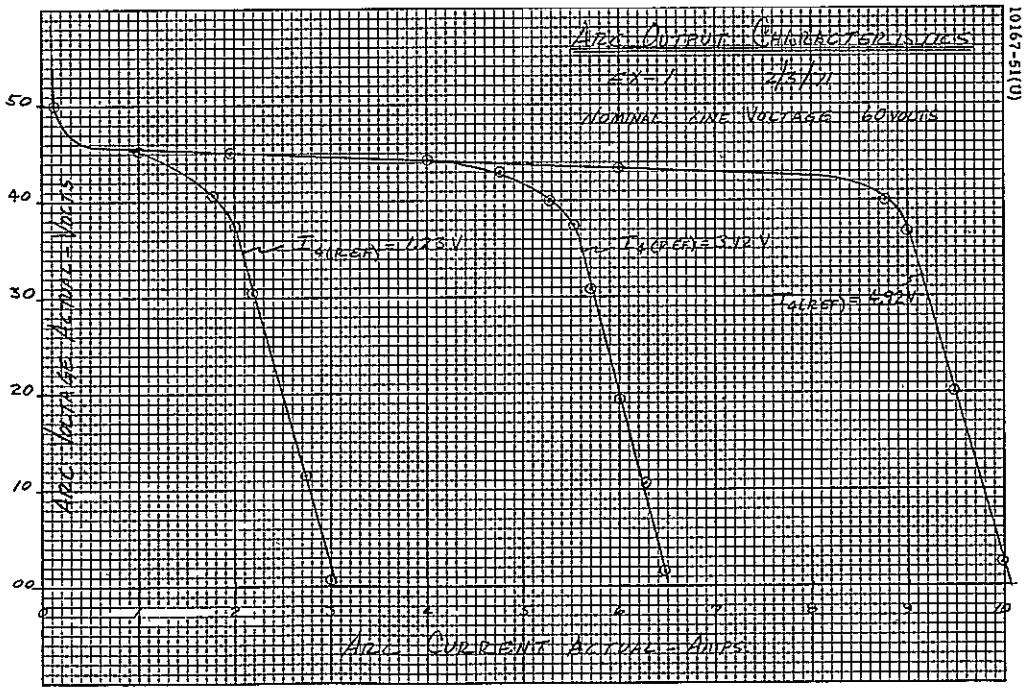

Figure 5-25. Arc Output Characteristics

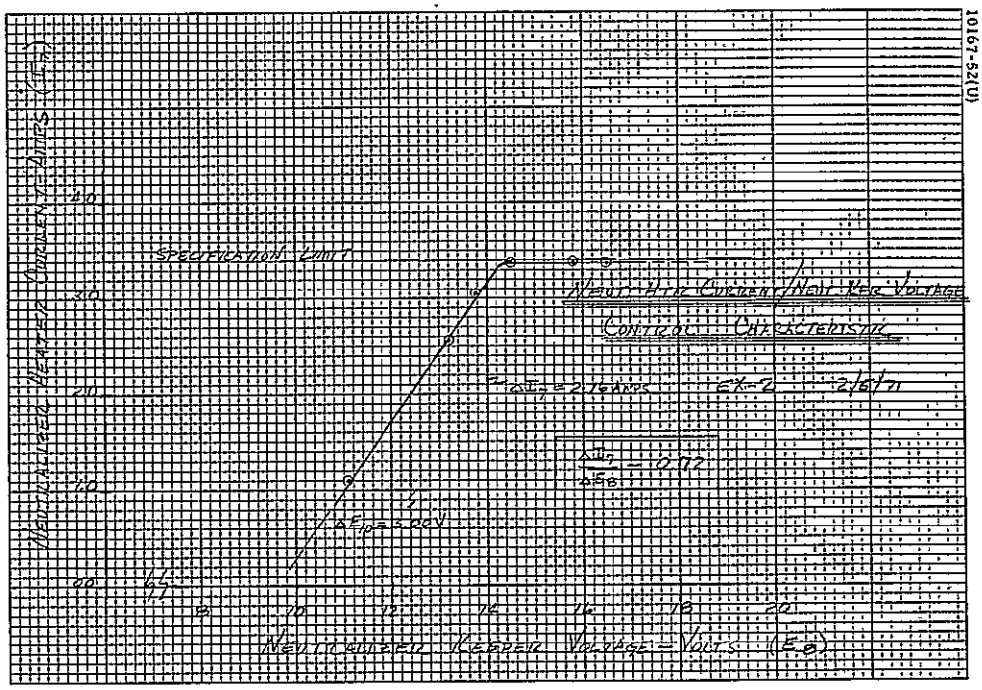

Figure 5-26. Neutral Heater Current/Neutral Keeper Voltage Control Characteristic

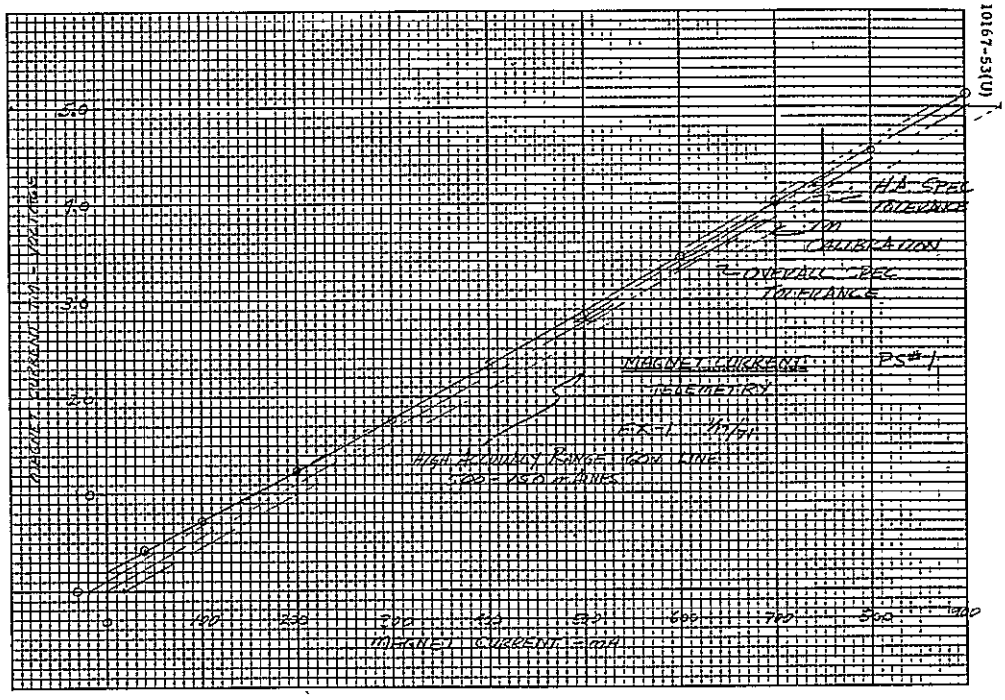

Figure 5-27. Magnet Current Telemetry

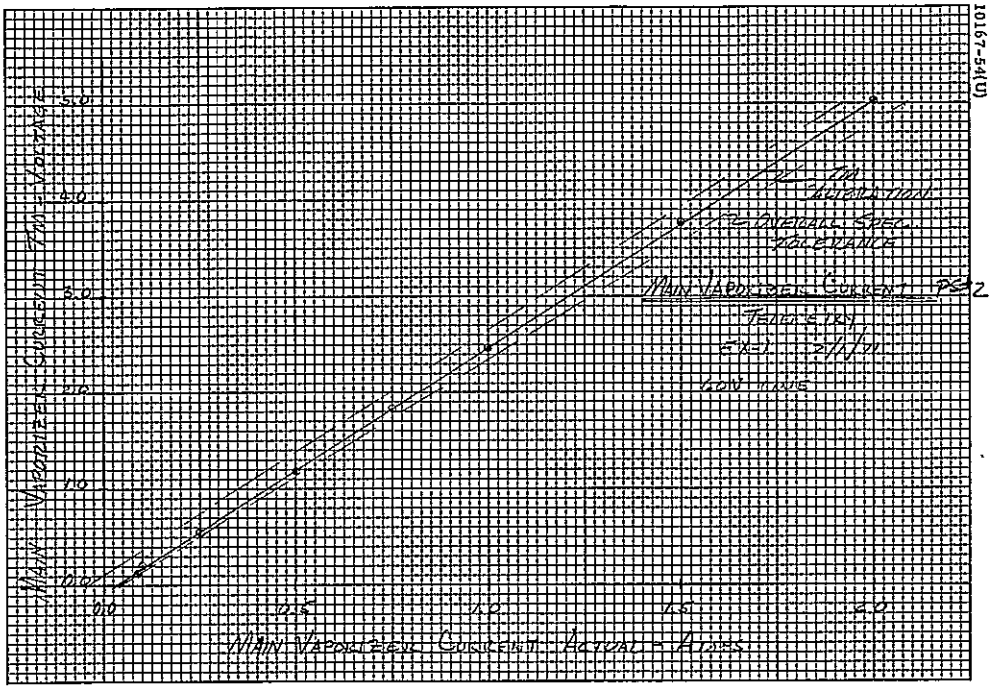

Figure 5-28. Main Vaproizer Current, PS No. 2

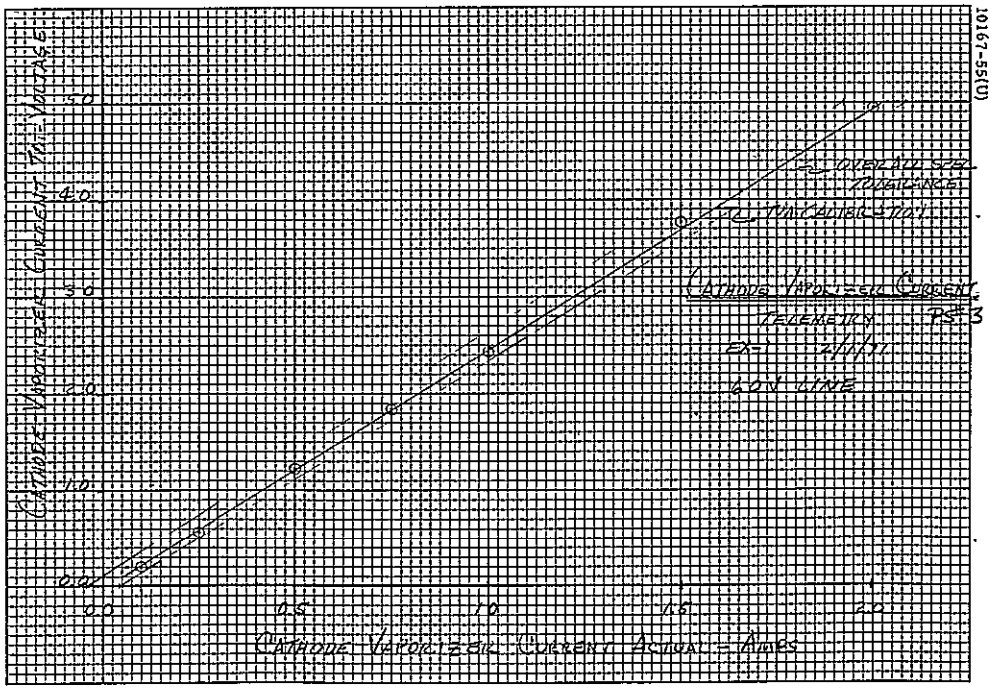

Figure 5-29. Cathode Vaporizer Current, PS No. 3

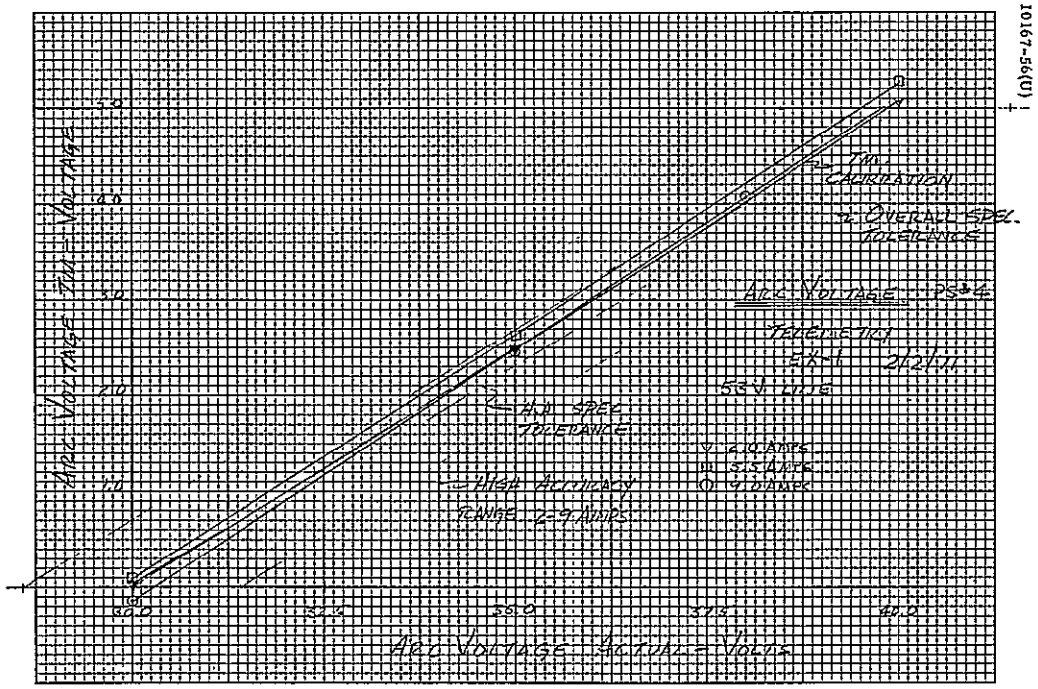

Figure 5-30. Arc Voltage, PS No. 4 — 53 Volt Line

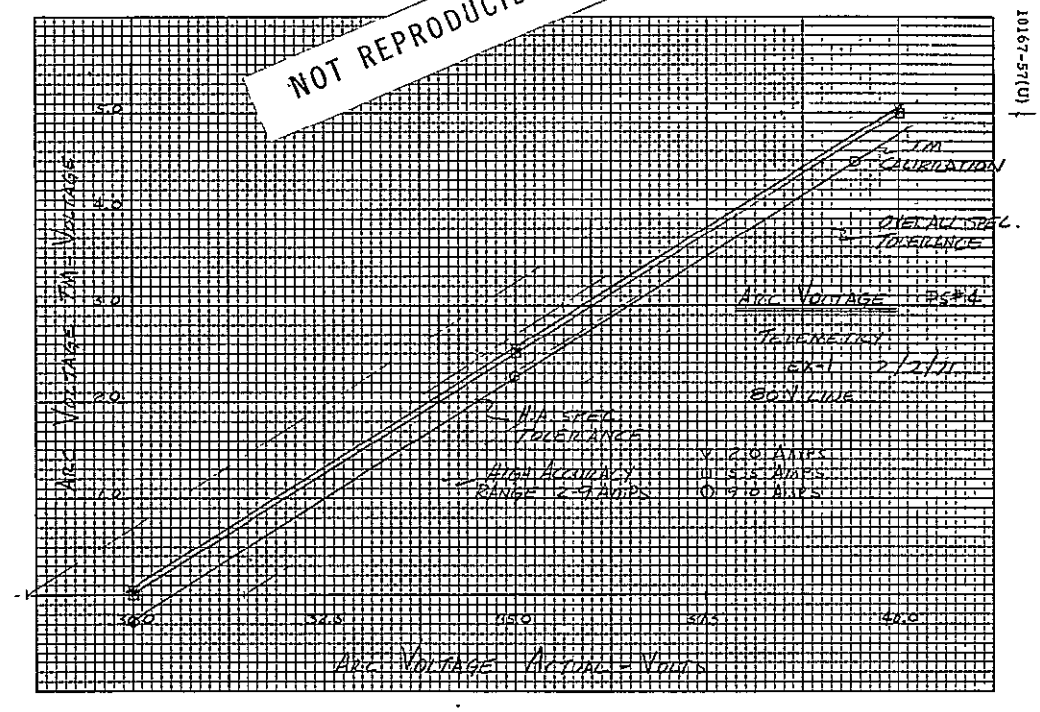

Figure 5-31. Arc Voltage, PS No. 4 — 80 Volt Line

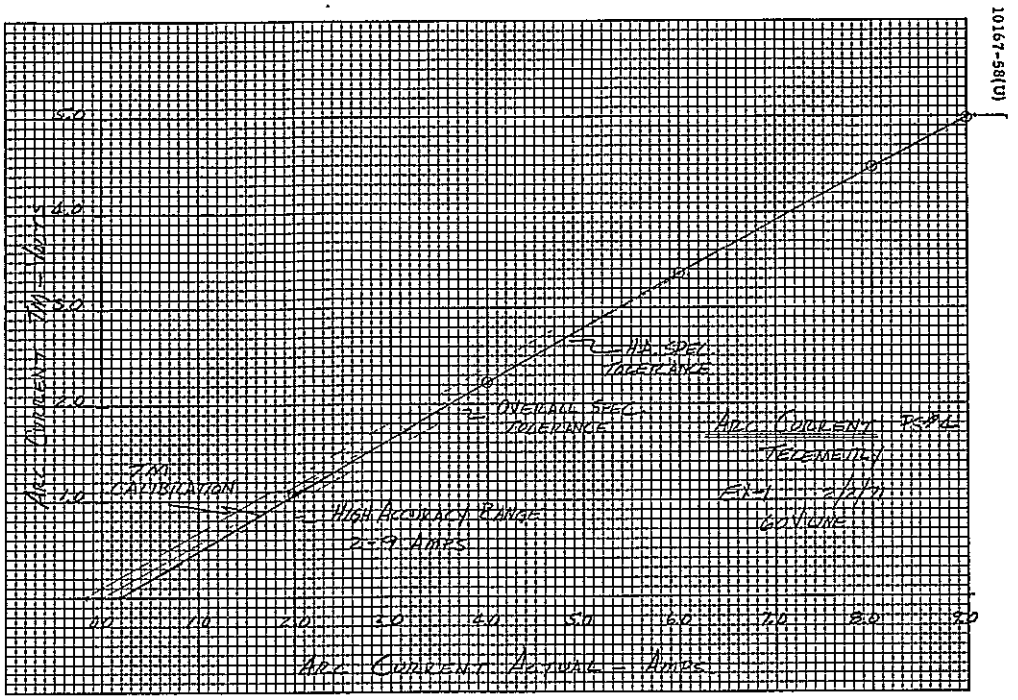

Figure 5-32. Arc Current, PS No. 4

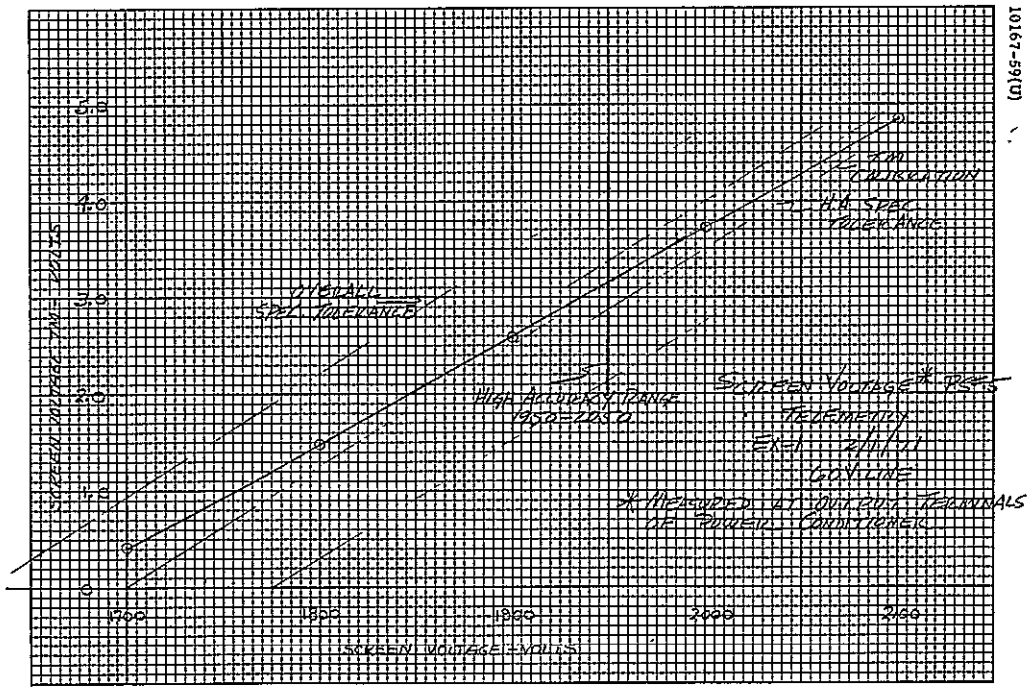

Figure 5-33. Screen Voltage*, PS No. 4

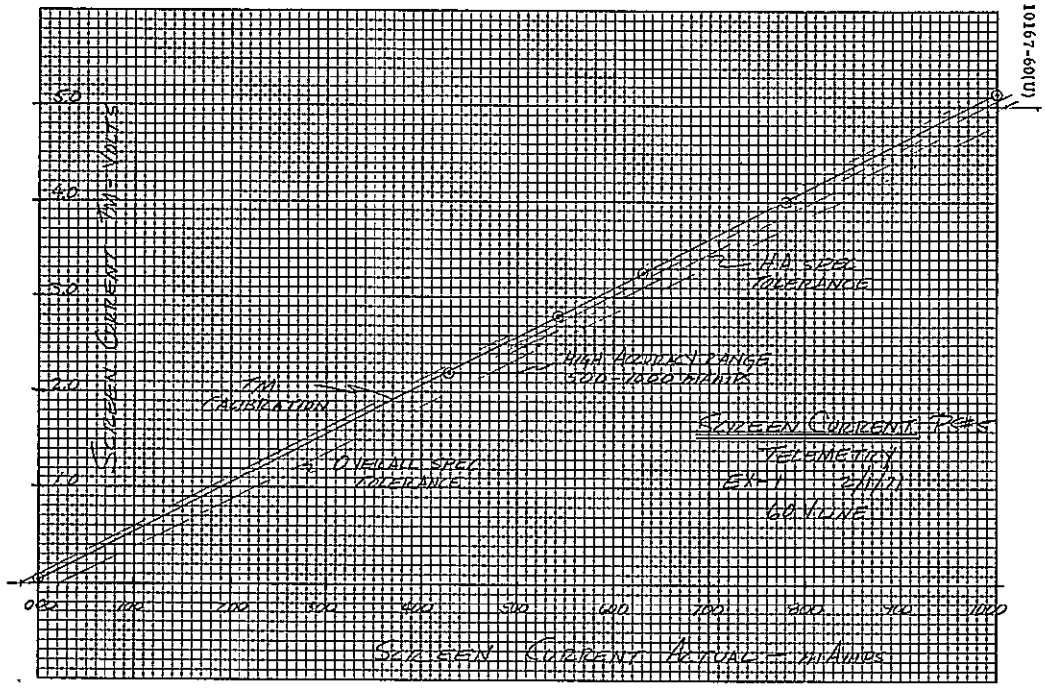

Figure 5-34. Screen Current, PS No. 5

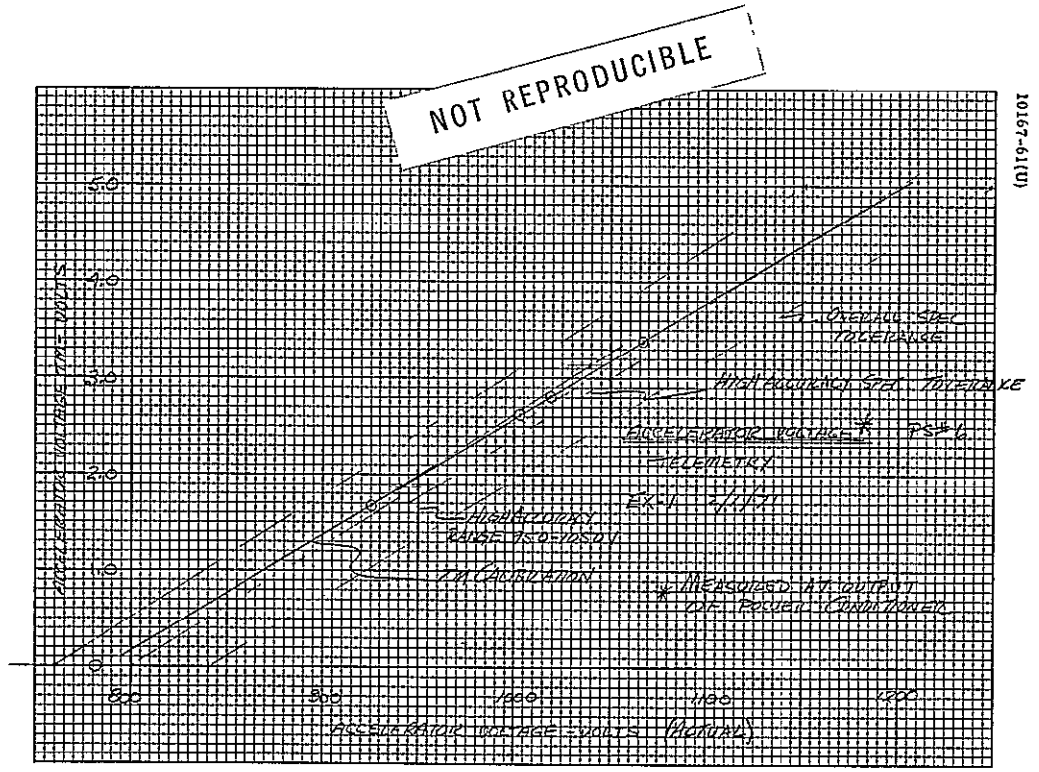

Figure 5-35. Accelerometer Voltage*, PS No. 6

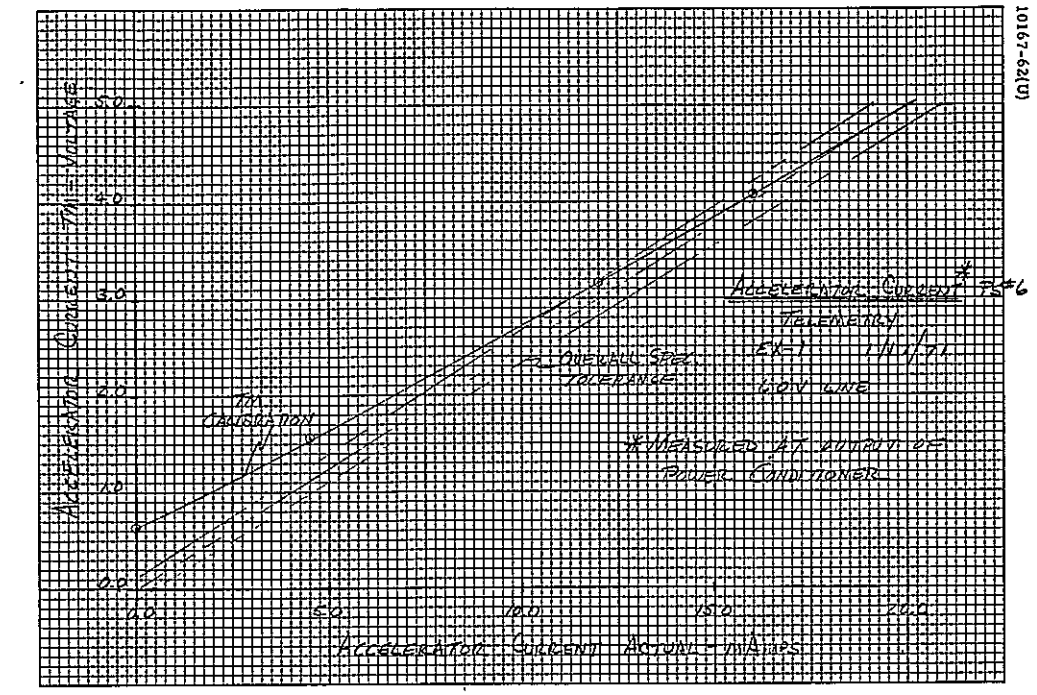

Figure 5-36. Accelerometer Current*, PS No. 5

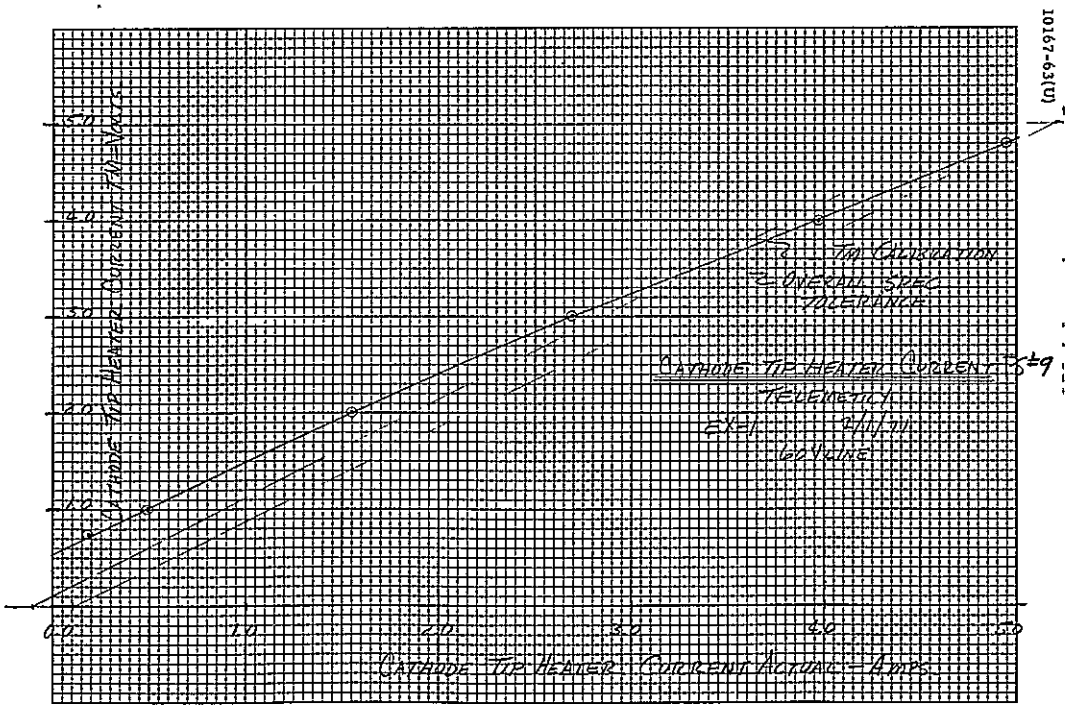

Figure 5-37. Cathode Tip Heater Current, PS No. 7

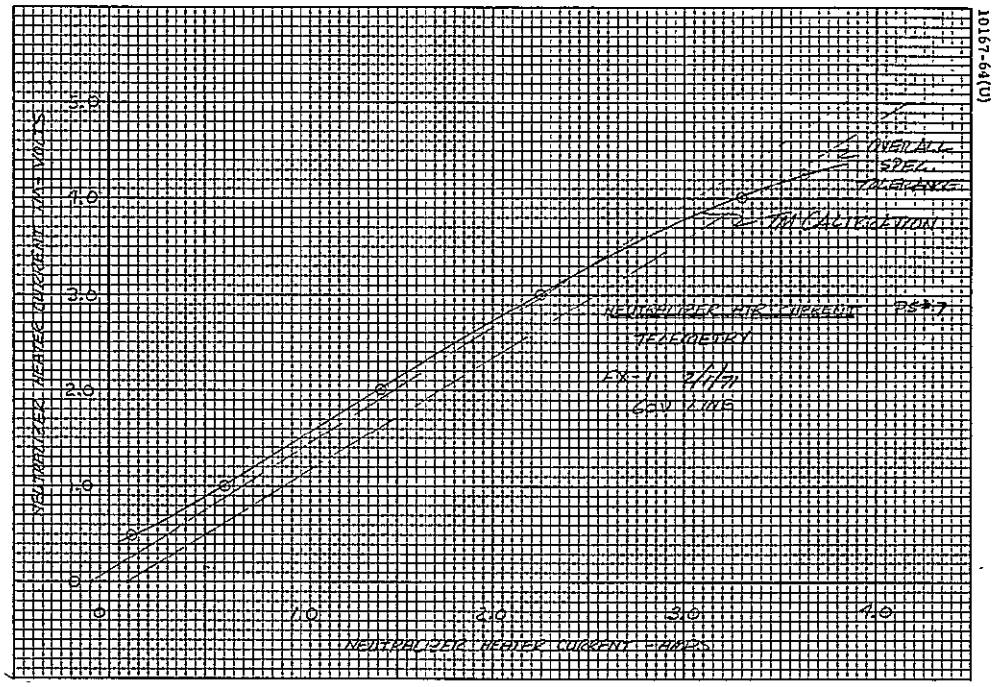

Figure 5-38. Neutralizer Heater Current, PS No. 7

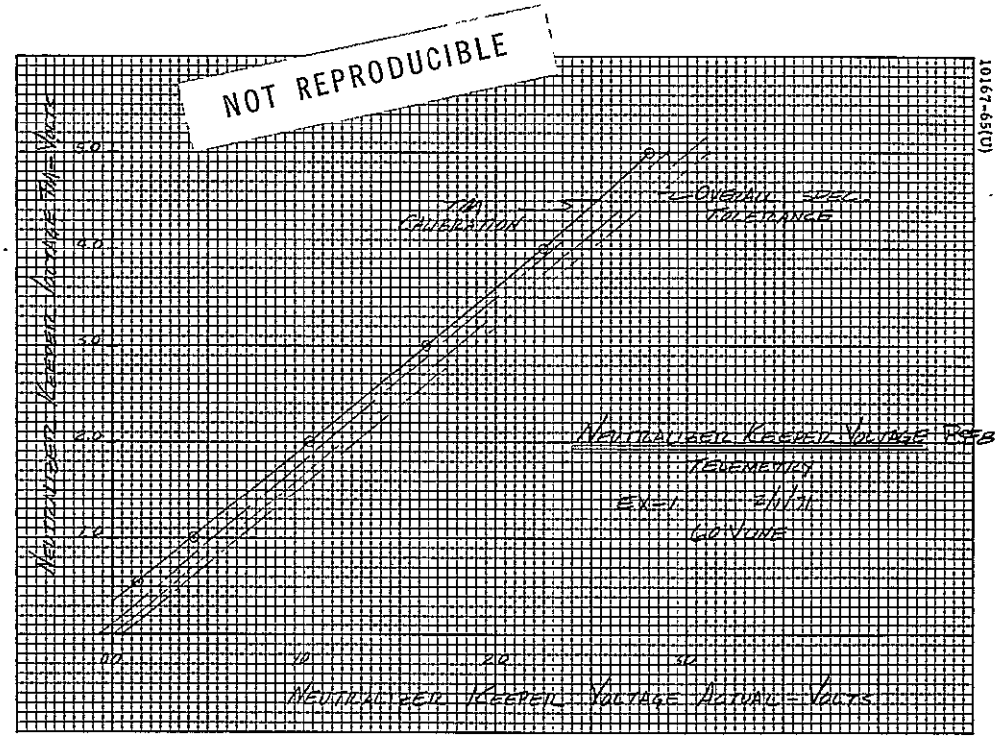

Figure 5-39. Neutralizer Keeper Voltage, PS No. 8

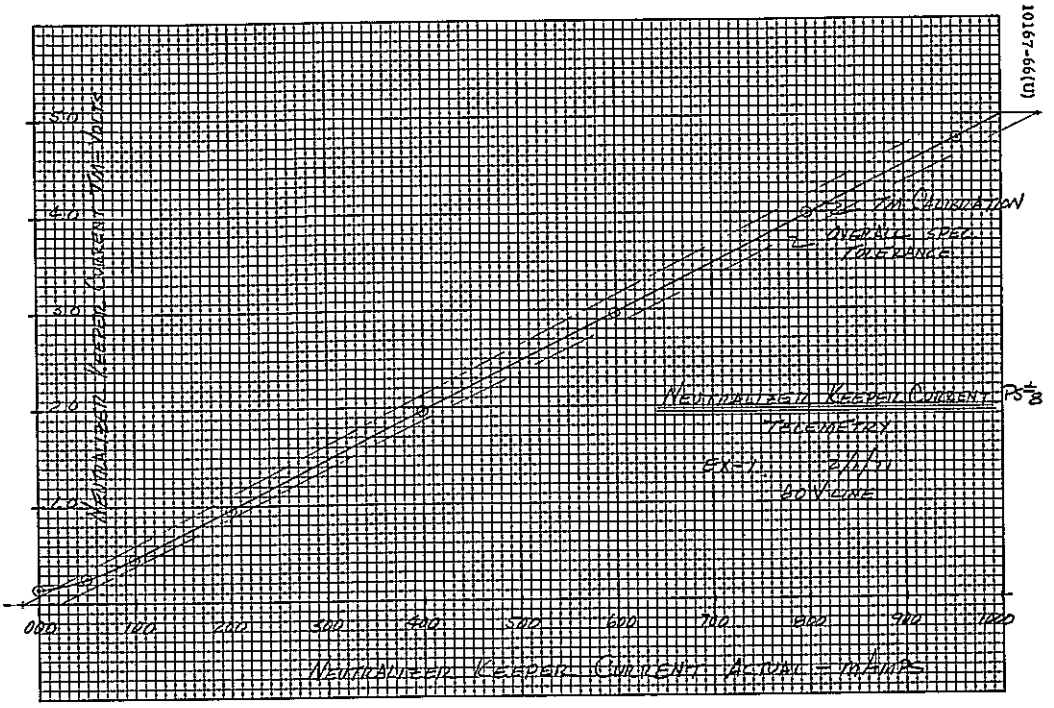

Figure 5-40. Neutralizer Keeper Current, PS No. 8

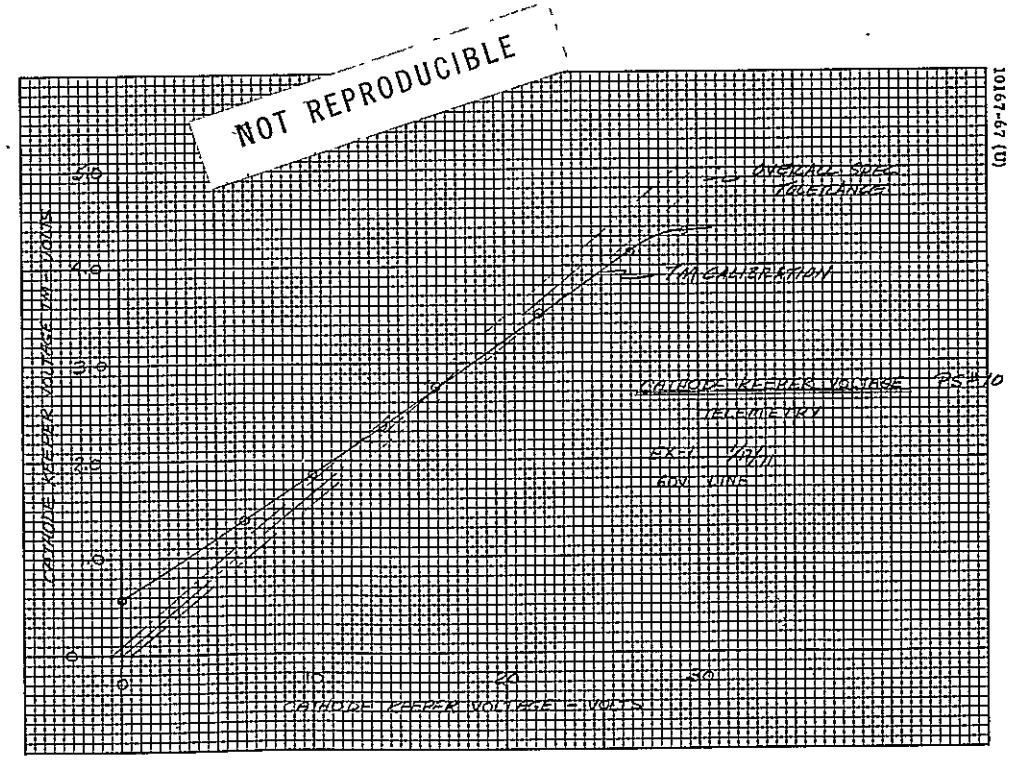

Figure 5-41. Cathode Keeper Voltage, PS No. 10

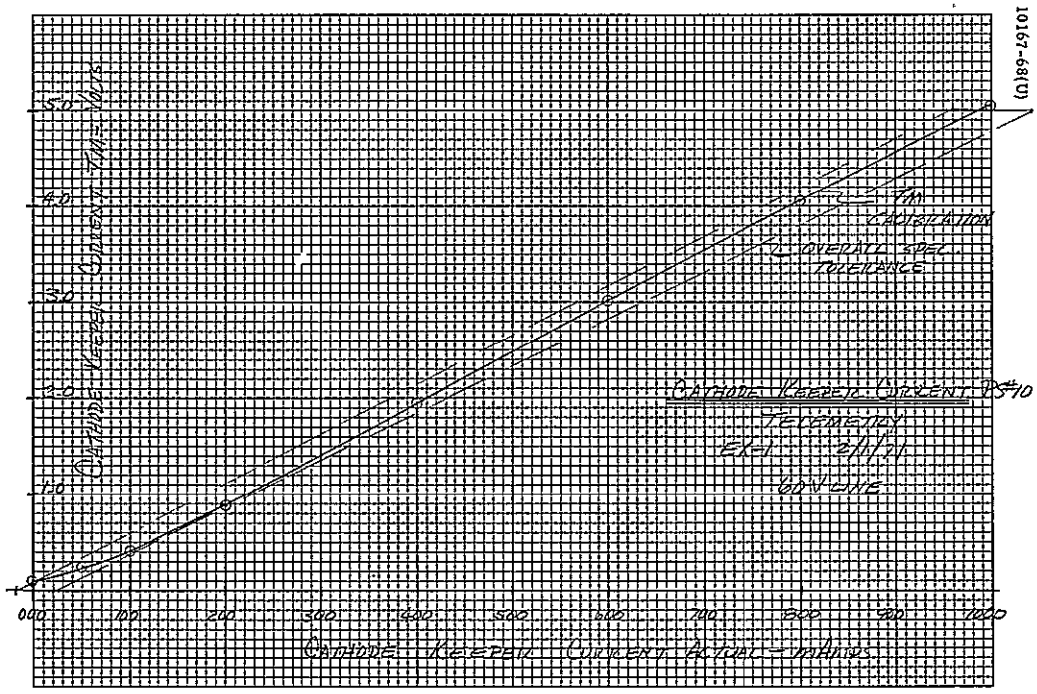

Figure 5-42. Cathode Keeper Current, PS No. 10

6. REFERENCES

1. King, H. J., et al. "Development and Testing of a Lightweight Flight Prototype Ion Engine System," Journal of Spacecraft and Rockets, May 1967.

2. Macie, T. W., et al. Integration of a Flight Prototype Power Conditioner with a 20 CM Ion Thruster, AIAA 9th Aerospace Sciences Meeting, New York, January 25-27, 1971.

APPENDIX A. BREADBOARD EFFICIENCY ANALYSIS

1) Screen Inverter

	40 Volt Line	80 Volt Line
Sat. Loss	= 5.04 watts	2.52W
Switching Loss	= 1.9	3.80
Base Drive	= 2.62	1.31
Line Cap	= 0.31	0.71
Transformer	= 3.96	2.65
Rectifiers	= 2.8	1.40
	16.63 watts/inverter	12.39 watts/inverter

% η = (250/266.6)100 = 94% % η = (250/262.4) x 100 = 95.1%

2) Arc Supply

Transistors	= 6.68	6.10
Base Drive	= 2.62	1.26
Line Caps	= 0.30	0.69
Transformer	= 3.82	2.55
Rectifier	= 5.60	5.60
Choke	= 2.50	2.50
Output Caps	= 2.00	2.00
	23.32 watts	20.70 watts

% η = (252/275.32) 100 = 91.6% % η = (252/272.7) x 100 = 92.4%

3) Cathode Supply

Transistors	= 4.25	2.87
Base Drive	= 1.40	0.70
Line Cap	= 0.25	0.80
Transformer	= 4.00	4.00
	9.90 watts	6.37 watts

% η = (200/209.9) x 100 = 95.3% % η = (200/206.4) x 100 = 96.8%

4) Accelerator Supply (Full Power)

Transistor Losses	
Sat	= 4.40
Sw.	= 1.20
Base Drive	= 1.60
Transformer	= 3.02
Rectifiers	= 0.80
Line Regulator	= 11.97
	22.99 watts

% η = (200/222.99) x 100 = 89.7%

5) 5 KHz Inverter and Regulator

Transistors	=	2.57
Base Drive	=	1.00
Transformer	=	2.10
Line Regulator	=	8.00
		13.67 watts

6) High Voltage Filter

Bleeder Networks	4 watts
Screen I Sense	1 watt
Accel. I Sense	0.5 watt
Screen Choke	2.0 watt
Accel. Choke	0.5 watt
	8.0 watts

7) Magnetic Modulator

Vaporizer	1.05 watt
Neut. Heater	2.10 watts
Neut. Keeper	1.40 watts
Magnet	1.65 watts
	6.20 watts

8) Control Module

Estimated	5.0 watts

4) Accelerator Supply (Full Power)

Transistor Losses		
Sat	=	4.40
Sw.	=	1.20
Base Drive	=	1.60
Transformer	=	3.02
Rectifiers	=	0.80
Line Regulator	=	11.97
		22.99 watts

$\%\mu = (200/222.99) \times 100 = 89.7\%$

5) 5 kHz Inverter and Regulator

Transistors	=	2.57
Base Drive	=	1.00
Transformer	=	2.10
Line Regulator	=	8.00
		13.67 watts

6) High Voltage Filter

Bleeder Networks	4 watts
Screen I Sense	1 watt
Accel. I Sense	0.5 watt
Screen Choke	2.0 watt
Accel. Choke	0.5 watt
	8.0 watts

7) Magnetic Modulator

Vaporizer	1.05 watt
Neut. Heater	2.10 watts
Neut. Keeper	1.40 watts
Magnet	1.65 watts
	6.20 watts

8) Control Module

Estimated	5.0 watts

TABLE A-1. SUMMARY OF LOSSES

Module	Losses	
	40V Line, watts	80V Line, watts
1. Screen inverter — Worst case — 71NV. x	(19.3)	(14.23)
Normal case — 81NV. x	16.6	12.39
2. Arc inverter	13.3	10.60
3. Accelerator inverter — Transient	11.0	11.0
Normal	3.75	3.75
4. Cathode inverter	9.90	6.37
5. 6 kHz inverter	5.67	5.67
6. 5 kHz line regulator	7.9	8.3
7. Accelerator line regulator — Transient	(11.97)	(12.5)
Normal	2.05	1.95
8. Arc rectifier — filter	10.1	10.1
9. High voltage filter	8.0	8.0
10. Magnetic modulator	4.8	4.8
11. Control module	5.0	5.0

APPENDIX B. EXPERIMENTAL EFFICIENCY ANALYSIS

Screen Inv.

53 V Line

Losses	Power Transistors	7.50
	Power Xfmr	3.50
	Line Caps	1.20
	+35V	4.00
	+5V	0.17
	Output Rectifiers	2.40
		18.77
	X8 Inv	8
		150.16
	Output Filter	3.42
	Harness Loss	5.84
		159.42
Power Out		2000.00
Power In		2159.72

$$\% \eta = \frac{P_{out}}{P_{in}} \times 100 = 92.7\%$$

80V Line

Losses	Power Transistors	9.82
	Power Xfmr	2.20
	Line Caps	1.20
	+35V	3.08
	+5V	0.15
	Output Rectifiers	2.40
		18.85
	X 8 inv.	8
		150.80
	Output Filter	3.42
	Harness Losses	2.57
		159.42
	Power Out	2000.00
	Power In	2159.42

$$\% \eta = \frac{P_{out}}{P_{in}} \times 100 = 92.8\%$$

TRANSISTOR LOSS CALCULATIONS

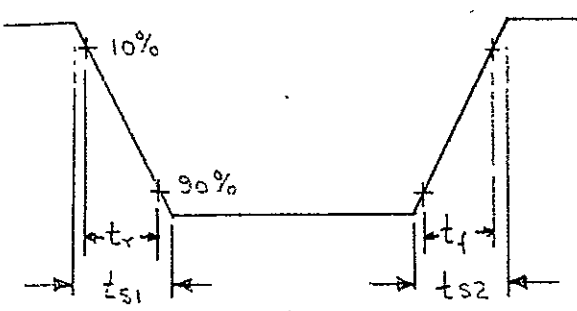

Collector to Emitter Voltage

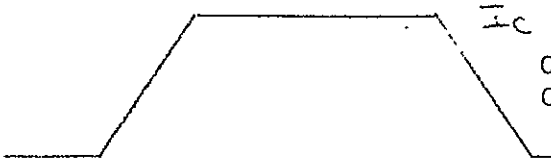

Collector Current

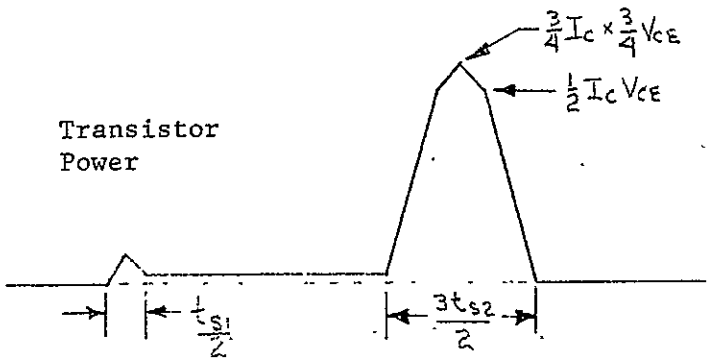

Transistor Power

Total Period = $\frac{1}{T}$

Pulse Width = $1/_T$

$$P_{xist} = \frac{1}{T}\left[\frac{I_c V_{ce}}{64} ts1 + \frac{I_c V_{ce}}{2} ts2 + \frac{I_c V_{ce}}{64} t_{s2} + V_{ces} I_c \tau\right] + \frac{T}{T} V_{BE} I_B$$

$$t_{s1} = \frac{tr1}{0.8} = 1.25\ tr$$

$$t_{s2} = 1.25\ tf$$

$$\tau = T\frac{53}{2\ V_{ce}} - (t_{s1} + t_{s2}) \approx \frac{53T}{2V_{ce}}$$

$$P_{xist} = \frac{V_{ce} I_c}{T}\left[\frac{1}{64}(t_{s1} + t_{s2}) + \frac{t_{s2}}{2}\right] + \frac{\tau}{T}\left[V_{ces} I_c + V_{BE} I_B\right]$$

$$= \frac{V_{ce} I_c}{2T}\left[\frac{1.25}{32}(tr + tf) + 1.25\ t_f\right] + \frac{\tau}{T}\left[V_{ces} I_c + V_{BE} I_B\right]$$

For max tr and tf $tr = tf$

$$P_{xist} = \frac{V_{ce} I_c t_f}{T}\left[\frac{1.25(33)}{32}\right] + \frac{53}{2V_{ce}}\left[V_{ces} I_c + V_{BE} I_B\right]$$

FROM THE XISTOR SPEC:

$$\frac{tr + tf}{2} < 0.7 \qquad \text{and} \qquad t_f + 0.6\ V_{ces} < 1$$

$$tr < 1.4 - tf \qquad \boxed{tf < 1 - 0.6\ V_{ces}}$$

$$tr < 1.4 - 1 + 0.6\ V_{ces}$$

$$\boxed{tr < 0.4 + 0.6\ V_{ces}}$$

If $V_{ces} = 0.5V$ max

$tr = 0.4 + 0.6\ (0.5) = 0.7$ $\qquad$ $tf = 1 - 0.6\ (0.5) = 0.7$

At 53 volt line and 250 w/inv out at η = 90%

assume $_{T}$ = T/2:

$$I_c = \frac{250}{(53)(0.9)} = 5.24 \text{ amps}$$

$$V_{ces} = 0.5 \times \frac{5.24}{8} = .327$$

$$P_{xist} = \frac{(53)(5.24)0.7}{100} \; 1.29 + \frac{53}{2(53)} \left[(0.327)(5.24) + (1.0)(0.8)\right]$$

$$= 2.5 + 1.25 = 3.75W$$

Total xistor losses at 53V = 7.50W

At 80 volt line and 250 w/inv out at η = 90%

$$P_{xist} = \frac{(80)(5.24)(0.7)}{100} \; 1.29 + \frac{53}{2(80)} \left[(0.327)(5.24) + (1.0)(0.8)\right]$$

$$= 3.78 + 1.13 = 4.91 \text{ W}$$

Total xistor losses at 80V = 9.82W

Input Line Drop

Average distance, top 4 inv. =	18 inches
Average distance, bottom 4 inv. =	32 inches
	50 inches
Plus ret	50
Total wire length	400 inches

Resistance 18 gage wire = 6.4 Ω/1000 ft.

$$\text{Total resistance} = 4\,\frac{16}{300} = \frac{4 \times 8}{150} = .2136\ \Omega$$

$$P_{lost} = 0.2136 \times (5.24)^2 = 5.84W$$

Arc Inv.

80V line, assume 87.8% η at 375 watts

$$P_{loss} = \frac{375}{.878} - 375 = 52 \text{ watts}$$

53V line, assume 87% η

$$P_{loss} = \frac{375}{.87} - 375 = 56 \text{ watts}$$

SUMMARY

80V line, total output power

Screen	2000
Arc	375
Accel	10
5 KHz Syst.	38
	2423

80V Line, Losses

Screen	156.79
Arc	52.00
Accel	3.00
5 KHz System	9.00
Controls	4.30
	225.09

$$\text{System Eff} = \frac{2423 \times 100}{2648.09} = 91.6\%$$

50V Line, total output power = 2423 W

50V Line. Losses

Screen	159.42
Acr	56.00
Accel	3.00
5 KHz System	9.00
Controls	4.30
	231.72

$$\text{System Eff} = \frac{2423 \times 100}{2654.72} = 91.4\%$$

TABLE B-1. EXPERIMENTAL INVERTER EFFICIENCY TEST RESULTS

Operation Level = 250 volts, 1 ampere, output 250 watts

Line Voltage	53 volts			80 volts		
Inverter Frequency	5 kHz	7.5 kHz	10 kHz	5 kHz	7.5 kHz	10 kHz
Power Dissipation per Module:						
1) Logic, drive, and filter circuits	6.8w/	6.4w/	8.3w/	6.4w/	6.5w/	6.05w/
2) Power transistors and comp. diodes	4.1	5.1	5.2	5.0	5.9	7.8
3) Output transformers		1.4	9.4		7.6	8.0
a) Core Loss		—	2.7		—	4.6
b) I^2R Loss		—	6.7		—	3.4
4) Rectifier	10.1	3.3	2.3	11.2	4.4	4.4
5) Output filter	2.75	3.05	2.9	3.3	3.6	3.2
Total power dissipation (without output filter)	21.0	22.2	25.2	21.95	24.4	26.25
Total power dissipation	23.75	25.25	28.1	25.25	28.0	27.45
Inverter efficiency (without output filter), percent	92.3	91.85	90.9	92.0	91.1	90.5
Inverter efficiency using meters (without output filter), percent	90.4	90.5	90.5	86.4	88.8	88.5
ΔEff ($Eff_{(cal.)} - Eff_{(meters)}$), percent	1.9	1.35	0.4	5.6	2 3	2 0
Screen system efficiency using calorimeter data, percent	92	91.55	90.5	91.6	90.8	90.2
Screen system efficiency using meter data, percent	90.1	90.2	90.3	86.0	88.5	88.2

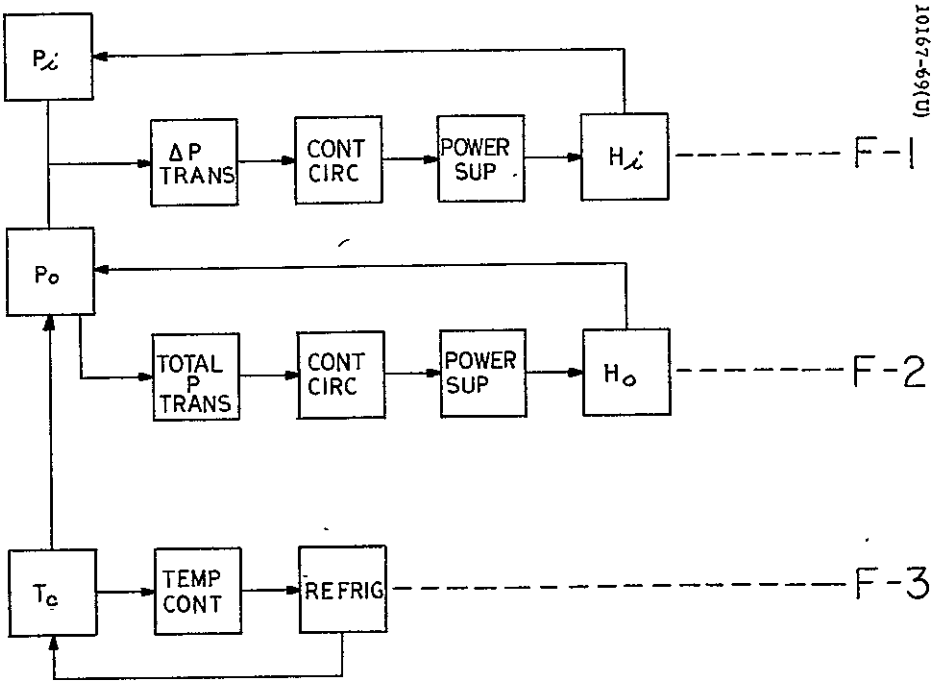

Figure B-1. Calorimeter Feedback Systems

CALORIMETER THEORY OF OPERATION

The calorimeter is of the isothermal type, which indicates heat generation rates by measuring the rate of boiloff of a liquid. The test item is placed inside the inner (test) chamber of the calorimeter. This chamber and the surrounding one are filled with one of the Freons. The two chambers are connected by a hole in the bottom of the test chamber. The Freon is maintained at the boiling point in both chambers by means of the calibration and feedback heaters in the test chamber and the heaters in the outer chamber. The pressure drop in the Freon vapor following through an orifice in the test chamber lid is sensed by a differential pressure transducer. The size of the orifice is adjustable, and is normally set to give a pressure drop of between 0.05 and 0.15 psid. The lower limit is set by the resolution of the transducer (0.0075 psid) and the upper limit by the difference in liquid levels in the two chambers (1 3/4 inch for a ΔP of 0.10 psid).

The calorimeter is capable of either manual or automatic operation. For manual operation, the test item is turned on, with the feedback heater disconnected. The system is then allowed to equilibrate thermally, and the signal from the differential transducer is determined by nulling the meter on the controller for the feedback heater. The actual value of the signal from the transducer need not be read; however, after thermal equilibration, the test item is turned off and the meter is again nulled by adjusting the calibration heater while the meter remains set at the same reading as it was when the test item was operating. The power to the calibration heater then equals the heat output from the test item.

For automatic operation, the feedback heater is connected and is set for a heat generation rate somewhat in excess of the anticipated heat output from the test item. When the test item begins to generate heat, the Freon flow rate increases, causing an increased pressure drop across the orifice. The increased output from the transducer causes the feedback heater to be turned down, and a constant flow rate of Freon vapor (and therefore a constant heat output from the test chamber) is maintained. The decrease in the power input to the feedback heater, compared to the power when no other heat source is operating, gives a measure of the heat generation rate of the test item. The circuit includes a zero suppression so that the decrease is read directly. Figure B-1 shows the three interconnected feedback systems. F-1, F-2, and F-3 refer to the individual feedback loops. Pi refers to the inner chamber pressure, Po to the outer chamber pressure, Hi to the inner chamber heater, Ho to the outer chamber heater, and Tc to the condenser temperature.

APPENDIX C. POWER LOSS AND EFFICIENCY MEASUREMENTS, JPL ION THRUSTER POWER CONDITIONER

1)	Total power output at P.C. (does not vary with line voltage).	2487.63W
2)	80V line calorimeter loss measurement	310 W
3)	57.6V line calorimeter loss measurement	300 W
4)	Losses in cabling from calorimeter internal connectors to P.C.	20 W

2) Above run at 950 ma beam current. An additional 50 ma would have increased the output power by 103.15 watts. The fixed losses due to drive power are 2.8 W out of 10.3 total calculated power for an effective increase in losses of 7.5 watts.

% η for (2) would then be

$$\% \eta = \frac{(2487.63 + 103.15)\ 100}{2590.78 + 310 - 20 + 7.5} = \frac{(2590.78)\ 100}{(2888.3)}$$

$$\eta = \begin{matrix} 89.39 \\ 89.699 \\ 90.01 \end{matrix} \quad \text{error band at } \pm 10\text{W}$$

3) Above was run at 925 ma beam current. An additional 75 ma would have increa ed the output power by 154.73. The fixed losses due to drive power are 3.37 out of 15.473W. Total calculated power for an effective increase in losses of 12.1W

% η for (3) would then be

$$\% \eta = \frac{(2436.05 + 154.73)\ 100}{2590.78 + 300 - 20 + 12.1} = \frac{2590.78}{2882.88} \times 100 = \begin{matrix} 89.56 \\ 89.87 \\ 90.18 \end{matrix}$$

APPENDIX D: ACCEPTANCE TEST SUMMARY EX-1

MAGNET SUPPLY (PS-1)		
Load Reg	Min. Load	I_1 = 640 mA
	Max. Load	I_1 = 641 mA
	Short Ckt	I_1 = 591 mA
Line Reg.	80V Line	I_1 = 641 mA
	53V line	I_1 - 641 mA
MAIN VAPORIZER (PS-2)		
Load Reg.	Nom. Load	I_2 = 1.92A
	Short	I_2 = 1.94A
CATHODE VAPORIZER (PS-3)		
Load Reg	Nom Load	I_3 = 1.92A
	Short	I_3 = 1.90A
ARC SUPPLY (PS-4)		
Load Reg	E_4 = 37.37V	I_4 = 4.9A
	E_4 = 20.10V	I_4 = 5.17A
	E_4 = 77.1 V	I_4 = 0
Line Reg	80V Line	I_4 = 8.03A
	53V Line	I_4 = 8.02A
Arc Standby	60V Line	I_4 = 8.03A
BEAM SUPPLY (PS-5)		
Load Regulation	V_5 = 2023.2V	I_5 = 0 A
	V_5 = 2025.2V	I_5 = 0.5A
	V_5 = 2028V	I_5 = 1.0A
Line Regulation	80V Line V_5 = 2034V	I_5 = 1.0A
	53V Line V_5 = 2033V	I_5 = 1.0A
Standby Test	60V Line V_5 = 2036	(1 inv. failed)
Trip Point	I_5 Trip = 1.09 to 1.10A	
Ripple	$V_{5\ pp}$ = 150V	I_5 = 1.0A

ACCELERATOR SUPPLY (PS-6)

Load Reg	V_6 = 1243.5V	I_6 = 0
	V_6 = 1063.5V	I_6 = 5.0 mA
	V_6 = 1020.5V	I_6 = 11.0 mA
	V_6 = 936V	I_6 = 50 mA
Line Reg	80V Line	V_6 = 1021.5V
	53V Line	V_6 = 1019.5V
Ripple	$V_{6\ pp}$ = 100V	I_6 = 11.0 mA

NEUTRALIZER HEATER SUPPLY (PS-7)

Load Regulation	Nom. Load	I_7 = 3.32A
	Short	I_7 = 3.24A

NEUTRALIZER KEEPER SUPPLY (PS-8)

Load Regulation	V_8 = 341.5	I_8 = 0
	V_8 = 308	I_8 = 6 mA
	V_8 = 30V	I_8 = 34.5 mA
	V_8 = 10V	I_8 = 785 mA
	V_8 = 1.08V	I_8 = 994 mA
Ripple	$I_{8\ pp}$ = 7mA at 500 mA load	

CATHOD HEATER (PS-9)

Load Regulation	V_9 = 8.67V	I_9 = 4.7A
	V_9 = 5.32V	I_9 = 4.67A
	Short	I_9 = 4.57A
Line Regulation	80V Line	I_9 = 4.81A
	53V Line	I_9 = 4.79A

CATHODE KEEPER (PS-10)

Load Regulation	V_{10} = 317V	I_{10} = 0
	V_{10} = 286.5V	I_{10} = 4.78mA
	V_{10} = 22V	I_{10} = 393 mA
	V_{10} = 10V	I_{10} = 802 mA
	V_{10} = 0	I_{10} = 1.0A
Ripple	$I_{10\ pp}$ = 7 mA at 500 mA load	

APPENDIX E: STRESS ANALYSIS

Table E-1 is a summary of the various configurations analyzed and the corresponding results. Model 5 of Table E-1 is recommended from a high resonant frequency, low deflection, and low weight standpoint.

DISCUSSION

The thruster plate basically consists of 20 electronic modules mounted on a frame which provides the system stiffness. Electronic components mounted on sheet metal plates comprise the electronic modules, while the frame is composed of an I-beam network. The models analyzed arose from various configurations of the frame, I-beam geometries, and module sheet thickness.

The structural dynamic analysis was performed by idealizing the distributed mass system with a lumped mass dynamic math model consisting of 30 mass stations. Figures E-1 and E-2 depict the frame geometries that were used in the models. The various frame I-beam configurations are shown in Figures E-3 through E-5. The last model variable is the module sheet thickness.

The model masses were obtained by lumping at the stations the masses of all the adjoining modules and I-beams. The model stiffness is based on 31 aluminum I-beam sections and 40 magnesium triangular sheet elements.

The model boundary conditions are dictated by the supports at the model periphery and at various stations within. For all models a clamped condition was used at the periphery. The supports within the periphery varied in number from model to model. Their use prevented translational motion in the direction perpendicular to the thruster plate plane.

The models are identified by the frame configuration, frame I-beam type, number of supports, and module sheet thicknesses and are summarized in Table E-1. The frame weights were derived from the component aluminum I-beams.

TABLE 1. THRUSTER PLATE DYNAMIC ANALYSIS SUMMARY

Model No.	Frame Configuration	Frame I-Beam	Number of Supports	Support Station No.	Module Sheet Thickness, inch	Frame Weight, pounds	Fundamental Frequency, hertz	Maximum Deflection, inch
1	I (Figure E-1)	A Figure E-3	1	13	0.050	3.744	193.	0.07
2		B Figure E-4	1	13	0.050	2.455	75.	0.47
3			4	7,9,17,19	0.050	2.455	75.	0.23*
4	II (Figure E-2)	C Figure E-5	1	23	0.032	2.859	159.	0.10
5			3	22,24,26	0.032	2.859	243.	0.05
6			4	20,22,24, 26	0.032	2.859	250.	0 04

*Estimated

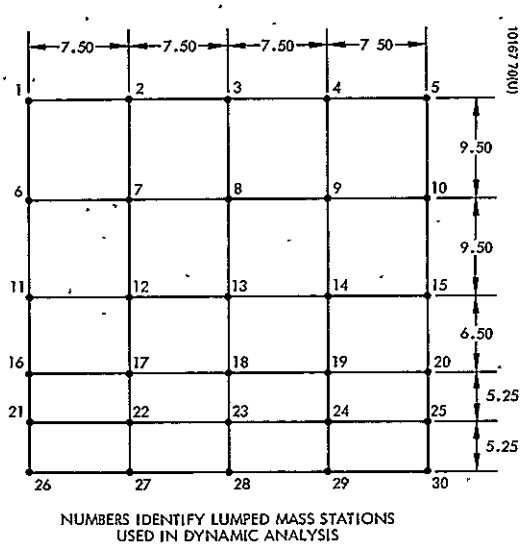

Figure E-1. Fran Configuration I

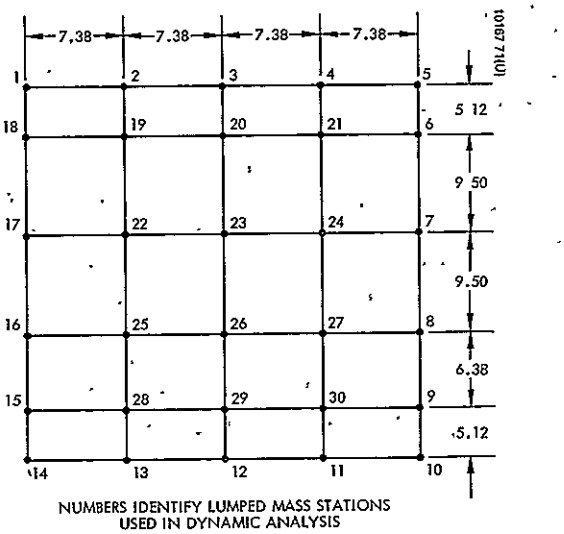

Figure E-2. Frame Configuration II

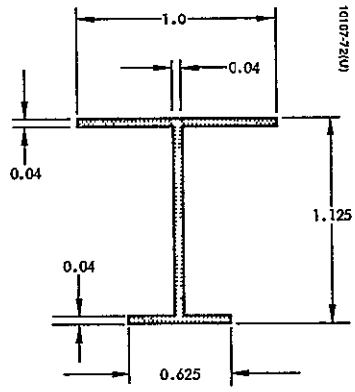

Figure E-3. I-Beam A (0.75 D Lightening Holes)

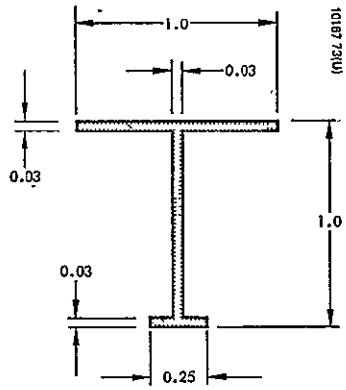

Figure E-4. I-Beam B (0.688 D Lightening Holes)

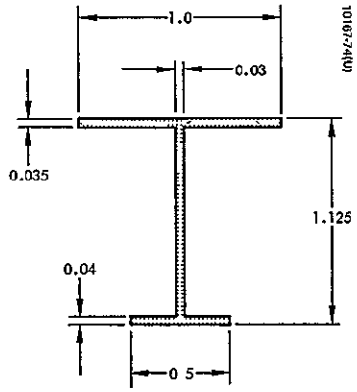

Figure E-5. I-Beam C (0.75 D Lightening Holes)

The model fundamental frequencies were obtained from the model mass and stiffness properties and are presented in Table E-1. The maximum deflections, also summarized in Table E-1, are based on the JPL component design qualification specification that requires a 9.0 g (0 peak) sinusoidal sweep frequency test.

CONCLUSIONS

The desirable thruster plate dynamic characteristics are a relatively high fundamental frequency and a low maximum deflection. Based on these criteria and a desirable low weight, the values in Table E-1 indicate that model No. 5 is the optimum of the six models analyzed. It consists of frame configuration II (Figure E-2) constructed with the I-beams of Figure E-5 and has three supports within its periphery. The modules mounted on the frame have sheet thicknesses of 0.032 inch. It has a fundamental frequency of 243 Hz and a 0.05 inch maximum deflection. Model No. 6 also appears feasible; however, an increase in frequency of 7 Hz and a 0.01 inch decrease in maximum deflection do not warrant the addition of another support to the thruster plate.

Control Number

BLANKET RELEASE FORM

In accordance with Memorandum of Understanding No. ____ between STID and OSSA ____; OART ____; OTDA ____; OMSF ____; the attached document can be Announced ____; Not Announced ____; and has a distribution limitation as follows:

- ☐ UNLIMITED
- ☐ U.S. GOVERNMENT AGENCIES AND CONTRACTORS ONLY
- ☐ U.S. GOVERNMENT AGENCIES ONLY
- ☐ NASA AND NASA-CONTRACTORS ONLY
- ☐ NASA HEADQUARTERS OFFICES AND CENTERS ONLY
- ☐ NASA HEADQUARTERS ONLY

GPL Blanket

Remarks:

☐ NASA CR 118651 ☐ TMX _____ N71-26525 ACCESSION NO. _____

Analyst _____

FF No. 864